The development of nanoscale techniques for the study of electrodes associated with biochemical processes.

Gordon, Daniel James

The development of nanoscale techniques for the study of electrodes associated with biochemical processes

Submitted to the University of Wales in fulfilment of the requirements for the Degree of Master of Philosophy

May 2011

Daniel James Gordon

Swansea University

Swansea University
Prifysgol Abertawe

ProQuest LLC.
789 East Eisenhower Parkway
P.O. Box 1346
Ann Arbor, MI 48106 – 1346

DECLARATION

This work has not previously been accepted in substance for any degree and is not being concurrently submitted in candidature for any degree.

Signed ..... (candidate)

Date ..... 22nd September 2012 .....

STATEMENT 1

This thesis is the result of my own investigations, except where otherwise stated. Where correction services have been used, the extent and nature of the correction is clearly marked in a footnote(s).

Other sources are acknowledged by footnotes giving explicit references. A bibliography is appended.

Signed ..... (candidate)

Date ..... 22nd September 2012 .....

STATEMENT 2

I hereby give consent for my thesis, if accepted, to be available for photocopying and for inter-library loan, and for the title and summary to be made available to outside organisations.

Signed ..... (candidate)

Date ..... 22nd September 2012 .....

Acknowledgements

I would like to thank my academic supervisor Dr Robert Lovitt for his support and help during my project, coming from a background with little biology experience made it tough, but his support made it possible.

Thanks also to Dr Chris Wright for help with investigations using the Atomic Force Microscopes and to Dr Alvin Tan for his instruction.

I would also like to thank Dr Byong-Hong Kim and Kyung Shik Kim for their training and hospitality when I was with them at KIST in Seoul.

Finally I would like to thank my friends and family for their support throughout, particularly Dr Elizabeth Sackett and Hannah Underwood for all their help.

Abstract

Bioelectrochemistry is a growing area with a great deal to offer technology, particularly in the fields of power generation, biosensors and medicine. The interfacial processes between electrodes and biological materials are central to understanding and exploitation of these processes.

The aim of this project was to investigate these processes by studying the interactions at the electrode surfaces. A number of techniques were employed to investigate the types of electrodes and the chemical reactivity with particular reference to biological materials

Initial studies of electrode characteristics were carried out through cyclic voltammetry studies of methyl viologen and oxygen. In the study different electrodes and different surface finishes are investigated. The topology of the electrodes is examined through the use of Atomic Force Microscopy (AFM), giving both images and statistical analysis of the surface roughness. Finally the bioelectrochemistry of proteins on the electrodes are investigated using the studies of laccase, azurin and the fouling of the electrode by bovine serum albumin.

Although establishing the basic methods and techniques required to study proteins on surfaces, the study did not give conclusive results as to electrode choice or the nature of the protein electrode interaction. It does however; indicate that a pyrolytic graphite edge plane electrode polished with alumina slurry is likely to be the best electrode for use with proteins. The studies with proteins need to be developed further and recent publications suggest several new methods that could be used.

During the work, many obstacles were encountered in the use of proteins, so this study puts forward possible methods of avoiding the same problems in the future. Likewise, new methods of investigation of electrode surfaces are put forward including Conducting-AFM, Electromagnetic Force Microscopy (EFM) and the imaging of double layers at a charged electrode using an AFM in fluid.

Table of Contents

Table of figures

1. Introduction

Whilst the human race is forever striding forward with new technologies, it is easy to forget that nature has already answered many of the problems that face us. For instance, whilst mankind is pushing towards alternative energy from hydrogen or sunlight amongst other sources, nature has already solved these issues, gaining energy from these sources through photosynthesis and hydrogen uptake.

Through millennia of evolution, nature has honed its techniques for energy production, sensing and adapting to its environment and processing information to a level far in advance of mankind's current technology.

With the emergence of new technologies, particularly in the field of nanotechnology, mankind is starting to understand the methods, materials and techniques used by nature, allowing us to start to harness some of natures "technologies" for our own use.

One key and exciting area is in the field of bioelectrochemistry, the harnessing of living cells and proteins through electrochemistry.

1.1. Bioelectrochemistry

Bioelectrochemistry is continuously an active area of research as it has so much to offer. The area covers topics as diverse as biological sensors, enzyme catalysis of reactions, investigation of electron transfer mechanisms, protein interfacial interactions, investigation of redox potentials, macromolecular recognition, electrode investigation, energy generation, biocorrosion and biomolecular electronics to name but a few (Armstrong et al. 1988; Mertens & Liese 2004; Murphy 2006; Yang et al. 2007). Some of these areas are of purely academic interest, whilst others offer real world solutions and commercial opportunities. In particular, there is great interest in bioelectrochemistry for fuel cells, biosensors and medicine. Enzymes allow the quick and efficient catalysis of reactions, that otherwise can be difficult or greatly energy consuming, for instance the evolution of hydrogen. It is the harnessing of the potential of proteins, enzymes and bacteria

that makes bioelectrochemistry such a wide ranging and exciting area, that still has so much to offer.

1.1.1. Fuel Cells

After over a hundred years of the world's economy being driven by fossil fuels, it is fast becoming apparent how the pollution caused by fossil fuels is effecting the environment, and also how quickly the resources will run out. To keep up with the energy demand other clean and renewable energy sources need to be found, developed and used. Hydrogen fuel cells are one potential solution to this problem.

Fuel cells work using an electrochemical reaction which converts the chemical energy directly into electrical energy. There are different types of fuel cells, but the ones that are the focus of a great deal of research is hydrogen fuel cells. The hydrogen fuel cells work on the following reactions in equation 1.1.

Anode:	$2H_2 \rightarrow 4H^+ + 4e^-$
Cathode:	$O_2 + 4H^+ + 4e^- \rightarrow 2H_2O$
Overall:	$2H_2 + O_2 \rightarrow 2H_2O$

Equation 1.1- The reactions within a hydrogen fuel cell

The reaction of the hydrogen fuel cell takes place over precious metal catalysts (Karyakin et al. 2002; Karyakin et al. 2005), usually platinum or an alloy of platinum, palladium or ruthenium. The only products of the reaction are water and energy (electrical and heat), in other words it is a pollution free energy source.

However fuel cells are expensive, currently around $200-2000 per kW (Karyakin et al. 2005). This is down to the material needed for a fuel cell. Most fuel cells, particularly for small scale applications, use platinum (Pt) as the catalyst. Even with the advances made in reducing the quantity of Pt needed as a catalyst, a 50kW fuel cell needs 100g of Pt (Karyakin et al. 2005). This may not sound like much until you consider that currently the entire world's annual Pt production is

195 tons (Karyakin et al. 2005). More importantly, the world's total Pt resources are 50,000 tons (Karyakin et al. 2005).

Another problem is that platinum suffers from poisoning. Reformed hydrogen is the cheapest form of the fuel, but contains 1-2.5% CO (Karyakin et al. 2005). Just 0.1% CO in hydrogen is enough to irreversibly reduce the activity of Pt electrodes by 100 times in just 10 minutes (Karyakin et al. 2005). The use of biogas is also not possible as it contain hydrogen sulphide, which poisons the electrode at an even faster rate (Karyakin et al. 2005). Even using pure fuels, the upper end of most fuel cells life expectancy is 1,500 hours (Cahan et al. 2002).

As platinum is such a good catalyst for many reactions, the theoretical efficiency of a fuel cell is 90-95%, but as the platinum is active in both hydrogen oxidation and oxygen reduction the real efficiency is 40-60% (Karyakin et al. 2005).

So with the threat of Pt supplies never being enough to satisfy peoples ever growing power needs, how can hydrogen be the fuel of the future?

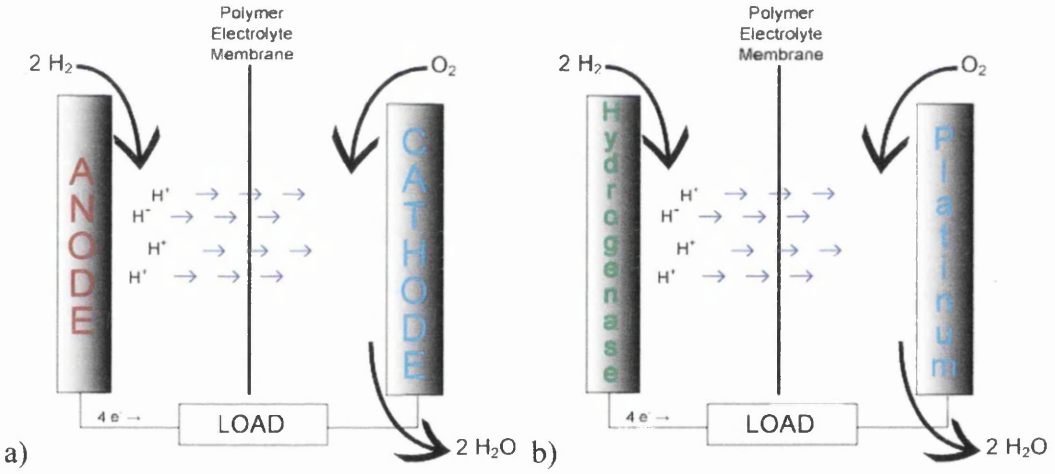

Figure 1.1- Comparison of a traditional fuel cell to a hydrogenase fuel cell. a) Shows a traditional fuel cell with an anode typically of platinum. b) Shows a current hydrogenase fuel cell, the platinum cathode can be replaced with another enzyme electrode such as laccase.

One possibility lies in biotechnology, in particular the enzymes known as Hydrogenases. Hydrogenase is a biocatalyst for both the evolution and reduction of hydrogen. When used with a suitable electrode, hydrogenase can be used as a replacement for noble metal catalysts in fuel cells. It has been shown by Jones et

al (Jones et al. 2002) that when hydrogenase is used as the catalyst it can have a turnover rate comparable to that of a Pt catalyst. Also, CO poisoning is not such a problem, whilst the Pt electrode would be irreversibly poisoned, hydrogenase is inhibited, but when the CO is removed, the enzyme will recover, in some cases making a 100% recovery (Karyakin et al. 2002). As hydrogenase is more selective about the reaction it catalyses, it is possible to use cheaper, less pure forms of hydrogen.

As hydrogenases can catalyse both from H_2 to $2H^+$ and the reverse reaction $2H^+$ to H_2, then as well as being used in fuel cells, hydrogenase can be used in the production of hydrogen by bioelectrolysis. This therefore can mean that if an advance is made in using hydrogenase for power production from hydrogen, it is quite probable that the same advance could improve the production of hydrogen.

1.1.2. Biosensors

Despite the quality of modern sensors, there is always a push for more information, faster, cheaper, more accurately and more easily. As a result, traditional analytical techniques are struggling to keep up with demand. Consequently, biosensors are moving to the forefront of technology offering fast results that are highly selective and sensitive (Ahmed et al. 2008), and potentially cheap enough to be single use and disposable (Murphy 2006). Biosensors are growing in use in many areas, but primarily the areas of interest are medicine, food production, environmental studies and agriculture (Ahmed et al. 2008; Murphy 2006).

There are three main types of biosensors; electrodes modified to react when they come in contact with the desired biological substance, electrodes which react with "tags" added to the biological matter and electrodes that use biological matter immobilised on the surface to detect an analyte (Ahmed et al. 2008; Murphy 2006). The former method relies on picking a suitable electrode, so when the analyte is present in solution it will react with the electrode. The second method is used for analytes that are not electrochemically reactive, thus the material is "tagged" or "labelled" with a suitable material that can be detected, e.g. gold nanoparticles have been used to tag DNA. The last type of sensor relies on

detecting the interaction of an immobilised protein, or other biological product, on the surface of the electrode with the analyte to produce an electrochemical reaction, e.g. glucose oxidase in the presence of glucose. This type of electrode can be highly sensitive and selective as most proteins and enzymes will only react with one analyte (Ahmed et al. 2008; Murphy 2006).

This final type of biosensor can be further grouped into one of three generations of sensor (Zhang & Li 2004). First generation biosensors used a natural mediator to shuttle the electrons between the electrode and protein, e.g. oxygen as a mediator for glucose oxidase (Zhang & Li 2004). However, the natural mediators have draw backs, high potentials are required which increases the chances of interference and if the concentration of the mediator changes the detection limits can vary (Zhang & Li 2004). As a result second generation biosensors used artificial mediators, e.g. dye molecules or conducting polymers, to overcome the issues (Zhang & Li 2004). These artificial mediators brought benefits such as reducing the decreasing the applied potential, and some mediators were small enough to diffuse in to the enzyme to react with the active site of the protein (Zhang & Li 2004). However, the mediators were not selective, resulting in other interfering reactions (Zhang & Li 2004). The third generation rely on direct electron transfer between the protein and the electrode. Since first being reported on in 1977 (Armstrong et al. 1988; Zhang & Li 2004), direct electron transfer has been of great interest as it removes the issues relating to mediators and also allows investigation of the mechanics and kinetics of the reactions (Leger & Bertrand 2008). However, not all proteins can be directly wired to the electrodes, limiting the current uses (Leger & Bertrand 2008).

To detect the material at the electrode, various electrochemical techniques are used including cyclic voltammetry and linear sweep voltammetry (which are both discussed later in this chapter), square wave voltammetry, normal and differential pulse voltammetry and electrochemical impedance (Allen 1966; Murphy 2006).

New biosensors are constantly being developed as new techniques are investigated, such as the use of nanoparticles to modify the electrode or protein to improve the electrochemical responses (Leger & Bertrand 2008; Padeste et al. 1998; Zhang & Li 2004). Direct electrochemistry advances allow new proteins to

be used and the linker molecules removed from other proteins already used, resulting in more sensitive electrodes. The use of direct electrochemistry also opens up the door to the use of other biological materials, as the protein absorbed on the surface can be used as a linker protein to materials that would otherwise not be reactive. Another technology is the use of different proteins on the same biosensor to improve performance, an example of this is the use of a disk electrode of glucose oxidase, surrounded by a ring electrode of bilirubin oxidase. The outer ring electrode is used to reduce any oxygen that may be present and hence increase the sensitivity of the glucose oxidase as a glucose sensor (Murphy 2006).

1.1.3. Medical applications

The medical area is just one of the areas biosensors are being used, but it is a large area that is of great interest. Biosensors are being used and investigated to improve the speed and accuracy of tests in many medical areas.

Biosensors are being used in the detection of genetic problems found in DNA. Certain genetic disorders are shown by certain sequences in DNA (Ahmed et al. 2008). By creating a biosensor to match this DNA sequence it is possible to quickly analyse samples for these genetic disorders. It has also been demonstrated that it is possible to detect DNA damage by measuring the oxidation peaks of DNA bases, avoiding the time consuming and expensive traditional assays that are normally carried out (Ahmed et al. 2008).

Immunosensors use much the same techniques as DNA sensing, allowing the detection of antibodies. The sensor is coated with an antigen, and the antibodies are tagged using an electrochemically active enzyme. When the antibody attaches to the antigen, the electrons can flow from the electrode to the enzyme and an electrochemical peak is seen (Murphy 2006; Padeste et al. 1998).

Biosensors are also being used in speeding up and simplifying the detection of hormones such as human chorionic gonadotropin, the indicator for pregnancy, peptides such as amyloid-β-peptides which are related to the on-set of Alzheimer's disease, and pathogens (Ahmed et al. 2008).

A large area of research in the medical field is that of *in vivo* sensors, which can allow real time monitoring of a patient. Currently the main use of *in vivo* biosensors is for the monitoring of glucose levels in diabetes patients to allow the correct dosage of insulin to be administered (Murphy 2006). Other studies include the monitoring of laccase and glucose in patients with brain injury and the monitoring of dopamine levels in rat brains to link with behaviour (Murphy 2006). Ultimately *in vivo* sensors may allow for automated systems, warning people of potential problems, or even automatically administering drugs to allow people with diseases to lead a normal life.

1.2. Proteins

The term 'protein' covers a very wide range of macromolecules, each very different from the next and requiring different conditions to survive and carry out their functions. This work will focus on one group of proteins, redox proteins.

1.2.1. Redox reactions

The redox reactions are some of the most fundamental to both chemistry and biology. A redox reaction is one in which the oxidation number of atoms change, i.e. they are reduced (gain electrons) or oxidised (lose electrons).

Redox proteins work as catalysts for redox reactions, either reducing or oxidising the substrate at a rate that makes it possible to sustain life (Bartlett 1990).

In general, redox proteins are very specific in which reaction they catalyse, usually only employing one substrate to produce one product (Ahmed et al. 2008; Leger & Bertrand 2008). By working in this way, the enzymes are very selective of the fuels that they use and hence the energy they produce. Thus redox enzymes are used to control redox reactions and make them useful. By utilising the redox enzymes, cells are able to produce energy and hence live (Adams & Stiefel 1998; Leger & Bertrand 2008; Yue & Waldeck 2005).

The redox-active site is deep inside of most redox enzymes. This keeps the centre isolated and allows the active site to maintain its own environment in spite of the

protein's surroundings. This imbalance is of benefit to the centre as it facilitates the selective electrical and chemical processes that it needs to maintain life.
In order to get the optimum results from redox proteins on an electrode it is essential to get a set up for fast electron transfer.

1.2.2. Hydrogenase

'Hydrogenase' is the term used to describe a class of enzymes that catalyse the conversions between H_2 and H^+ and vice-versa. Hydrogenases can be found in a great number of microorganisms, particularly in sulphate reducing bacteria (Guiral-Brugna et al. 2001). Each of these types of hydrogenase can have different properties, e.g. the temperature range they operate at, turnover rate, susceptibility to inactivation by oxygen.
The wide range of hydrogenases can be classed into three classes: metal-free hydrogenase, [Fe]-hydrogenase and [NiFe]-hydrogenase (Leger, Jones, Roseboom, et al. 2002). The classes are based upon the structure of the hydrogenase's centre, as described in the following sections. However, hydrogenases from the same class can have very varied properties.

1.2.2.1. Metal-free hydrogenase

These are the least common of the hydrogenases and are usually not covered in much detail in the papers found during this study, so will not be discussed here in any great detail.
Although called 'metal-free', it is not necessarily an appropriate term for this class of hydrogenase, as a recent study (Lyon et al. 2004) has shown that methylentetrahydromethanopterin dehydrogenase contains functional iron, although it is not catalytically active.

1.2.2.2. [Fe]-hydrogenase

The [Fe] or iron hydrogenase has a Fe-S centre that is highly reactive. [Fe]-hydrogenase has the highest turnover rate of the hydrogenases, according to Hallenbeck and Benemann (Hallenbeck & Benemann 2002) it can be as high as $6000s^{-1}$ for *Clostridium pasteurianum* and even $9000s^{-1}$ for *Desulfovibrio spp.*

The high reactivity of the enzyme has its downsides too, namely [Fe]-hydrogenase are far more susceptible to being oxidised than other classes of hydrogenase. Although oxidation is reversible by exposure to an H_2 environment, it is not desirable as it deactivates the enzyme.

1.2.2.3. [NiFe]-hydrogenase

The [NiFe]-hydrogenase consists of both small and large subunits. The small subunit contains three iron-sulphur clusters, two [4Fe-4S] and one [3Fe-4S]. The large subunit contains a complex nickel iron centre (Hallenbeck & Benemann 2002).

[NiFe]-hydrogenases are mainly "uptake" hydrogenases, i.e. their function is to derive reductant from H_2. However, they can be used in both directions and even being used in hydrogen evolution, the turnover rate is in the region of $98s^{-1}$ (Hallenbeck & Benemann 2002). In the uptake direction a rate of five or six times that rate could be expected (Hallenbeck & Benemann 2002).

A number of the papers covering the use of hydrogenase on an electrode use a [NiFe]-hydrogenase (de Lacey et al. 2005; Jones et al. 2003; Karyakin et al. 2002; Kovacs et al. 2006; Leger, Jones, Albracht, et al. 2002; Leger, Jones, Roseboom, et al. 2002; Morozov, Karyakina, Zadvornyi, et al. 2002; Morozov, Karyakina, Zorin, et al. 2002; Morozov, Vignais, et al. 2002; Pershad et al. 1999; Vincent, Parkin, et al. 2005; Vincent, Cracknell, et al. 2005). This is probably due to the fact that [NiFe]-hydrogenase is more resistant to environmental conditions than [Fe]-hydrogenase and also maintains a fairly high turnover rate. Plus for some [NiFe]-hydrogenases, if they are inactivated by CO, the effect can be completely reversed by placing in an H_2 atmosphere.

Guiral-Brugna et al (Guiral-Brugna et al. 2001) also state that in experiments showing the effects of pH, electrode polishing, presence of methyl viologen, strong electrolyte, presence of protein and the concentration of hydrogenase, [NiFe]-hydrogenase yields qualitatively similar results at lower catalytic currents.

1.2.2.4. States of hydrogenase

There are three states that hydrogenase enzymes may be in: active, inactive (ready) and inactive (unready). When the enzyme is active, it will catalyse the hydrogen reaction straight away. When in the ready state, the enzyme is inactive but a few minutes in a H_2 atmosphere will get it to the active state. When in the unready state, the enzyme requires incubation in a H_2 atmosphere for up to an hour before it reaches the active state.

1.2.3. Laccase

Laccases are multicopper oxidases that are found in many plants, fungi and micro-organisms (Shleev et al. 2005; Solomon et al. 1996). Within plants and fungi, laccase is known to be used in pigment formation, lignin degradation and detoxification (Solomon et al. 1996). Laccase is also known to catalyse the oxidation of ortho-diphenols and para-diphenols, aminophenols, polyphenols, aryl diamines and some inorganic ions (Shleev et al. 2005).

The key to the reactivity of laccase is the construction of its centre, which contains four copper ions in a cluster. The four ions are classified into three types, T1, T2 and T3. The centre is formed from a single T1 site, containing a single ion, with a trigroup of a T2, also single ion, and T3 containing two ions (Portaccio et al. 2006; Solomon et al. 1996; Xu et al. 1996). The T1 site is core to the electron transfer and capture, T2 activates the molecular oxygen and T3 the oxygen uptake.

Laccases are of interest as they can be used within biological fuel cells, as the catalyst on the cathode (Shleev et al. 2005), thus could be used with hydrogenase to create a fuel cell containing no precious metals. They are used in creating biosensors and have been shown to sense phenolic compounds (Portaccio et al. 2006). Laccases can also be used in bioelectroorganic synthesis (Shleev et al. 2005).

Laccases have been used in bioelectrochemistry and reported on as far back as 1977 (Hill 1996). Interestingly, laccases, like hydrogenases, have also been shown to work efficiently on pyrolytic graphite edge plane electrodes (PGE), absorbing

to sub-monolayer coverage. Despite the high turnover achieved on the PGE electrode, it has also been shown that modification of the electrode using anthracene-2-diazonium creates an electrode with twice the current density of laccase absorbed at the standard polished electrode (Blanford & Armstrong 2006). Gold has also been shown to be a suitable electrode for laccase. However, despite laccase showing a reaction in electrochemical tests, the product is hydrogen peroxide instead of water, implying that the natural electron pathway is not being used (Pita et al. 2006). Modifying the electrode, by soaking of thiol to form a self assembled monolayer, returned the laccase to producing water, showing that correct surface is of importance to allow the laccase to work in its natural way (Pita et al. 2006).

Some laccases are very dependant on a particular substrate for the reaction to take place. However most plant and fungi laccases are less specific and will work with a number of substrates (Solomon et al. 1996), including catechol (Portaccio et al. 2006) and syringaldazine (Harkin & Obst 1973).

Laccase from the plant *Rhus vernicifera* is the most studied of all the laccases (Solomon et al. 1996), and the one studied here.

1.2.4. Azurin

Like laccase, azurin is also a copper protein. However, azurin is small (Pascher et al. 1992) and only contains a single copper ion at its core (Solomon et al. 1996). The single core is of type T1 as described before. As the enzyme is small, the centre lays only 7Å from the solvent accessible surface (Hirst & Armstrong 1998) allowing for fast electron transfer (Jeuken, McEvoy, et al. 2002). Azurin is believed to be used in intermolecular electron transfer (Solomon et al. 1996), although its exact function is still being debated (Jeuken, McEvoy, et al. 2002).

Azurin, like laccase, will absorb easily at a PGE electrode, only needing to be smeared across a bare electrode (Jeuken & Armstrong 2001; Jeuken, McEvoy, et al. 2002), thus allowing for direct electrochemistry of the protein film (Hirst & Armstrong 1998) and fast electron transfer (Jeuken & Armstrong 2001). Azurin has also been shown to absorb onto gold electrodes, although this requires a long period of soaking (Chi et al. 1999).

The bioelectrochemistry of azurin from *Pseudomonas aeruginosa* appears to be widely reported on (Andolfi et al. 2006; Chi et al. 1999; Hirst & Armstrong 1998; Jeuken & Armstrong 2001; Jeuken, McEvoy, et al. 2002; Pascher et al. 1992), and it is the enzyme used in this study. The redox potential is reported to be in the range 300 to 350 mV, however this can vary depending upon pH (Pascher et al. 1992), the scan rate in cyclic voltammetry and even the potential at which the electrode is poised before the experiment takes place (Jeuken & Armstrong 2001), so care must be taken to get reproducible results.

1.2.5. Cytochrome c

Cytochrome c can be found in plants, animals and unicellular organisms; in fact it is essential in most forms of life. The functions of cytochrome c include electron transfer and enzyme catalysis and it is used in the fundamental processes of respiration, photosynthesis and in the induction of apoptosis (Yang et al. 2005; Yue et al. 2006).

Unlike laccase and azurin but similar to hydrogenase, cytochrome c has a Fe based heme centre with a structure well documented in literature (Armstrong et al. 1988).

Electrochemical response of cytochrome c has been thoroughly investigated over a number of years and was in fact the first protein found to show a quasi-reversible redox response at a modified gold electrode (Armstrong et al. 1988). Various electrodes have been used in the electrochemistry of cytochrome c, but bare metal electrodes of Au, Pt, Ni and Ag have shown poor responses (Armstrong, Bond, Hill, Psalti, et al. 1989). This is down to the rate of electron transfer being dependant on the nature of the electrode the protein is attached to (Armstrong, Bond, Hill, Oliver, et al. 1989) and the orientation at the electrode (Bartlett 1990). At bare gold electrodes cytochrome c is known to denature, hence modification of the electrode with linker molecules gives better responses as the protein is attached to the electrode, but not denatured (Yue & Waldeck 2005). The centre of cytochrome c is known not to be central in the protein; hence the orientation when attaching to the electrode is essential. In the perfect orientation the centre is thought to be within 0.5nm of the electrode, however in the worst

case this becomes 2.8nm, reducing or even stopping electron transfer (Bartlett 1990).

By contrast to the metallic electrodes, cytochrome c has been shown to attach to graphite electrodes, without modification, and deliver good electrochemical responses and fast electron transfer (Armstrong, Bond, Hill, Psalti, et al. 1989).

1.3. Electrodes

Electrodes and their characteristics can be essential in getting the best electrocatalytic reaction from a redox protein. For instance, most redox protein reactions are very fast at bare metal electrodes, but Cytochrome c is extremely slow (Armstrong, Bond, Hill, Psalti, et al. 1989). This is caused by the denaturing and absorption of the protein at the electrode surface.

Not only the material the electrode is made from, but also the surface can have an effect on the reaction. In a study of hydrogenase, it was shown that polishing a pyrolytic graphite electrode with emery paper produced much better results than polishing with alumina slurry (Guiral-Brugna et al. 2001). So both the electrode material and any surface modification should be considered in the selection of an electrode.

Metal electrodes are used most commonly, with gold being very popular, however with many proteins modification of the surface is needed and linker molecules are used. With the increase of direct electrochemistry, i.e. without linker molecules, carbon based electrodes are being more widely used as they allow direct absorption for a wide range of proteins (Armstrong 2002) and do not require the use of precious metals.

1.3.1. Pyrolytic graphite electrodes

Pyrolytic graphite (PG) is formed by the decomposition of hydrocarbon gas at 3300K in a vacuum, when the carbon reforms, it does so in a structure where in one direction the atoms are hexagonally arranged in a planar structure (PGB, the basal plane or ab layer) and in the other the atoms are randomly oriented (PGE, edge plane or c direction). There is also a more oriented version of PG called

highly oriented pyrolytic graphite (HOPG); it is formed by heating pyrolytic graphite to over 3000K and submitting it to high pressure. This can result in graphite with orientation within 0.4° and with crystals of up to an infinite size, although in practice they tend to be 1-10 μm.

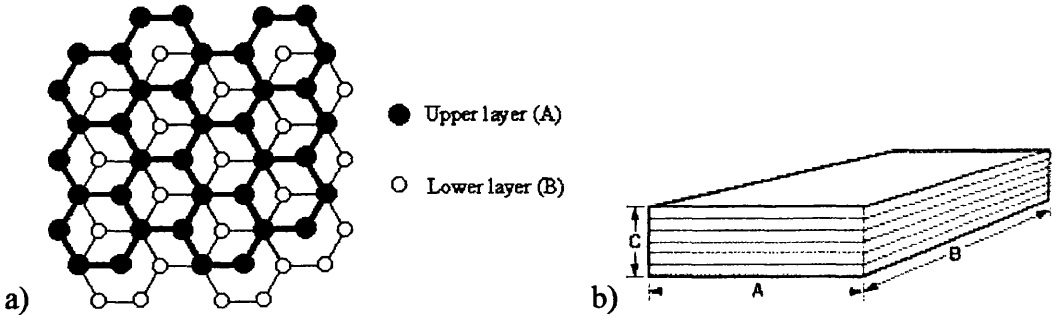

Figure 1.2- The structure of pyrolytic graphite. a) Shows the layout of two planes of pyrolytic graphite, b) An illustration of how the multiple ab layers are built up in the c dimension

Both pyrolytic graphite and HOPG have very different properties depending upon the orientation of the planes. In the ab direction the graphite is very conductive of electricity and heat, however in the c direction, the graphite is very resistive.

In redox reactions, the basal plane has been shown to be considerably slower than the edge plane (Armstrong, Bond, Hill, Psalti, et al. 1989; Guiral-Brugna et al. 2001). It has been proposed that this is due to the basal plane crystals being inert or nearly inert and if the surface was homogeneous, the plane would be completely inactive (Armstrong, Bond, Hill, Psalti, et al. 1989). A real basal plane is not homogeneous, as such the edges of the crystals and the surface defects expose the edge plane and it as these points that the reaction happens. As the surface defects can be as low as 0.2% for HOPG (Banks et al. 2005), this would explain why there is the large difference in reactivity. This theory is also supported by the fact that the capacitance of the basal plane decreases as the number of defects increases due to the increased current leakage (Kim et al. 2003). Also at the exposed edge sites on the basal plane friction is increased by approximately 100% and the attractive force by approximately 20% and this increase in force stays even after fresh cleavage in a vacuum and under liquid (Mechler et al. 1998). This being the case, the basal plane offers interesting

possibilities to study the effect of surface modification as reactive edge plane could be seen next to unreactive basal plane.

The edge plane, as indicated above, is in comparison very reactive (Armstrong, Bond, Hill, Psalti, et al. 1989). It offers a larger surface area and lower electrical resistance. Plus, the edge plane has a lower capacitance (Kim et al. 2003), which would imply more current flows from the edges. The edge plane also exhibits stronger friction and attractive forces (Mechler et al. 1998), which implies that the surface is more reactive, due to a stronger interaction between the scanning force microscopy probe and the surface.

So the edge plane appears to be the more reactive plane, but the basal plane could offer interesting results of active areas with the surrounding area being unreactive. With these differences in mind, the mass transport diffusion patterns are very different between the two electrodes. The basal plane has isolated reactive sites surrounded by large unreactive areas, the patterns of the diffusion from these sites maybe thought of radial away from the site (Armstrong, Bond, Hill, Psalti, et al. 1989). The edge plane is in effect lots of these reactive sites close together, thus they all over lap to such an extent that the diffusion pattern can be taken as linear. This difference will be important when working on a micro- or nano- scale (Armstrong, Bond, Hill, Oliver, et al. 1989; Banks et al. 2005).

Preparing the electrode varies depending upon which plane is being used. The basal plane is prepared by cleaving, this is done either with a clean razor blade, or more commonly with HOPG by using scotch tape to remove the top layer. Edge plane electrodes are prepared by polishing with alumina or diamond slurry down to 0.3-0.25 μm, followed by thorough sonication in water.

1.3.2. Carbon filament material

Carbon filament material (CFM) is a carbonised viscose cloth with pyrocarbon (from thermolyzing benzene). CFM has been designed for fuel electrodes (Karyakin et al. 2005). Very little else was found in literature about this material.

1.3.3. Carbon Nanotubes

Carbon nanotubes (CNTs), as the name suggests, are well ordered hollow all-carbon nanomaterials of high aspect ration (Yang et al. 2007). There are two categories of CNTs, single-walled carbon nanotubes (SWCNTs) and multi-walled carbon nanotubes (MWCNTs) (Mechler et al. 1998; Yang et al. 2007). The former can be thought of as a rolled sheet of graphine with a typical diameter of 0.4 nm to 3 nm (Gong et al. 2005; Yang et al. 2007), the latter is formed of co-axial multilayer graphine tubes with diameters of 1.4 nm to 100nm (Gong et al. 2005; Yang et al. 2007). As a result of this construction, and as DNA has been shown to attach only to the ends and defects of CNTs (Yang et al. 2007), it is believed that the ends and defects behave much like pyrolytic graphite edge plane, whilst the walls like basal plane (Gong et al. 2005).

CNTs have aroused interest in a number of research and industrial fields due to their properties which include high surface area, high mechanical strength, light weight, chemical and thermal stability and electrical conductivity (Gong et al. 2005; Yang et al. 2007).

Within the biological fields, there has been a great deal of interest in CNTs in a number of areas including electrocatalysis, direct electron transfer to proteins, sensors and biosensors (Gong et al. 2005; Yang et al. 2007). However, until recently, there has been issues with the insolubility of CNTs within aqueous and organic solutions, causing them to aggregate together due to van de Waals forces between the tubes (Gong et al. 2005; Yang et al. 2007). This issue has now been overcome, whilst maintaining electrocatalytic properties, through the modification by Nafion coating (Gong et al. 2005; Yang et al. 2007).

CNTs bring great benefits to bioelectrochemistry, firstly their structure provides a large surface area and the possibility of bonding either outside or within the tube (Gong et al. 2005; Yang et al. 2007). Also the high aspect ratio gives the possibility of electron transfer directly into the centre of large proteins (Yang et al. 2007). The unique structure of SWCNTs, being only on atom thick, offers the possibilities of improving the sensitivity of sensors, as any absorption on the CNT changes the properties of the whole tube (Yang et al. 2007). However CNTs do

have drawbacks, firstly they lack specificity (Yang et al. 2007), secondly they can denature absorbed biomolecules (Gong et al. 2005; Yang et al. 2007), thirdly electron transfer can be slow on pristine CNTs (Yang et al. 2007) and finally they are potentially toxic to the environment and to health (Yang et al. 2007).

Electrodes have been made from CNTs by either randomly dispersing them on an electrode substrate or by confining them with a polymer or paste (Gong et al. 2005). Reported ways of binding the CNTs have included the use of Nafion, polypyrole, polyaniline, silicate sol-gel or by mixing the CNTs with mineral oil to form a paste and packing into a cavity (Gong et al. 2005). When attaching to an electrode, layer by layer films may be built up on the substrate, such as glassy carbon (Gong et al. 2005), by using alternate layers of poly(diallydimehtylammonium chloride) (PDDA) and CNTs, this techinique allows the CNTs to maintain their electrochemical properties.

1.3.4. Metallic electrodes

Various metallic electrodes have been used in the studies of redox proteins, such as platinum, silver, nickel and probably most widely gold (Armstrong, Bond, Hill, Psalti, et al. 1989). However, it can be noted from the list that these are usually precious metals, not ideal for trying to produce a competitive commercial product. Gold is often used due to its high stability (Pita et al. 2006), however, as mentioned above in the case of cytochrome c, often gold electrodes need modification to allow the proteins to perform at optimum rates, or at all (Armstrong, Bond, Hill, Psalti, et al. 1989; Hill 1996). Thus gold electrodes are often modified by thiols (Pita et al. 2006), 4,4'-bipyridyl or 4,4'-bipyridyl disulphide or peptides (Hill 1996).

As a result of needing these linker molecules, it is not possible to get the same direct electrochemistry as it is with carbon based electrodes, as the electrons must flow through the linker molecule and the protein being studied. Hence it is more difficult to determine the thermodynamic and kinetic properties of the protein being studied (Armstrong et al. 1988).

In this study, metallic electrodes were avoided on the whole in favour of the direct electrochemistry on carbon based electrodes using protein film voltammetry.

1.3.5. Protein film voltammetry

In protein film voltammetry (PFV), a redox enzyme is adsorbed onto an electrode, typically to sub-monolayer coverage. Now, as the enzyme and electrode are in contact, electron transfer can occur between the electrode and the enzyme's buried active site, usually via a chain of redox groups. This allows the potential for fast electron transfer and more importantly, the current is directly proportional to the turn over rate of the enzyme allowing investigation of the proteins kinetics and energetics (Leger & Bertrand 2008).

The characteristics of the surface that the enzyme is absorbed onto can play a large part in the efficiency of PFV as it is likely that any one technique is not suitable for all proteins (Leger & Bertrand 2008). As mentioned earlier, the electrode could cause denaturing of the enzyme resulting in low turnover rates. Likewise, the way that the enzyme is absorbed onto the surface can result in either a good or poor route from the electron transfer, once again affecting the turnover rate.

So for good results from PFV it is essential to have not only the best material for the electrode, but also for the surface to have a suitable morphology and suitable chemical properties. To further complicate matters, for each type of enzyme, these sets of parameters may change, e.g. the case of Cytochrome c at bare metal electrodes compared to other redox proteins (Armstrong, Bond, Hill, Psalti, et al. 1989).

Protein films can be produced in different ways. The simplest way is to use a carbon or gold electrode, onto which the enzyme is absorbed, either through "painting" the electrode with a protein solution or cycling the electrode in the solution (Leger & Bertrand 2008). This way creates electrodes with the enzyme in direct contact with the electrode; hence the enzymes are locked closely to the electrode potential. It also allows for fast electron transfer rates.

If metal electrodes are used, the proteins are usually attached using protein linker molecules or surfactants. These are usually allowed to build their own layer on the electrode by soaking or a similar method, hence usually they are known as self assembled monolayers (SAMs). To date, the best electrode-protein interface with

a known structure has been achieved by using a gold mirror electrode with SAMs using cytochrome c (Armstrong et al. 1997). Investigations into different SAMs have shown that shorter SAMs allow faster electron transfer, but a lower fraction of the enzymes are electrically active, indicating that a greater number of the proteins are incorrectly oriented (Armstrong et al. 1997).

Surfactants can be used to produce a more favourable environment for the proteins on the electrode. Surfactants have a hydrophobic part and a hydrophilic part. The surfactant is typically laid down on the electrode as a monolayer (one molecule thick). The protein can then be absorbed onto the surfactant, or more layers built up. For electrochemical purposes, the thinner the layer of surfactant the better, as more layers slow the electron transfer.

1.3.5.1. LB Films

A Langmuir-Blodgett (LB) film is type of surfactant film, built up using the LB method. This involves creating a monolayer of the surfactant on surface the of a liquid (typically water) and then dipping the electrode into the liquid and removing it whilst keeping the surface pressure constant (KSV Instruments Ltd n.d.). The surfactant will then ideally transfer to the electrode surface one layer at a time.

1.3.5.2. Polylysine

Polylysine is a positively charged polymer widely used for adhering living cells and proteins to synthetic substrates. Because of these properties it is among the materials used to create SAMs on electrodes (Xiao et al. 1999). The result is to produce very stable electrodes with the proteins strongly bonded.

1.3.6. Electrode modification

The modification of an electrode can be key to getting the best out of it by creating a favourable environment for a protein on the surface.

So far, only a little modification of CFM has been found in literature, and the techniques are only designed for improved characteristics with hydrogenase. The first is electropolymerization of pyrrole, this is done by controlled oxidation of 2mM pyrrole at 0.95 V in CH_3CN containing 0.1M TBAP (Tetrabutylammonium

perchlorate) (Karyakin et al. 2005; Morozov, Vignais, et al. 2002). The other technique is to hydrophilise the electrode, this has been achieved by either bathing in concentrated sulphuric acid, a mixture of concentrated sulphuric acid and concentrated hydrogen peroxide or boiling in a saturated potassium hydroxide solution and then washed with phosphate buffer solution (0.05M KH_2PO_4, 0.1M KCl, pH 7.0) for 48 hours (Karyakin et al. 2002; Morozov, Karyakina, Zadvornyi, et al. 2002). This can also be achieved by an electrochemical method, using the above phosphate buffer solution as an electrolyte and taking the electrode through anodic and cathodic current of 1-20 mA cm^{-2} in air and cycling the electrode from -0.8-1.3 V in an argon atmosphere (Morozov, Karyakina, Zadvornyi, et al. 2002).

Modification of PG electrodes can be done in many ways, the simplest is polishing. By polishing the electrode, either basal or edge, to different grades will give an electrode with different properties. For instance if the electrode is polished with emery paper, the surface is rougher, hence has a higher surface area, and is more hydrophobic than when polished with alumina slurry. The emery paper polished electrode then exhibits a better shaped sigmoidal response than the alumina polished one (Guiral-Brugna et al. 2001).

It is possible to form edge sites on the basal plane by oxidation. This produces pits with a basal plane bottom and edge sites around the edge (Mechler et al. 1998). The modification is carried out by heating the sample to 500-750°C in air and leaving for a period of time (Chu & Kinoshita 1997; Mechler et al. 1998). Typically, heating at 650°C for 30 minutes gives etch pits one monolayer deep and approximately 100-200nm in diameter(Chu & Kinoshita 1997). The pits that are formed have edge planes exposed at the sides and the bottom is basal plane. The pits show improved absorbency compared to the surrounding basal plane, indicating that the edge plane has a higher absorbency. Pits can also be produced by using a Nd:YAG laser, this can produce pits of > 2.5 μm diameter with exposed edge sites. However using a laser damages the surrounding lattice due to the heat of the laser (Chu & Kinoshita 1997).

Patterns can also be etched into the surface using AFM, as yet this technique has not been found in papers, but is worthy of further investigation.

Modification of gold electrodes was covered above in the metallic electrodes section, but usually involves either the modification by adding of surface linker molecules or by polishing with alumina slurry (Pita et al. 2006).

As discussed in section 1.3.3, carbon nanotubes are naturally hydrophobic, hence modification make CNTs water soluble. However, this hydrophobicity this can provide a good environment for absorption of complementary biomolecules such as proteins or DNA (Yang et al. 2007). A number of techniques have been reported for the modification of CNTs, the most common being covalent functionalization of carboxylic acid residues through the use of strong acids, thus allowing direct interactions with some biolmolecules, or with a biofunctional spacer to provide a link to the biological molecule (Yang et al. 2007). In addition, azide photochemistry has been used to functionalize the sidewalls and tips of CNTs (Yang et al. 2007).

1.3.7. Electrode materials and technology – a summary

In this study the plan was to avoid the use of platinum and other precious materials and focus on using more common materials. Gold was also contemplated, despite being a precious metal, but as it is not always suitable for use in direct electrochemistry, it was ruled out.

Whilst an interesting area of study, carbon nanotubes would not allow the investigation of electrode topology that solid carbon based electrodes would, hence were also ruled out for this study, but could offer a new route of investigation on enhancing the electrodes in a future study.

Out of the two sets of carbon electrodes, each appears to be preferred by different groups. The PGE electrode is used by Armstrong, et al. (Armstrong, Bond, Hill, Oliver, et al. 1989; Armstrong, Bond, Hill, Psalti, et al. 1989; Armstrong et al. 1988; Jeuken, Jones, et al. 2002; Jones et al. 2003; Leger, Jones, Albracht, et al. 2002; Leger, Jones, Roseboom, et al. 2002; Pershad et al. 1999), Guiral-Brugna et al. (Guiral-Brugna et al. 2001), and called "state of the art" by Mertens and Liese (Mertens & Liese 2004). The CFM electrodes are used by Morozov et al. (Karyakin et al. 2002; Karyakin et al. 2005; Morozov, Karyakina, Zadvornyi, et

al. 2002; Morozov, Karyakina, Zorin, et al. 2002; Morozov, Vignais, et al. 2002). Although the two types of electrode have not been found in direct comparison yet, both are reported in hydrogenase fuel cells to be comparable to a Pt electrode in a hydrogen fuel cell (Jones et al. 2002; Karyakin et al. 2002). This implies that the two are comparable in performance; however the effects of surface modification and examining enzymes on the surface would be easier to study with PG as the surface could be polished flat first, allowing investigation of the surface with an AFM or other microscopes.

1.4. Electrochemistry

Electrochemistry is a branch of chemistry where the chemical reactions either produce electricity, such as in batteries or fuel cells, or electricity is put in for the reaction to take place, as in electrolysis or the use of biosensors. The work in this study covers the latter of the two types of experiment using a potentiostat to drive the reaction in a standard electrochemical cell. As the study is into the reactions of redox proteins, it was chosen to use cyclic voltammetry as both reduction and oxidation peaks are seen.

1.4.1. Potentiostat

In its simplest form a potentiostat is an amplifier that keeps the potential between two electrodes, the working and the reference, to a constant value.

To understand a little more about the development of the potentiostat, it is necessary to look back to the 17th century. Sir Humphrey Davy found that if you dip an iron wire (or iron electrode) in diluted sulphuric acid (electrolyte) it instantly starts to corrode (Doelling 2000). By inserting a second electrode that would not corrode, e.g. platinum wire, and connecting the iron wire to the negative pole of a current source, such as in figure 1.3, the platinum to the positive and then increasing the voltage the corrosion will slow or even stop. If you connect the electrodes the other way around then the rate of corrosion will increase (Doelling 2000).

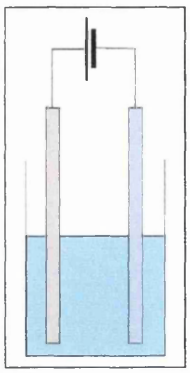

Figure 1.3- A diagram of a basic electrochemical cell

To further understand this phenomenon, it was attempted to find the current-voltage (IV) curve of the reaction. However, if the current is controlled and the potential measured, the results vary depending upon whether the potential is increasing or decreasing (Doelling 2000).

Attempting to try the other way, controlling the potential and measuring the current, oscillations of several hundred millivolts would occur in the range between the active dissolution and passivity regions (Doelling 2000). This was due to use of manually adjusted voltage sources, when the current dropped from 100mA in the active region to 1μA in the passive, the low resistance of the power supply would cause a potential shift of 100mV back to the active state.

It was not until the 1950s, with knowledge of D.C. amplifiers that the problem of the stability was solved through the use of a difference amplifier (Doelling 2000).

1.4.1.1. Theory of potentiostats

The electrochemical cell contains three electrodes, the working electrode, the counter or auxiliary electrode and the reference electrode (Doelling 2000; Gosser 1993), see figure 1.4. The working electrode is held at earth, the counter electrode supplies the potential difference in the cell. The reference electrode, usually silver-silver chloride or calomel, creates a 'half-cell' with a salt bridge.

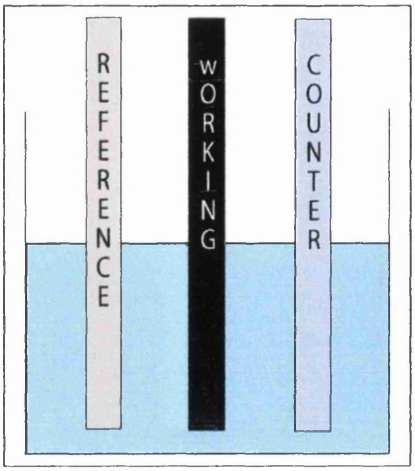

Figure 1.4- A diagram of a typical electrochemical cell containing, from the left, a reference electrode (a half cell), a working electrode and counter electrode

The potentiostat works by keeping the potential between the stable reference electrode and the working electrode as close as possible to zero (Doelling 2000). This is done by taking the difference signal between the two electrodes, amplifying it and inverting. The two electrodes are connected to the two inputs of a difference amplifier. The signal from the difference amplifier is then fed to the counter electrode and this creates a potential across the cell between the working electrode (held at ground) and charged counter electrode (figure 1.5). This gradient is such that any potential difference between the working electrode and reference electrode is cancelled out (Doelling 2000).

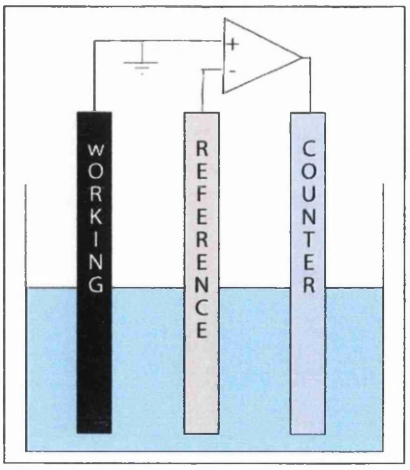

Figure 1.5- A basic potentiostat for equalising the potential at the reference and working electrodes

Now that the potential between the working and reference electrode can be kept close to zero, a potential difference can be created in the cell by driving the working electrode to a different potential compared to the reference electrode. This is achieved by adding the desired potential between the working electrode and the working electrode input to the difference amplifier (Doelling 2000).

Likewise, it is now desirable to measure the current flowing through the cell. This can be achieved by putting a small, known value, resistance between the output of the amplifier and the counter electrode. By measuring the potential across the resistor, the current can be derived from Ohm's Law (figure 1.6) (Doelling 2000).

The potential of the working electrode is now variable and allows experiments investigating a potential offset compared to the reference electrode and the resultant currents.

More detail of potentiostat design is discussed in appendix III.

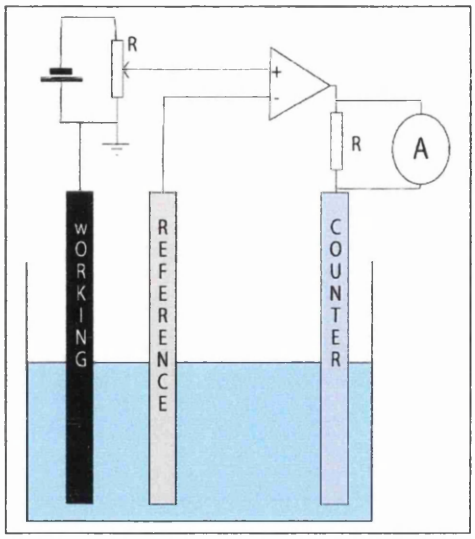

Figure 1.6- A basic potentiostat with potential control

1.4.2. Cyclic Voltammetry

Cyclic voltammetry (CV) is a potential-controlled reversal electrochemical experiment, i.e. the potential is swept up and back across a range of potentials at a set scan rate. By analysis of the current that flows at the different potentials, it is possible to determine some details about the kinetics and thermodynamics of the electron transfer at the electrode (Gosser 1993).

The sample being studied is set up in a three electrode cell. The working electrode is made of, or coated in, the sample being tested. The counter electrode completes the circuit with the working electrode, and the reference electrode gives the reference potential that all measurements are taken against (Gosser 1993). In most cases in this study, the working electrode will be a form of graphite with or without a protein film, the counter electrode will be a platinum wire electrode and the reference electrode, a calomel (essentially a second half cell with a salt bridge and an electrode). The whole cell must usually be made anaerobic by either vacuum or by purging with a suitable gas, e.g. N_2.

A potential can then applied to the working electrode, if a zero start point is not desired, and can then be held for a set period of time for the system to stabilise.

The potential is then cycled between the maximum and minimum set potentials at a rate set by the scan rate, this creates a triangle shaped waveform of potential as

seen in figure 1.7. Other scan types can be used, e.g. a faster scan rate on the reverse sweep, or just a sweep in one direction (this is linear sweep voltammetry). Typically in the cases that will be investigated, the maximum potential is likely to be of the order of a few hundred mV and the minimum of minus a few hundred mV with a scan rate from tens to hundreds of mV s^{-1} (Armstrong, Bond, Hill, Psalti, et al. 1989).

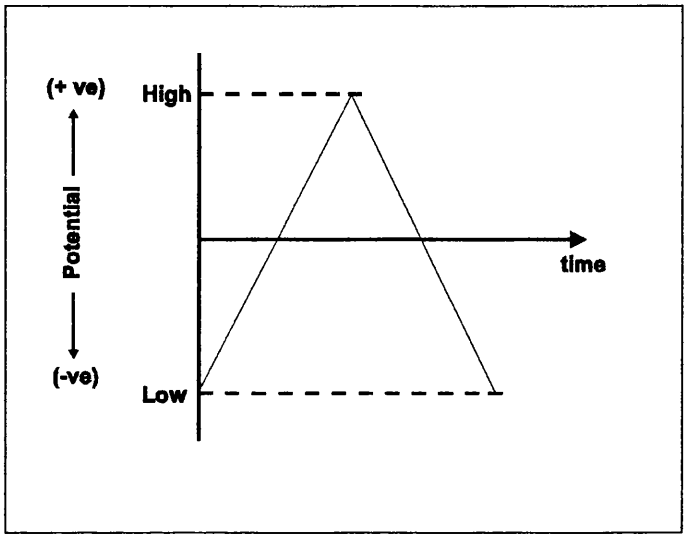

Figure 1.7- Example of a cyclic voltammetry potential scan

The results from the scan are then plotted as current versus potential. Figure 1.8 shows an example output plot from a scan, the most obvious points of this scan are the peaks at points A and B. Peak A occurs during the forward sweep, where the potential is increasing. On approaching this peak, the reduced reactant (R) starts to be oxidised (O) at the working electrode and diffuses away from the electrode down the diffusion gradient, R also diffuses towards to electrode down its own diffusion gradient. At peak A, the potential is such that any R that reaches the electrode will be instantly oxidised, so the reaction rate is then limited by the rate of mass transport of R to the electrode. Likewise, on the reverse scan, peak B is reduction peak, as this point is approached the oxidised substance that can reach the electrode is reduced.

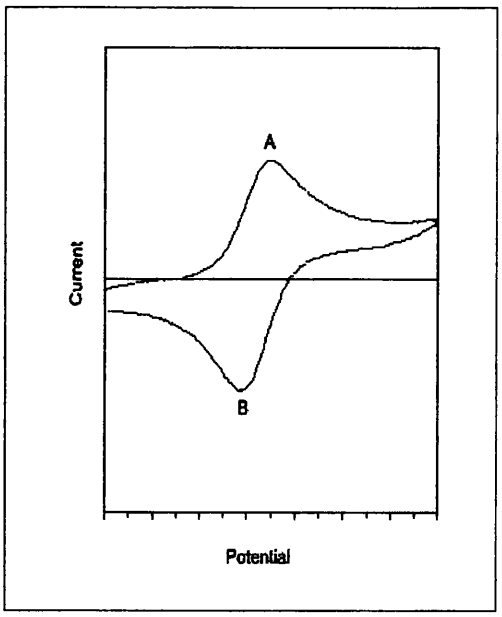

Figure 1.8- Example cyclic voltammogram

In cyclic voltammetry there two types of reaction that take place. The first is an electrical reaction (E) and the second is a chemical reaction (C). The simplest reaction is a reversible E reaction (E_r) (Gosser 1993).

In an E_r reaction, as there is no chemical reaction, the O that is produced in the forward sweep can be reduced back to R on the reverse sweep (Gosser 1993). As a result, the cyclic voltammograms show almost symmetry between the forward and backwards sweeps. With repeated cycles, the current will show similar results on each repetition with a slight reduction in current as not all O is reduced back to R. The requirements for it to be an E_r reaction are:

- The difference in cathodic and anodic peak potentials is around the 57-60 mV range. (Although in practice this can often be more like 60-70 mV) (Gosser 1993).
- The difference between the initial sweep peak and half-peak (where the current is half of the peak current) potentials is 56 mV/*n*, where *n* is the number of electrons (Gosser 1993).
- The shifted ratio of the cathodic peak current to the anodic peak current is unity. In shifted ratio the peak current is measured from the point that the current would have followed if there was no peak, to the top of the peak (Gosser 1993).

- The forward scan peak current should be proportional to the square root of the scan rate (Gosser 1993).

An EC mechanism is one where after oxidation or reduction the product chemically reacts to become a new product (Gosser 1993). As such the reverse peak will be diminished compared to the forward peak, or non-existent. The ratio of the cathodic peak to the anodic peak will depend on a function of the chemical rate constant and the scan rate. As the chemical rate increases in comparison to the scan rate, the forward peak will increase in height and shift to a different potential, whilst the reverse peak will become smaller and shift potential (Gosser 1993).

There are various cases of the EC mechanism, dependant upon the electrode kinetics in comparison to the chemical kinetics:

- If the electrode and chemical kinetics are both slow. In this case the forward peak shifts -59 mV per tenfold change in scan rate. This is an irreversible reaction (Gosser 1993).
- If the electrode kinetics are fast and the chemical kinetics are slow. In this case the scan appears the same as the E_r reaction. This is a reversible reaction (Gosser 1993).
- If both the electrode and chemical kinetics are fast, then the peak potential shifts by -30 mV for every tenfold change in scan rate (Gosser 1993).
- If the chemical kinetics are fast and the electrode kinetics slow, this creates an irreversible reaction with no backwards peak (Gosser 1993).

In an ECE mechanism, the product of the first electrical reaction then chemically reacts before the reverse sweep (Gosser 1993). During the reverse sweep, both the product of the chemical reaction and, if any remains, the first electrical reaction are then reduced or oxidised. This type of reaction results in a voltammogram with a reduced reverse peak and a second peak on the reverse sweep, see figure 1.9. If the chemical kinetics are much faster than the electrode kinetics, then on the reverse sweep only peak of the product from the chemical reaction will appear.

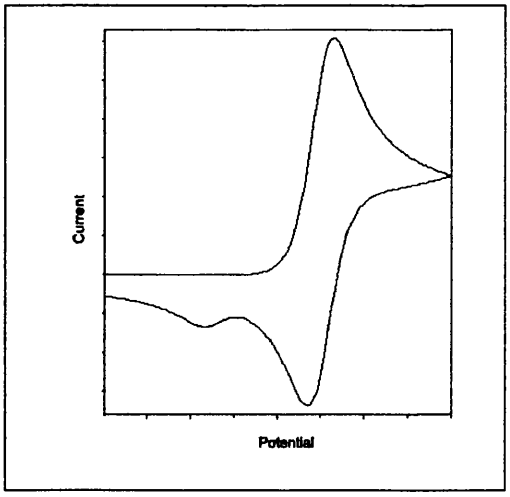

Figure 1.9- An example of an ECE voltammogram

1.5. Atomic Force Microscopy

The AFM has proved itself a very useful tool in nano-biology, as well as many other areas including surface science, material engineering, data storage, aerospace, and the list goes on (Wright & Revenko 2004). This is due to its flexibility and the wide range of techniques that it can be used for.

The AFM is a scanning probe microscope that works by moving a sharp probe over the surface. This probe, or tip, typically has an end radius of 10-50 nm and is mounted on the end of cantilever which bends as a result of forces between it and the surface. The deflection of the cantilever is measured by reflecting a laser off the back of the cantilever and onto a photodiode array composed of either two or four photodiodes, called a position sensitive photodiode (PSPD) (Mechler et al. 1998). The two photodiode array, measures purely the vertical deflection of the cantilever, the four photodiode array measures the horizontal frictional forces as well. The force is calculated by using the difference signal between the photodiodes, measuring the deflection of the laser and hence the deflection of the cantilever. As the cantilever obeys Hooke's law, it is then possible to calculate the force between the tip and the surface. The tip is then moved over the surface in a raster scan by using a sensitive positioning device made from piezo-electric ceramics.

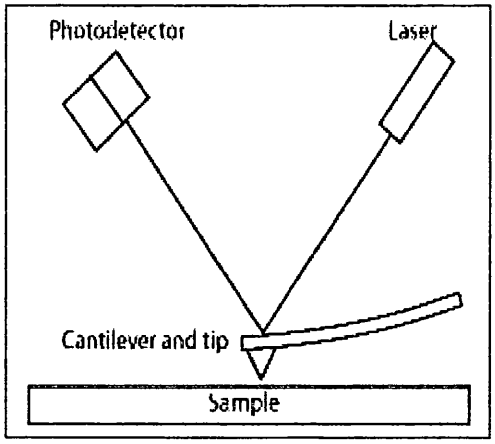

Figure 1.10- Typical AFM setup with laser and photodetector

An AFM has three main scanning modes; contact, non-contact and tapping. Contact mode, as the name suggests, is where the tip is in contact with the surface and dragged across it, many people think of this mode as resembling a stylus on a record. The tip is not actually in "contact" as such, but is being repulsed from the surface. This mode allows scans to be done under liquid and various other techniques like C-AFM (see section 1.5.3) to be employed. In contact mode, large lateral forces are created making it unsuitable for softer samples (Hansma et al. 1994; Wright & Revenko 2004), but can be used for building an image of the surface friction (Lateral Force Microscopy LFM). In tapping mode, the cantilever is oscillated at its resonant frequency in air, gas or liquid, and allows positioning above the sample such that the tip only touches the same for a small fraction of the oscillation. As the tip only touches the surface for a short time, the lateral forces in tapping mode are very small making it suitable for softer or poorly immobilised samples (Hansma et al. 1994). Other methods can be used for gaining images when using tapping mode, for example phase, where the phase difference of the driving piezos between oscillations is used to create the image. Another technique used with tapping mode is constant force mode, where the oscillations are kept almost constant via a feedback system. The image is then derived from the variations in oscillation that occur before the feedback system regulates a change. Non-contact mode is not widely used due to the difficulty of operation. The probe is oscillated as with tapping mode, but far enough above the surface that it does not enter the repulsion force zone. This can be very hard to

maintain in ambient conditions as surface water may form a capillary bridge to the tip and cause a "jump to contact". Then the AFM will in effect be working in tapping mode.

1.5.1. AFM in biology

AFM has become a very powerful tool in physical biology due to its ability to image in ambient, vacuum and liquid environments, thus being able to create an environment native to the sample and without special pre-treatment that may cause damage to the sample (Bowen et al. 1997), e.g. drying the sample for Scanning Electron Microscopy (SEM).

Due to the flexibility and resolution of AFM it has been possible to image viruses, bacterial cells, mammalian cells, plant cell wall ultrastructures, proteins, enzymes and DNA (Bowen et al. 1997). Using the AFM it is even possible to image biological samples at a sub-nanometre resolution as has been shown by Muller et al. (Muller et al. 1997). As the technology improves it is possible to image faster. Thus, due to the fact that the AFM can be used in any environment, biological processes can be seen working in real time. The images can then be played back in sequence to see a "video" of the process.

As the AFM is of a 'mechanical' nature, rather than using electromagnetic waves or electron beams, it can be used to apply forces to samples, measure interaction forces and even manipulate the sample on a nanoscale (Rief, Gautel, et al. 1997). When the tip is brought into contact with the surface and then pulled away, various forces are experienced and these give some of the properties of the sample (Mechler et al. 1998). As the tip is brought to the surface it will experience either an attraction or repulsion force as the tip gets near to the surface. As the tip reaches the surface and is pressed against the surface, the repulsion force will increase to match the force with which the tip is being pushed into the sample. If the sample is soft, this will result in nanoindentation, which allows the Young's modulus of the sample to be found. Then as the force is removed for the tip, the reaction force will also reduce. As the cantilever is then lifted away from the surface, an attraction force between the tip and the sample appears. This force will keep increasing until the force from the cantilever becomes greater than the

attraction force, at this point the tip will snap away from the sample (Bowen et al. 1997; Lindsay n.d.). Interactions between a sample and a surface can be investigated in a similar way by coating the tip, or attaching a sample to the tip. The force between the sample and the surface can then be measured as the tip is brought to the surface and away again.

Single molecules can also be investigated by stretching them. The molecule is attached to the substrate and imaged to check that it is a single molecule and not denatured by attaching to the substrate at multiple points. The molecule is then attached to the tip; this can be done by pushing the tip hard into the molecule. The cantilever is the moved away from the surface and the forces measured as a function of the separation. This technique was first demonstrated by Rief et al. (Rief, Gautel, et al. 1997; Rief, Oesterhelt, et al. 1997). Their study of titin immunoglobulin showed that as the as the tip moved away from the surface, the force would increase and decrease in a saw-tooth waveform. The waveform is caused by increasing the force until one section of the molecule starts to unfold, the force required then decreases as the section is straightened out, then the force increases again until the next section starts to unfold. This unfolding gives details of the structure of the molecule and the forces within it.

1.5.2. AFM in fluid

The ability to image under liquid is a great asset of the AFM, as not only is it the natural environment for many biological materials, but also forces under liquid tends to be of an order of magnitude less. Thus the unwanted forces are also decreased allowing increased resolution and decreased image distortion.

However, imaging under liquid is more difficult than in air as the damping effect of the liquid, hydrophobic and hydrophilic forces, double layers and the movement of the liquid, among other forces, must be taken into account. Although these forces are usually undesirable in trying to get the best quality image, some of these forces can actually be imaged and add more information to a scan, not just the topography. One such case is imaging the electrostatic forces of a double layer.

1.5.2.1. Double Layers

Double layers form on the surface of objects in a liquid. If the surface of the object is charged, then it will attract ions of the opposite charge within the liquid towards the surface and repel those of the same polarity (Gosser 1993). This results in an excess of ions close to the objects surface relative to the bulk solution. A diagram of a double layer is shown in figure 1.11.

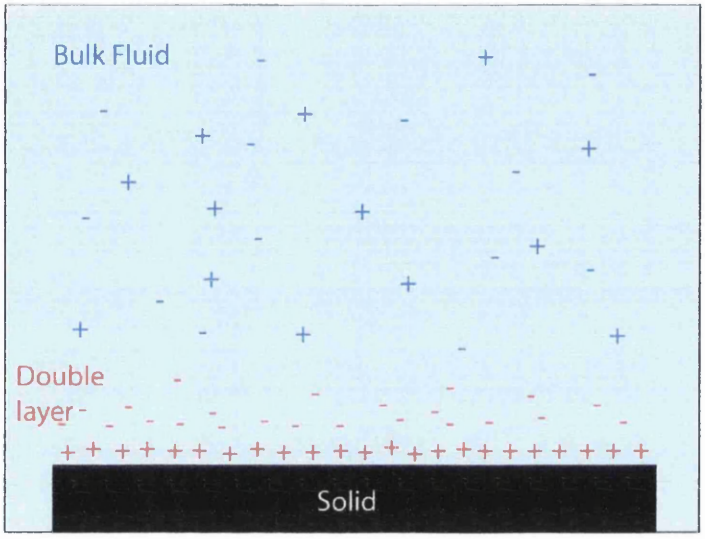

Figure 1.11- A diagram of the formation of a double layer at surface in contact with a solution containing ions

It has been shown that it is possible to image the double layers using an AFM in "electrical double layer mode" and hence get an image of how the double layer follows the surface (Bowen et al. 1997). The forces exhibited by the double layer are repulsive; hence a set force is used to create the image. By increasing the force it is possible to move the tip further through the double layer, closer to the surface and improve the level of detail in the image. Likewise, increasing the ionic strength of the fluid compresses the double layers and hence brings the tip closer to the image resulting in more detailed images (Bowen et al. 1997).

Another technique for imaging double layers, but this time at a charged electrode is scanning electrochemical potential microscopy (SECPM) (Hurth et al. 2007). In this technique the electrode being scanned is used as the working electrode in an electrochemical cell. The AFM tip, made of Ag coated PtIr, is then charged to a potential a few hundred millivolts above the potential of the counter electrode and

the current that flows used to determine the set point of the tip. Thus the tip scans the surface imaging a height where the current is constant.

It was also noted during investigation of SECPM that ionic strength affects the rate of decay of potential as the tip moves away from the electrode. As in the imaging of double layers, the higher the ionic strength the faster the potential decay with respect to distance (Hurth et al. 2007).

1.5.3. Other techniques

Due of the mechanism AFM uses to image the surface, it is possible to add more functionality with little modification. Conducting AFM (C-AFM) is one such development. In C-AFM the probe is run in contact mode whilst the potential difference is created across the sample between the conducting chuck and a conducting tip by applying a DC bias to the tip. As the topography is scanned, the current is recorded at the same time, thus building simultaneous images of topography and current.

Electrostatic Force Microscopy (EFM), also known as Electric Force Microscopy, by comparison does not touch the surface, but is a derivative of tapping mode that images the electric field above the sample. Following the scan of a line on the surface, a potential is applied to the sample or tip. The tip is then raised above the sample and a line scanned whilst the tip vibrated. The changes to the tips resonant frequency and phase are then used to create the EFM image.

1.6. Aims

As stated at the start of this section, bioelectrochemistry has a great deal to offer, but key to this is ensuring the interaction between the electrodes and the proteins is optimised and consistently reproducible.

To this end, the main aim of this investigation was to investigate the best electrode material and modification for improving protein interactions. This was to be achieved through the three steps below:

- The investigation of the modification of electrodes, primarily carbon based, through the use of electrochemistry and AFM imaging, to optimise electrochemical reactions with chemical compounds.
- The investigation of electrode blocking or fouling of electrochemical reactions through the use of BSA.
- The investigation of redox protein interactions with modified electrodes using azurin and laccase.

2. Methods and Materials

2.1. Equipment

2.1.1. Electrochemical

All electrochemical work was carried out using a Bioanalytical Systems (BAS) Epsilon potentiostat/galvanostat controlled via a PC running BAS Epsilon EC software with a C3 cell stand. This set up allowed for many types of test to be run, but within this work the main techniques used was cyclic voltammetry.
As well as the Epsilon system, a potentiostat was designed in house for use within the AFM (appendix III).

2.1.1.1. Cyclic Voltammetry Operation

The electrochemical cell was set up as in figure 2.1, using a platinum wire auxiliary electrode (BAS) and a silver-silver chloride reference electrode (BAS), the working electrode and electrolyte was varied depending upon the experiment.
The cell was then purged with nitrogen (oxygen free, BOC Gases) and stirred for 20 minutes before a test run was carried out on the cell. If the test run showed any peaks, the cell was purged and stirred for another 20 minutes and another test carried out. If peaks still existed the electrode would be re-polished and the same method followed. After these checks, if the peak persisted the electrolyte was changed and the tests re-run. Only when all peaks had been removed would the experiment begin.
Depending upon the substance being tested the range of scan was chosen, typically within -1000 mV to 1000 mV. Scans were then run at various rates from ranging from 50 mVs^{-1} to 1000 mVs^{-1}. Different ranges and rates were chosen depending upon the experiment.

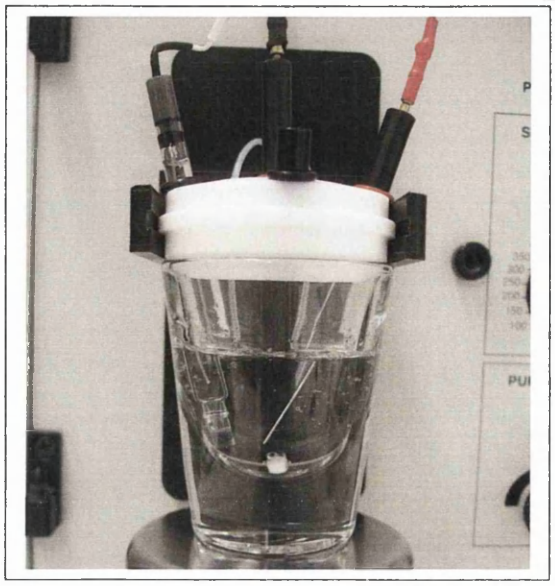

Figure 2.1- The electrochemical cell set up containing, from the left, an Ag/AgCl reference electrode, GC working electrode and platinum counter electrode

2.1.2. Electrodes

The auxiliary and reference electrodes were supplied by BAS. The glassy carbon (GC) and platinum (Pt) working electrodes were also supplied by BAS. Both electrodes were circular and had diameters of 3mm for the GC and 1.6mm for the Pt.

The pyrolytic graphite electrodes were constructed in house as described in the following section.

2.1.2.1. Design and Construction

The pyrolytic graphite edge (PGE) and basal (PGB) plane electrodes were constructed from material grade pyrolytic graphite (Le Carbone, Great Britain). Two electrodes were designed for different applications.

The first electrodes were designed to only expose either a basal or edge plane and to be flat enough to work under whilst being examined by the AFM. The electrode also allows for easy polishing of the electrode surface. The electrode is set in a non-conducting two-part epoxy resin (Buehler); a wire is connected to the rear face of the electrode using silver-loaded epoxy. The wire is lead through a bottom

plate and sealed with a quick setting epoxy. The whole assembly is then bolted together with nylon nuts and bolts and a rubber o-ring between the layers to seal the back of the electrode. This set up creates an electrode set in an un-reactive surround and only a few millimetres high and sits flat so it can be scanned by the AFM.

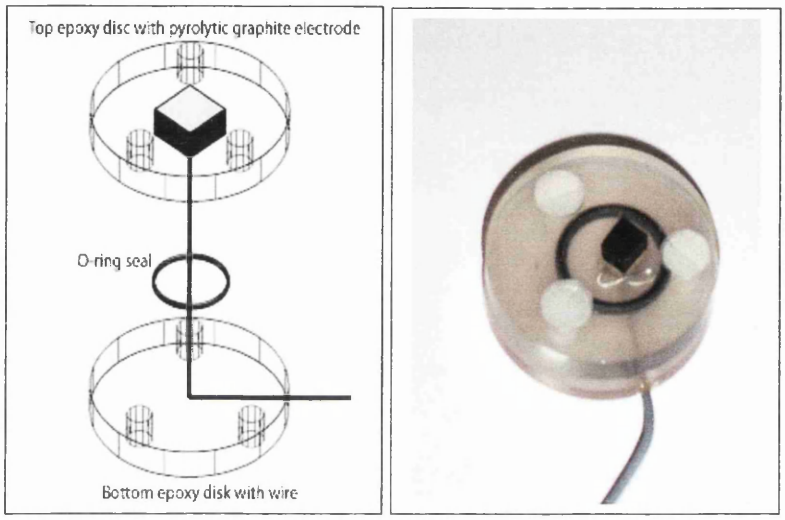

Figure 2.2- Construction of first electrode

The first electrodes worked well for scanning with the AFM, but were too large to be used in an electrochemical cell. Hence other electrodes were designed for use in the electrochemical cell and under the AFM. These electrodes had smaller surface areas; they were 2mm by 2mm, measured to within 5 microns. The electrode tip was removable so it could be mounted in different set ups for the long length needed for the electrochemical cell and the small height needed for the AFM.

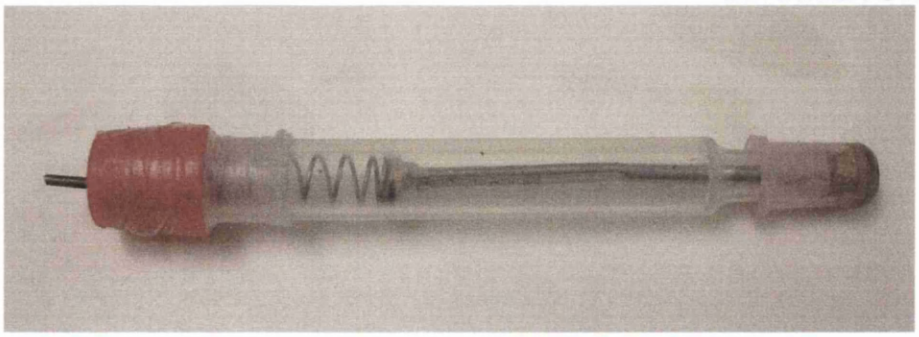

Figure 2.3- Second in house electrode made, note removable tip

The electrode was set into the tip using silver-loaded epoxy (RS) and stood slightly proud of the surface. The electrode and silver-loaded epoxy were then covered in non-conducting epoxy, which was left to set before being ground back to reveal the electrode surface, but not the silver-loaded epoxy. The electrode was then polished to a suitable finish using progressively finer grades of diamond (Kemet) and alumina (BAS) polishes.

2.1.3. Atomic Force Microscope

2.1.3.1. Digital Instruments Dimension 3100

The Dimension 3100 was used with a NanoScope IV controller and Digital Instruments Nanoscope version 6.12r2 software.

Through the use of different probes the Dimension could be used for both tapping and contact modes of operation. Contact mode in fluid was possible by using a different probe holder and appropriate seals.

The dimension can also be used for Magnetic Force Microscopy (MFM) through use of a different probe. Conducting Atomic Force Microscopy (C-AFM) is possible by using an add-on module and scanning in fluid is possible by using an appropriate probe holder and seals.

Figure 2.4- Digital Instruments Dimension 3100

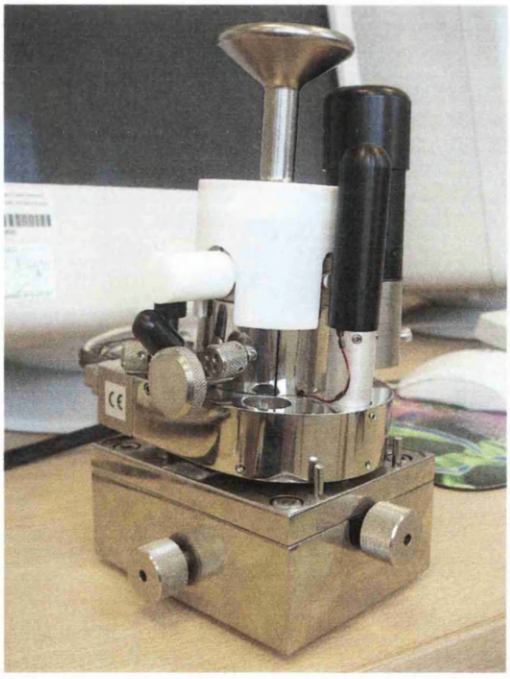

Figure 2.5- Topometrix Explorer

2.1.3.2. Topometrix Explorer

Two Explorers were used in this investigation, both were the same Topometrix Explorer model and used associated controllers and Digital Instruments SPMLab NT version 6.0.2 software. One of the Explorers was set up for tapping mode and the other for contact and contact in liquid.

2.2. Materials

2.2.1. Electrodes

The electrodes were made from pyrolytic graphite from Le Carbone. For the original electrodes the electrode was encased in 2-part epoxy resin from Buehler. The wire was then attached with silver loaded epoxy from RS and sealed using rubber O-rings and nylon nuts and bolts, also from RS. The wire was then sealed into the back disc using Araldite.

The smaller electrodes used the same pyrolytic graphite and silver loaded epoxy. This time the electrode was set in Araldite epoxy. The rest of the electrode was constructed from a syringe and luer tip, both from Fischer Scientific.

All other electrodes were sourced from Bio Analytical Systems (BAS).

The carbon electrodes were polished using Alumina slurry, on a Buehler polishing pad, both from the BAS CV3 Polishing Kit, as per the instructions in Electrode Polishing and Care, document A-1302, from BAS. The platinum electrode was also polished as described in the document, using the material supplied in the CV3 kit.

All other diamond polishes were from Kemet. There were three grades of diamond compound 0.5, 0.25 and 0.1 μm. All diamond polishes were used on a Kemet PAN-W polishing pad with Kemet Lubricating Fluid Type GW2.

The reference silver-silver chloride electrodes were stored, as per BAS instructions, in a 3 M sodium chloride solution.

2.2.2. Electrochemistry

All solutions used in the electrochemistry were made using deionised water, purified to greater than 15 MΩ/cm using a Millipore Elix 5 purification system. All solutions were degassed using vacuum and oxygen free nitrogen from BOC. Three buffers were used in the experiments: a pH 5.0 acetate buffer and pH 7.0 and 9.0 phosphate buffers. The buffers were composed as shown in the tables 2.1 and 2.2. The buffers were then boiled, purged with nitrogen and autoclaved.

Table 2.1- Acetate buffer composition

	Concentration
Sodium acetate	100 mM
Acetic acid	Added to pH 5.0

Table 2.2- Phosphate buffer composition

	Concentration
Potassium hydrophosphate	50 mM
Potassium hydroxide	Added to correct pH

For many experiments methyl viologen was used as a reactant, this was sourced from Sigma, and the solution prepared at time of use.
The cell was purged, when appropriate with oxygen free nitrogen also from BOC.

2.2.3. Bacteria and Proteins

2.2.3.1. Proteins and Enzymes

The laccase was from *Rhus vernficera* and in the form of a crude acetone powder (120 unit/mg). The azurin was from *Pseudomonas aeruginosa* and came as a lyophilised powder of approximately 70% protein. The Bovine Serum Albumin (BSA) was also a lyophilised powder of greater than 96% and along with the laccase and azurin was sourced from Sigma.

2.3. Methods

2.3.1. Electrochemistry

The electrochemistry experiments followed the same basic format, just with slight differences depending upon the material being tested.

The cell would be thoroughly washed in de-ionised water prior to each experiment. Likewise the reference and counter electrodes would be washed with deionised water. The working electrode would then be polished using a suitable polish, as described below, and thoroughly rinsed with de-ionised water.

The cell would then be carefully filled with purged buffer, the cell placed into the cell stand and the electrodes placed into the cell. The cell was then purged with N_2 and stirred for 20 minutes to ensure it was anaerobic.

Following this period CV scans were carried out over a suitable range of potentials and scan rates to ensure that there were no major peaks coming from the buffer or electrode finish. If peaks occurred then the working electrode was re-polished and the test re-run. If the peaks persisted then the buffer was changed.

Following this test the experiment could begin.

2.3.1.1. Polishing the electrode

The electrodes were polished using the polishes as described above in section 2.2.1 in accordance with the BAS Electrode Polishing and Care document A-1302.

2.3.1.2. Cyclic voltammetry (CV) of Methyl Viologen

Once the cell had been pre-tested then Methyl Viologen was added to the cell, in powdered form, to a concentration of 1 mM. The cell was then stirred and purged for another 20 minutes to ensure anaerobic conditions were maintained.

Cyclic voltammetry scans were then carried out over the range 0 to –800 mV at scan rates of 50, 100, 200, 300, 400, 500, 600, 700 and 800 mV/s.

2.3.1.3. CV of different electrode finishes

The testing of different electrode finishes was done using Methyl viologen and oxygen and the technique was much the same as in sections 2.3.1.2 and 2.3.1.5. Then following the CV run the electrode would be removed, polished to a new finish and thoroughly flushed with de-ionised water. The electrode would then be returned to the cell and the cell purged and stirred for 20 minutes to ensure anaerobic conditions were maintained.

2.3.1.4. CV of different electrodes and finishes

Each electrode was polished with the alumina slurry and then flushed thoroughly with de-ionised water before the experiment started. The cell was then tested with the glassy carbon electrode and the buffer alone, before the methyl viologen was added and the test run as in section 2.3.1.2. The electrode was then changed, the cell purged with N_2 for 20 minutes and the test re-run.

Following all electrodes having been tested, all electrodes were polished with the 0.1μm diamond polish and all electrodes were tested. This process was then repeated for the 0.25 and 0.5 μm diamond polishes.

2.3.1.5. CV of oxygen

The CV of oxygen was carried out in the same way as described in section 2.3.1, but an aerobic buffer was used in place of the anaerobic buffer and the cell was not purged. No testing of the buffer was carried out at the start of the test, but the cell was thoroughly purged at the end to get a buffer response.

To test different polished finishes on the electrodes, the electrodes were tested with one finish, removed and polished, thoroughly flushed and then returned to the cell for the next test.

2.3.1.6. CV of Enzymes and Proteins

Before the experiment, the appropriate electrode was selected, polished to a suitable grade and tested with buffer as described above. The experiment was then carried out in one of two ways: Either the protein was added to the cell to suitable concentration, or the electrode had a drop placed on it's surface and was left for a

period of time to allow absorption before the electrode was flushed and returned to the cell.

Laccase: A solution of 10mg/ml in phosphate buffer (pH 7.0, 50mM) was placed on to the electrode, so the surface was just covered. The electrode was then left for 20 minutes before the solution was gently flushed with de-ionised water. The electrode was then returned to the cell and used immediately. Scans were run over the range –50 to 1000 mV at scan rates of 50 to 1000mV/s.

Laccase + Pyrocatechol: The experiment was carried out as for the Laccase. The cell then had 10mM Pyrocatechol added as a substrate to the phosphate buffer (pH 7.0, 50mM) and the laccase was retested. Finally the electrodes were re-polished and the pyrocatechol tested without laccase present.

Azurin: 1 ml of de-ionised anaerobic water was added to the bottle of Azurin as bought from Sigma. Just enough solution to cover the surface of the electrode was used and left for 20 minutes. The excess solution was then removed by syringe and the electrode returned to the cell. The tests were run immediately. CV scans were carried out over the range 0 to 600 mV and scan rates 50 to 600 mV/s.

Bovine Serum Albumin (BSA): BSA was used to investigate the blocking of the electrode instead of electrochemical activity. BSA was used in two different ways. The first method was to carry out with methyl viologen as described above in section 2.3.1.2. After the methyl viologen had been tested, BSA was added to the cell to a concentration of 1mM and purged for 5 minutes. The CV runs were carried out over a range to 0 to –800 mV at scan rates of 50 to 800 mV/s. Following this test the cell was left to stand for 20 minutes with the electrode soaking and the test repeated.

The second method was to again run the methyl viologen experiment. The electrode was then removed from the cell, dipped in 10mM BSA solution for five minutes and allowed to dry for 1 hour. The cell was continually purged for that time to ensure conditions were maintained. The electrode was then returned to the cell and the experiment run as above. The electrode was then returned to the solution and soaked for 20 minutes and then allowed to dry for an hour and then retested. Finally the electrode was soaked for a period of 1 hour, dried for 1 hour and retested.

For both methods with BSA the experiment was also carried out using the GC, PGE and PGB electrodes, all polished with alumina slurry.

2.3.1.7. CV of BSA with Poly-D-lysine

A solution of Poly-D-lysine hydrobromide (Sigma) was made with 5mg added to 50ml of de-ionised water. The solution was used to coat the electrode by smearing 1.5µl of the solution across the surface of the PG electrodes and 3µl across the GC electrode. The electrodes were then left to stand for 5 minutes in air. Any excess solution was then removed by aspiration and the electrodes allowed to dry for two hours.

The Poly-D-lysine film was used to coat the electrode before it was dipped in BSA. Otherwise the experiment was carried out in the same was as the BSA 'dipping' experiment above.

2.3.2. Atomic Force Microscopy (AFM)

The AFM has 3 methods of use for normal operation: contact, non-contact and tapping mode. During this work, only contact and tapping mode were used. The methods used will be described for use in air, followed by how the use in fluid differs. Then the more specialist techniques of double layer imaging and conducting AFM will described.

2.3.2.1. AFM in air

Contact AFM: The AFM was set up with a suitable tip and set up as per the appropriate manual for the Dimension or the Explorer. In both cases the tip would be lowered until it touched the surface. The force (set point) would then be reduced until the tip left the surface and increased again until it just touched. From this starting point the force and proportional and integral gains would be adjusted until the tip would consistently follow the same contours on the trace and retrace. At this point the scan would be carried out.

Tapping AFM: Likewise the AFM was equipped with an appropriate tip and set up according to the manual. The tip was tuned before each approach and the tip lowered using the software. The set point, proportional and integral gains were then adjusted to get a consistent trace and retrace before the scan was started.

2.3.2.2. Conducting AFM

The conducting AFM was performed using the Dimension with the Digital Instruments C-AFM add on module and a C-AFM head. To ensure conductivity, gold plated tips were used.

C-AFM is carried out in contact mode, so the AFM was set up in the same way as above in section 2.3.2.1

The sample was then placed in contact with the chuck in such a way as to ensure a good connection. This usually involved bonding the sample to a metal disc using conducting epoxy (RS). If the sample had a resistance of less than 1 kΩ care needed to be taken, as the current would be too great for the module, so the resistance had to be increased.

Once the AFM and sample were set up a small potential was applied to either the sample via the chuck, or to the tip or to both. The scan was then run as normal using an extra channel to record the current.

3. Results

3.1. Electrochemistry of bare electrodes

3.1.1. Introduction

In order to have a good understanding of the electrodes' behaviour and an idea of which materials and finishes were going to give the best interaction with proteins, it was decided to investigate the electrochemical responses of the bare electrode. The electrodes and finishes that gave the best chemical reaction would give a good indication of the starting point to investigate the best surface to react with the proteins.

3.1.2. Cyclic voltammetry of methyl viologen

The electrochemistry of methyl viologen is well studied, therefore giving a good starting point. When a solution of methyl viologen is reduced it turns a dark shade of blue, oxidation returns the solution to colourless. Thus, as well as any electrochemical data recorded, there is a visual indication of the reaction taking place.

The experiments carried out were based on changing either the electrode or the conditions of the cell to investigate how the reaction was influenced.

Before experimenting with the variables, an experiment was carried out using the Glassy Carbon (GC) electrode polished with alumina and a solution of 10mM methyl viologen in 50mM phosphate buffer. The results can be seen in figure 3.1.

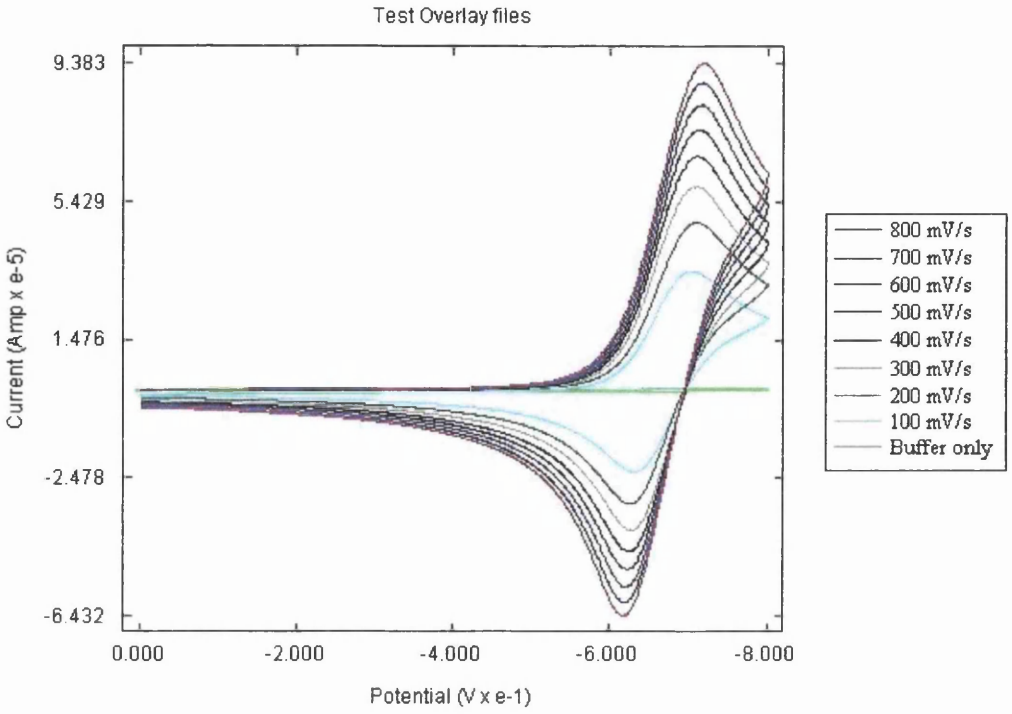

Figure 3.1 - The effect of scan rates on a CV of of 10 mM methyl viologen (see section 2.3.1.2 for method)

From the scan in figure 3.1, it is possible to see that there is a reduction peak at just over – 700 mV and an oxidation peak at just over -600 mV. It can also be seen is that as scan rate increases the, peaks separate. At 100mV/s the reduction and oxidation peaks are at -704 mV and -628 mV respectively. When the scan rate is increased the peaks move apart to -717 mV and -615 mV. This separation shows that electron transfer is slow enough to be effected by the increasing scan rate. The reaction shown is a quasi-reversible reaction.

To enhance the reaction, various techniques were tried to improve the reactivity of the electrode. These involved modification of the electrode and change to the environment of the cell.

A successful modification would not only show itself through larger peaks, but also through the peaks not separating, or separating less, when the scan rate was increased. This would show that the modification had resulted in faster electron transfer.

3.1.2.1. Electrode polishing and materials

The experiment was carried out as described in section 2.3.1.3, polishing with all grades of polish.

The first experiment was carried out using the GC electrode polished using the alumina slurry and diamond compounds.

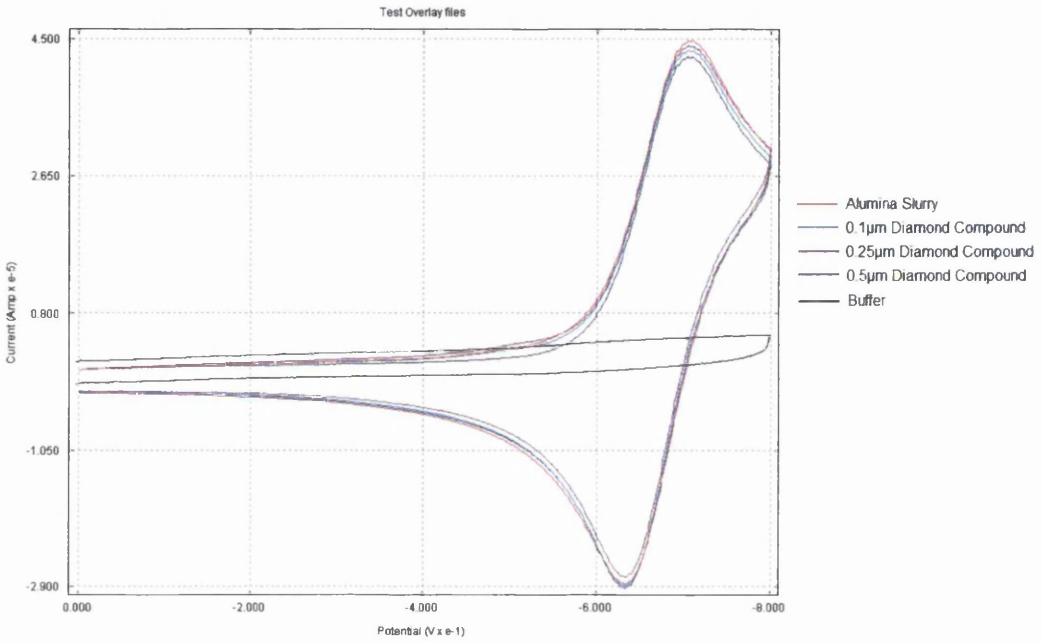

Figure 3.2- The effect of polished finishes on a CV of methyl viologen at 800mV/s using a GC electrode

From the scan in figure 3.2 it is possible to see that despite the different surface finishes, there is no difference to the potential at which the peaks occur, implying that there is no difference in the electron transfer rate.

Table 3.1 shows the currents for each of the reduction peaks.

Table 3.1 – The effect of different polishing techniques on the reduction peak currents in cyclic voltamograms

Alumina		0.1µm Diamond		0.25µm Diamond		0.5µm Diamond	
100mV/s	800mV/s	100mV/s	800mV/s	100mV/s	800mV/s	100mV/s	800mV/s
13.8	35.02	13.97	36.96	14.5	36.11	13.75	38.62
12.14	33.52	12.72	33.86	13.13	32.36	13.01	38.62
12.31	29.48	14.74	29.25	14.14	34.16	19.18	34.8
Average							
12.75	32.67	13.81	33.35	13.92	34.21	15.31	37.34

From the average values, it can be seen that at both 100 and 800mV/s the current peak increases with the coarseness of the diamond compound and the diamond compounds all give a higher current than the alumina slurry.

It is also possible to see that the 0.5μm diamond compound polished electrode gives a peak of around 10% greater than that of the electrode polished with 0.25μm diamond compound, both at 100 and 800mV/s. Compared to the alumina this percentage increase is around 15% at 800mV/s and even higher, around 20%, at 100mV/s .

So whilst it is not instantly obvious from the scans, and there is little difference in electron transfer characteristics, the coarser the polish used, the higher the current peak is on methyl viologen reduction.

3.1.2.2. Stirring of the electrochemical cell

Stirring of the MV solution was the first variable to be investigated. This was carried out using the stirrer built into the cell stand. (see section 2.3.1 in materials methods)

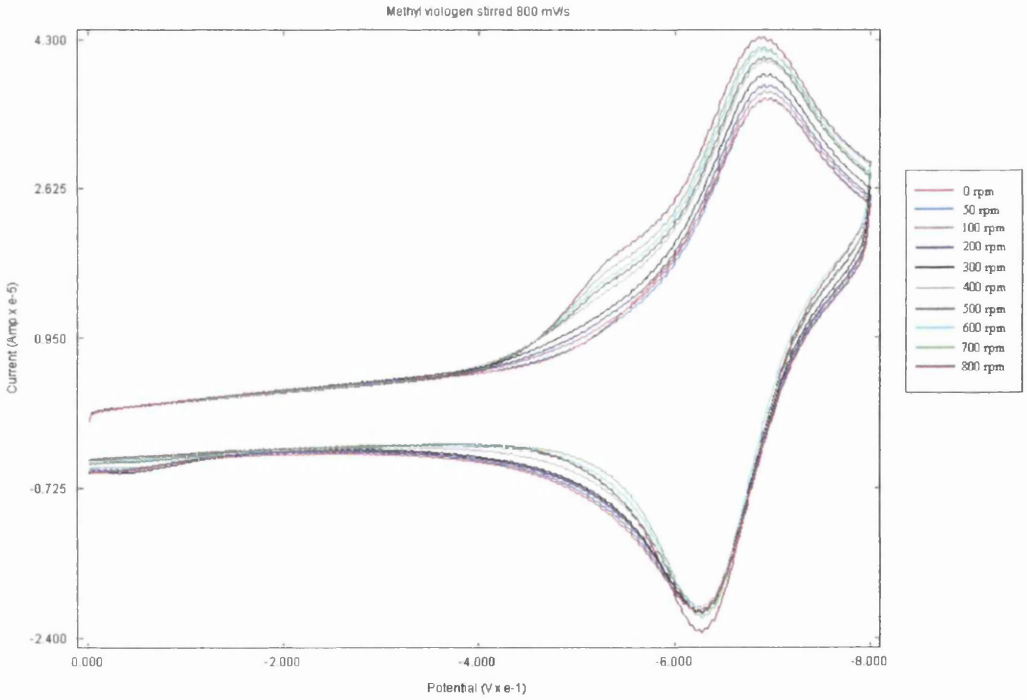

Figure 3.3- The effect of stirring rate on the CV methyl viologen at 800mV/s. The rate was varied from 0 to 800 rpm

Immediately noticeable in figure 3.3 on the scan at 800mV/s is that the stirring increases the current at the reduction peak and also at potentials less than -4 volts. At the oxidation peak however there was less of a difference. The increased reduction peak can be put down to the movement of the solution over the electrode. This will mean that once the methyl viologen was reduced, it was moved away from the surface allowing fresh solution to pass over. This implies that the reaction at the electrode is usually limited by mass transport without the stirring. The movement of the solution also accounts for the similarity at the oxidation peak. As the reduced methyl viologen is moved away from the electrode, the solution at the electrode surface will be normal solution containing the same amount of reduced methyl viologen, and the fact that more was reduced in the forward scan does not affect the result.

An observation that also came from the stirring of the solution is that it is important to match the rate of stirring to the rate of the scan, if you want to be able to interpret the scan, as can be seen in figure 3.4.

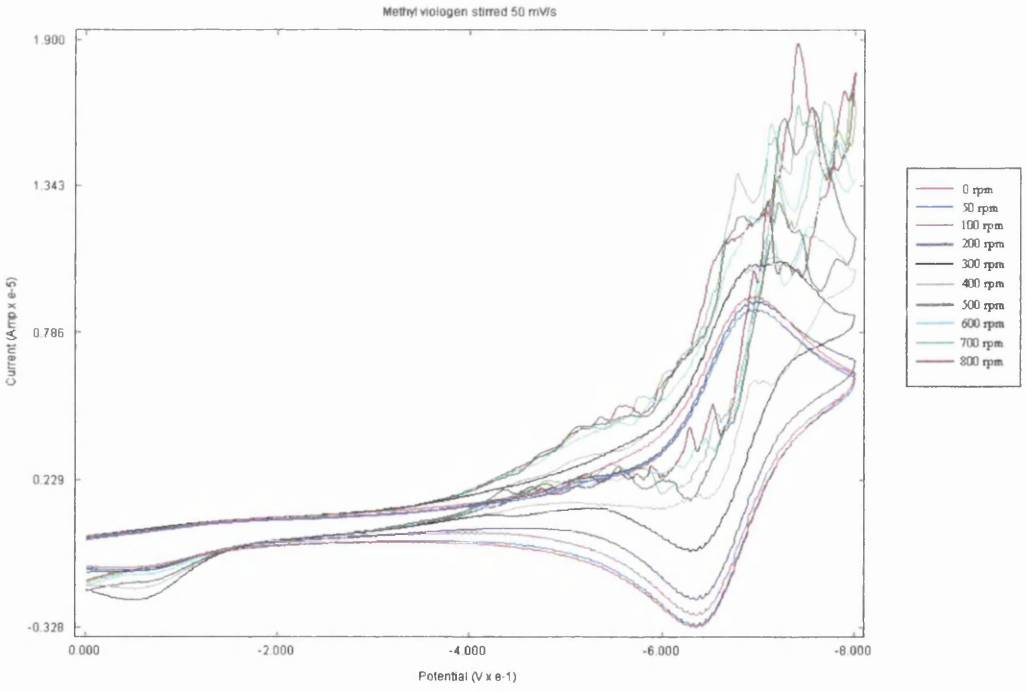

Figure 3.4- The effect of stirring rate on the CV methyl viologen at 50mV/s. The rate was varied from 0 to 800 rpm

Despite the fluctuations on the scan it was still possible to see that stirring increases the reduction peak. However, as most of reduced methyl viologen has been moved from the electrode, there is almost no oxidation peak.

Comparing the slow and fast scan rates, it is possible to see that the stirring has more of an effect at the lower rate, as may be expected because there is more time to clear the reduced substance from the electrode surface. Taking reduction peak values at 800 mV/s, the peak is increased in height to 28.8μA during stirring at 800rpm, compared to 25.3μA when not stirred. This is an increase of around 14%. When the slower scan rate of 50mV/s is considered, the 800rpm peak was 9.6μA compared to 4.2μA with no stirring. This is an increase of around 130%.

3.1.2.3. The effect of pH

As the pH of a solution is a measure of the activity of hydrogen ions in the solution, it follows that the pH will have an effect on the electrochemical response.

So the same experiment was run on methyl viologen, this time varying the pH using a pH 5.0 acetate buffer, and pH 7.0 and pH 9.0 phosphate buffers. The results of the 800 mV/s scan at the various pH values can be seen in figure 3.5.

From figure 3.5, it is obvious that increasing the pH does not necessarily increase the current peaks. Whilst the pH 7.0 and pH 9.0 peaks are higher than the pH 5.0, the pH 7.0 is the greatest peak, hence it appears that the there is an optimum pH above which the electrochemical reaction becomes inhibited by the increasing pH. The pH can affect the redox potential of the MV and there was shift in the peak to more reduced values at high pH.

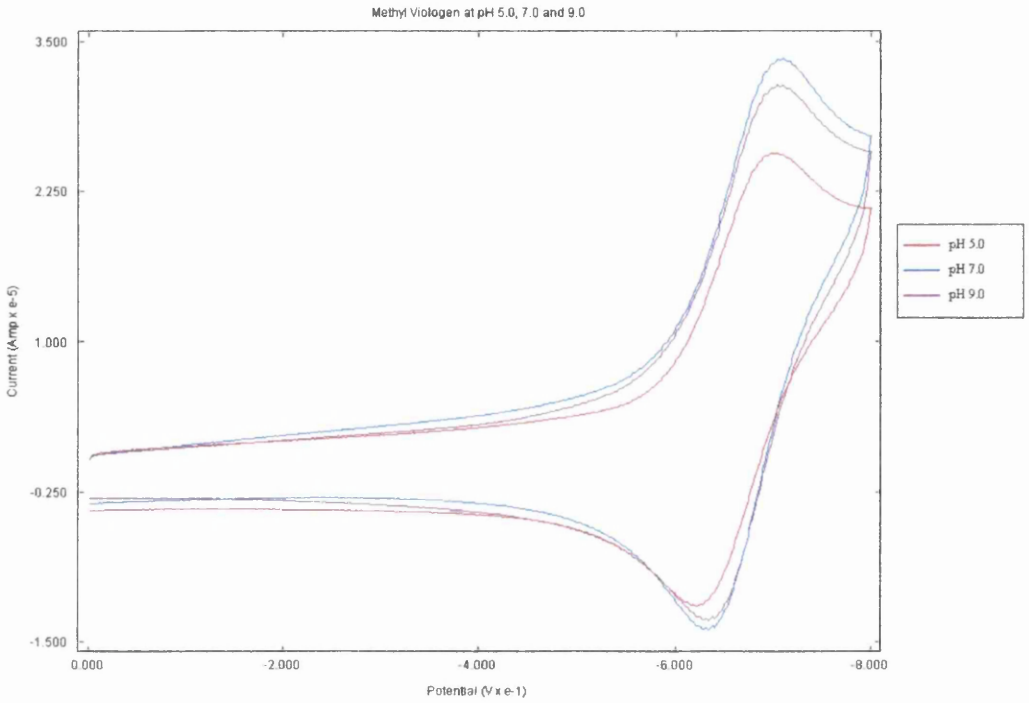

Figure 3.5- The effect of pH on CV of methyl viologen at a 800mV/s. Three values of pH were used, pH 5.0, pH 7.0 and pH 9.0

Table 3.2 - Current peaks for the CV of methyl viologen at various levels of pH and scan rates

		Reduction Peak (mA)		
pH	Scan Rate (mV/s)	Experiment 1	Experiment 2	Average
5.0	50	7.53	4.68	6.105
7.0	50	8.58	5.86	7.22
9.0	50	5.23	6.05	5.64
5.0	800	22.8	18	20.4
7.0	800	31.2	22.9	27.05
9.0	800	22.5	21.5	22

Table 3.2 shows that at both high and low scan rates, the pH 7.0 reduction peaks are the greatest.

3.1.2.4. Electrode materials

As well as the electrode surface, the material the electrode is made from can also make a difference to a reaction.

Four different materials were tested with methyl viologen; platinum (Pt), glassy carbon (GC), pyrolytic graphite edge plane (PGE) and pyrolytic graphite basal (PGB) plane.

A brief experiment was carried out to compare the materials. For this test, the GC, PGE and PGB electrodes were polished using alumina slurry, the Pt electrode was polished with 1μm diamond polish followed by alumina slurry as recommended in the BAS polishing guide.

As the electrodes were both bought and made in house the surface areas were not the same, the GC had a surface area of 7.07 mm^2, the PGE and PGB were 4 mm^2 and the Pt 2.01 mm^2. So in the following experiments that involved using the different electrodes, the results were all normalised to give current for a surface area of 1 mm^2.

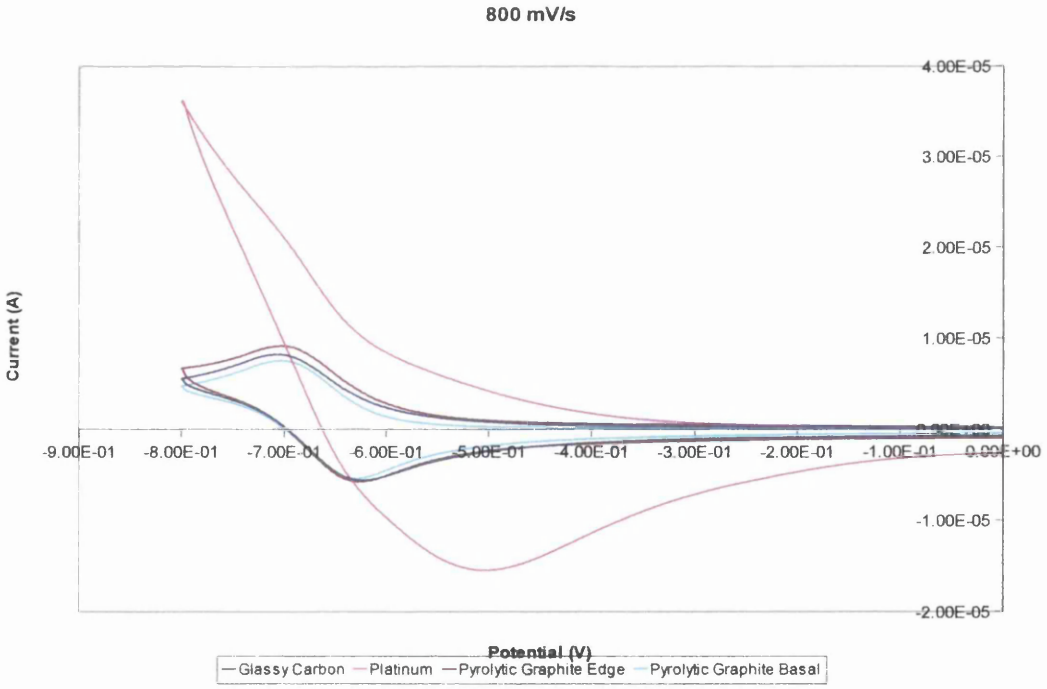

Figure 3.6- The effect of different electrode materials on the CV of methyl viologen at 800 mV/s

During this preliminary experiment, the Pt electrode stood out as reacting differently to the carbon based electrodes. Figure 3.6 shows how the response of the Pt electrode was very different, the reduction peak is off the end of the 800 mV scale and much higher. The oxidation peak is around -500 mV and also much greater. As these potentials are considerably different to the reduction potential of methyl viologen, it was assumed that the Pt electrode was actually catalysing a different reaction. As a result, the carbon based electrodes were focussed on and the results of the carbon electrodes at a slow and fast scan rate can be seen in figures 3.7. and 3.8.

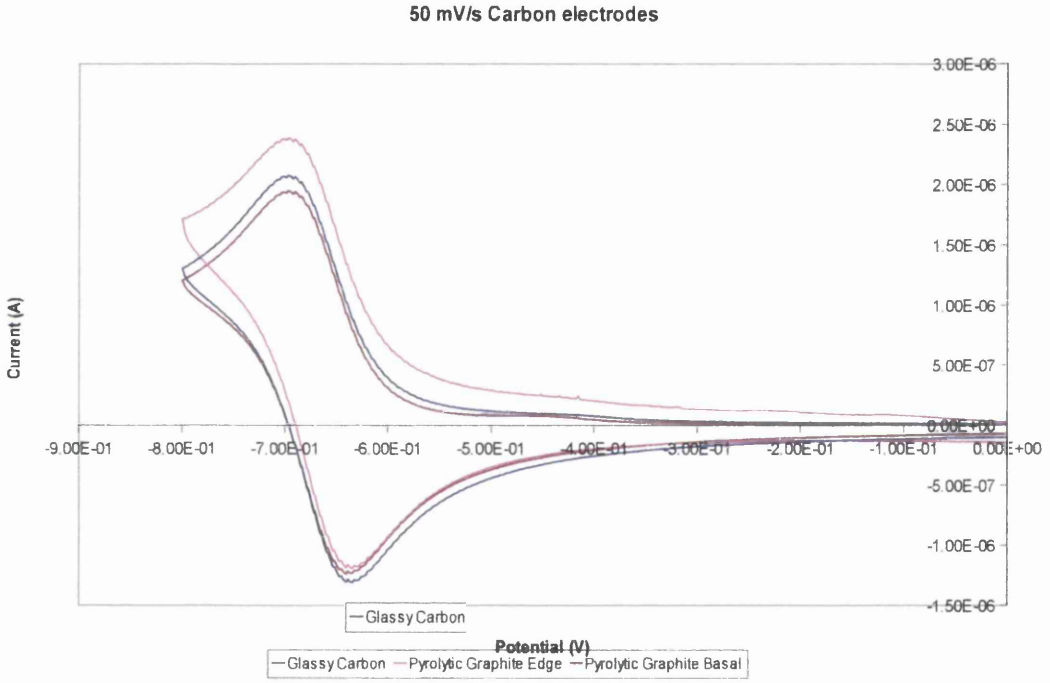

Figure 3.7- The influence of the type of carbon electrode on the CV of methyl viologen using 50 mV/s scan

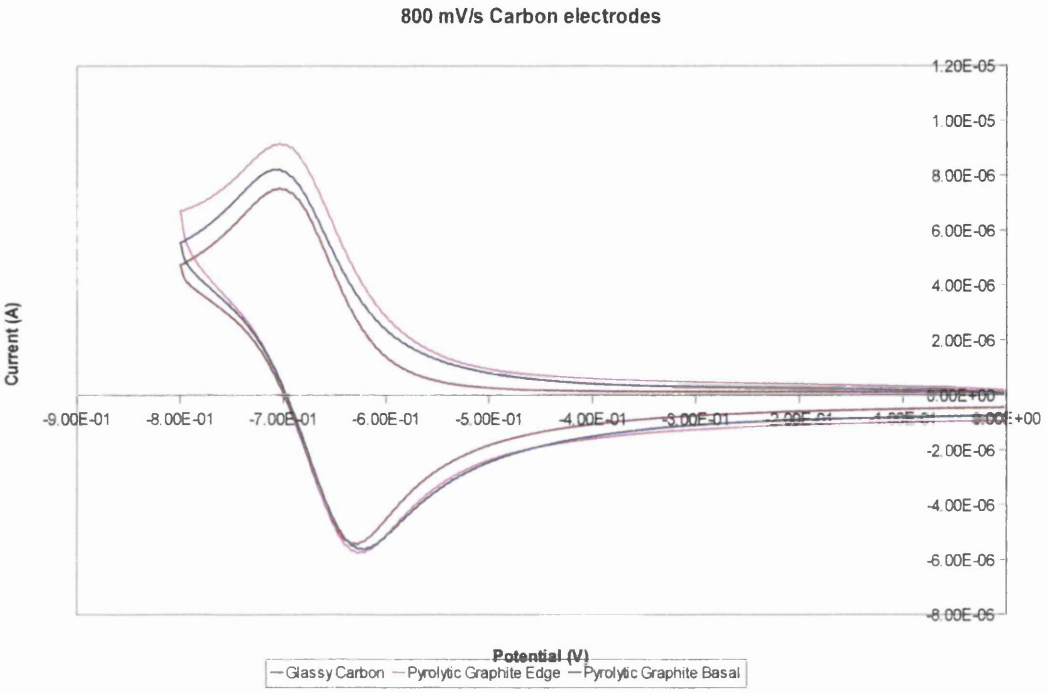

Figure 3.8- The influence of the type of carbon electrode on the CV of methyl viologen using 800 mV/s scan

At both slow and fast scan rates, the PGE electrode produces the greatest reduction peaks. The oxidation peaks at low scan rates are very similar in height. However as the scan rate increases, the PGE electrode gets both the greater oxidation and reduction peaks.

Also at higher scan rates, it is noticeable that the GC electrode peaks separate more than both the pyrolytic graphite electrodes, implying slower electron transfer. The PGB electrodes peaks are actually the closest, so despite not having the greatest current peaks, the electron transfer is actually faster than that of the PGE.

3.1.3. Cyclic voltammetry of oxygen

Usually great effort is taken to ensure there is no oxygen in an electrochemical cell. As oxygen is so reactive, it will create a current peak great enough to overshadow any other reaction that is present. Also the oxygen will react with

products of the electrochemistry, creating an EC reaction, which could stop the true reaction of the chemical under test from being seen.

However as oxygen is readily available and has a strong reaction, it can easily be used to test the reaction of a gas at the electrodes.

The tests were carried out both with a still cell and with stirring, different polished finishes to the electrode were also tested without stirring. As before the GC, PGE and PGB electrodes were used and the results normalised before they were compared.

3.1.3.1. CV of oxygen with and without stirring

As mentioned above, oxygen gives a large current peak, which can be clearly seen in figure 3.9. The oxygen and purged scans follow very similar traces above -0.3 V. Below this value, the peak grows sharply.

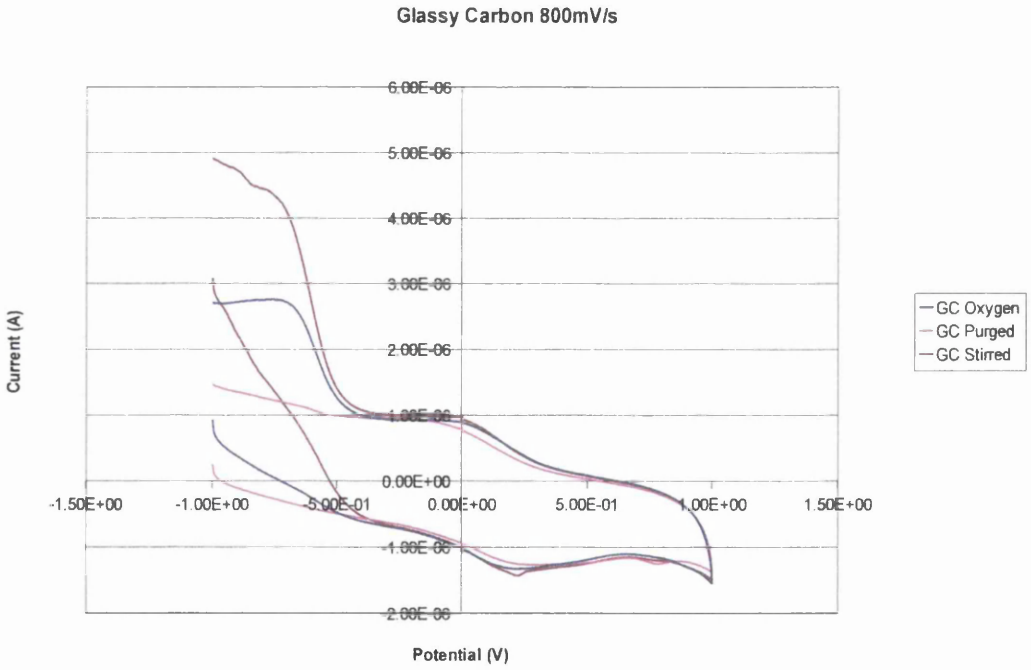

Figure 3.9- CV of oxygen on GC at 800mV/s both stirred and unstirred

Stirring the solution also has a large effect, when the still reduction peaks at 2.8μA around -760mV, at the same point the stirred solution has a current of 4.4 μA and the current is still rising. This indicates that mass transport is a limiting factor in a still cell.

When comparing the GC electrode to the PGE and the PGB electrode (figures 3.10 and 3.11) the first thing that is obvious is the nature of the PGE scan. As the solution under test was the same as the other electrodes, it can only be concluded that there was some damage to the electrode surface. However despite repeated polishing and retesting it was not possible to get a smooth result.

Comparing the PGB to GC, the current of the PGB electrode was considerably lower, the reduction current peaking at 1.4 μA for the unstirred and 1.8 μA for the stirred. This was less than half the current of the GC electrode. The other point is the position of the peaks, the stirred result has a peak around -770 mV very similar to that of the GC, but the still result has its reduction peak at -880 mV. This is far more similar to the peaks of the PGE which are around -850 mV for both scans.

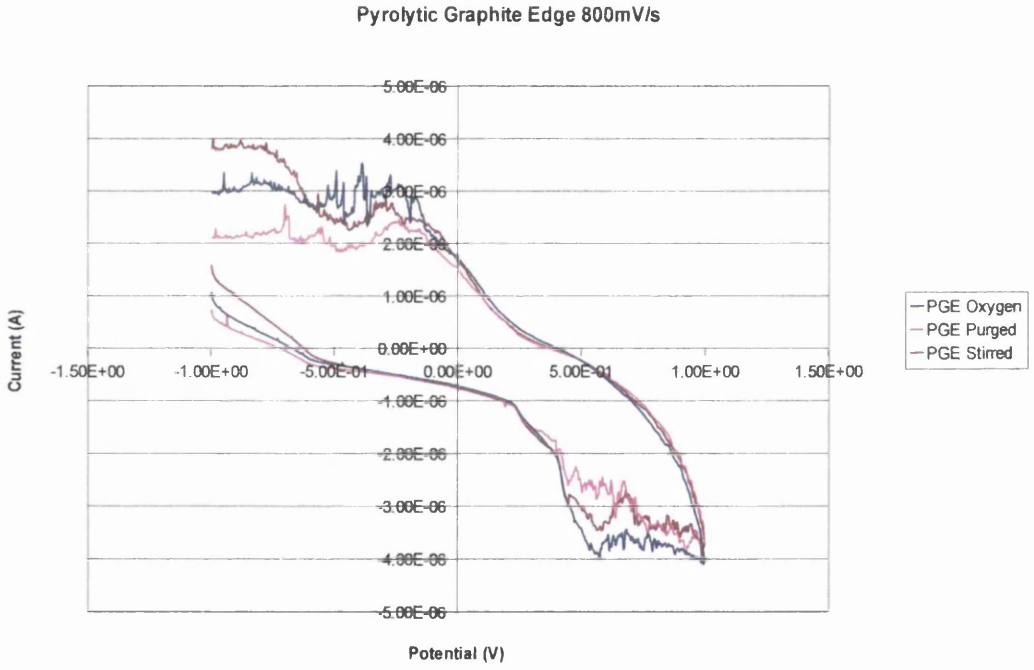

Figure 3.10- The effect of stirring on CV of oxygen with PGE at 800 mV/s

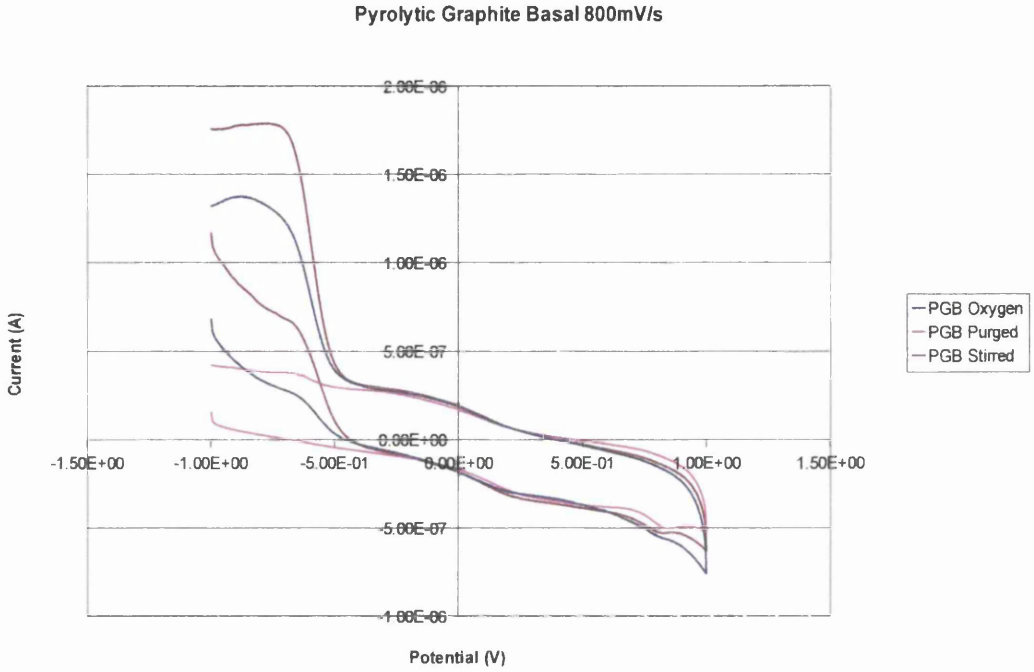

Figure 3.11- The effect of stirring on CV of oxygen with PGB at 800 mV/s

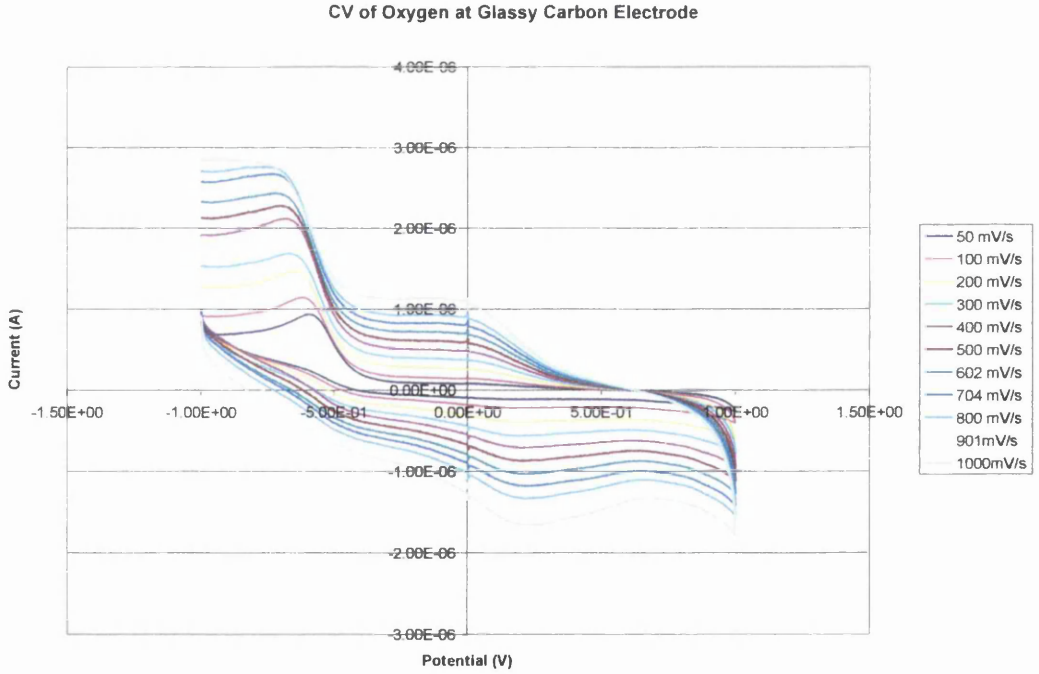

Figure 3.12- The effect of scan rate on the CV of oxygen at GC

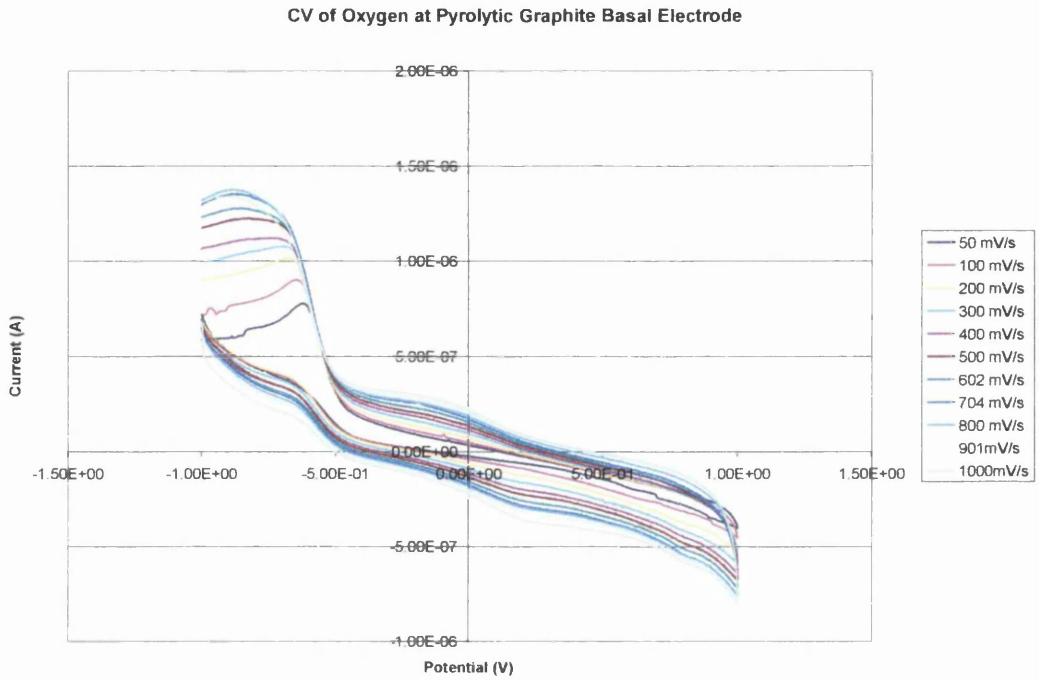

Figure 3.13- The effect of scan rate on the CV of oxygen at PGB

Comparing the reduction peaks for both PGB and GC as the scan rate increases, the PGB peaks start reaching a limit around 700 mV/s, with the GC reaching a limit around 800 mV/s. This shows that at these rates, there is a factor limiting the rate of turnover at the electrode surface. In the stirring scan, see figure 3.14, the scans are not limited at these scan rates, so the limiting factor is most likely mass transport.

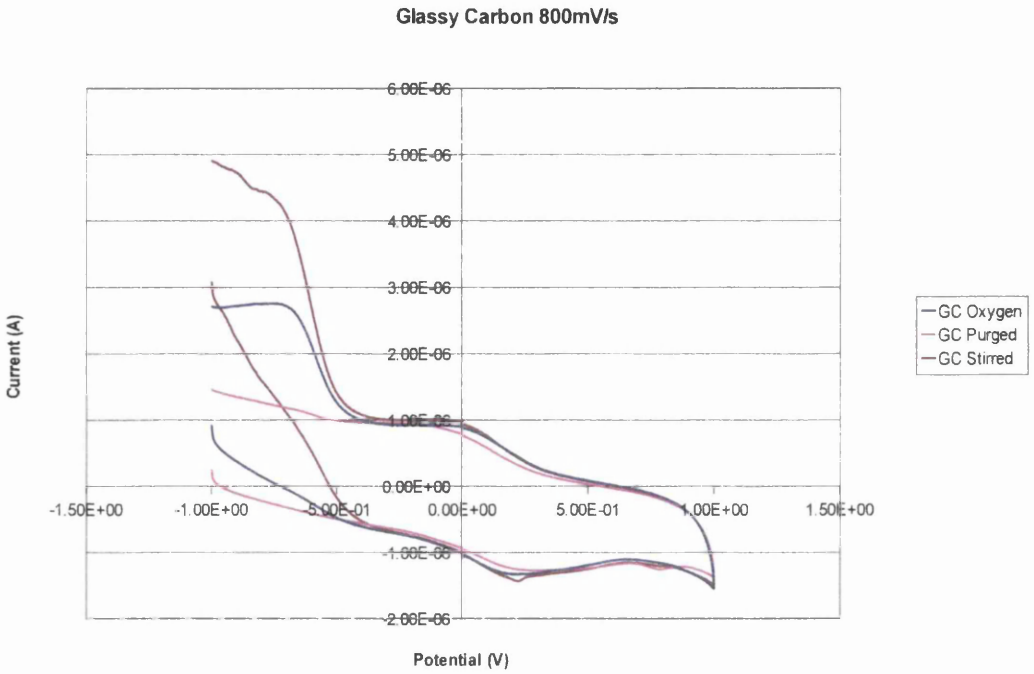

Figure 3.14- A comparison unstirred and stirred cell CV's of oxygen at GC electrode

Also in figures 3.12 and 3.13 it is noticeable that the reduction peak moves to a more negative potential as the scan rate increases. In the case of the GC electrode, the peak moves from around -600 mV at 50 mV/s to -770 at 1000 mV/s. For the PGB electrode the peak is also at -600 mV at 50 mV/s, but at 1000mV/s the peak has moved to around 900 mV/s. This implies that electrode transfer to oxygen from the PGB electrode is slower than that of the GC electrode.

3.1.3.2. Polishing of electrodes

Polishing the electrodes has the potential to greatly affect their reactivity as it changes their topography, surface area and the reactive sites on the surface.

In this experiment the carbon based electrodes were polished with alumina slurry and the three diamond polishes. These were tested with oxygen as before, once again the results were normalised to a surface area of $1mm^2$.

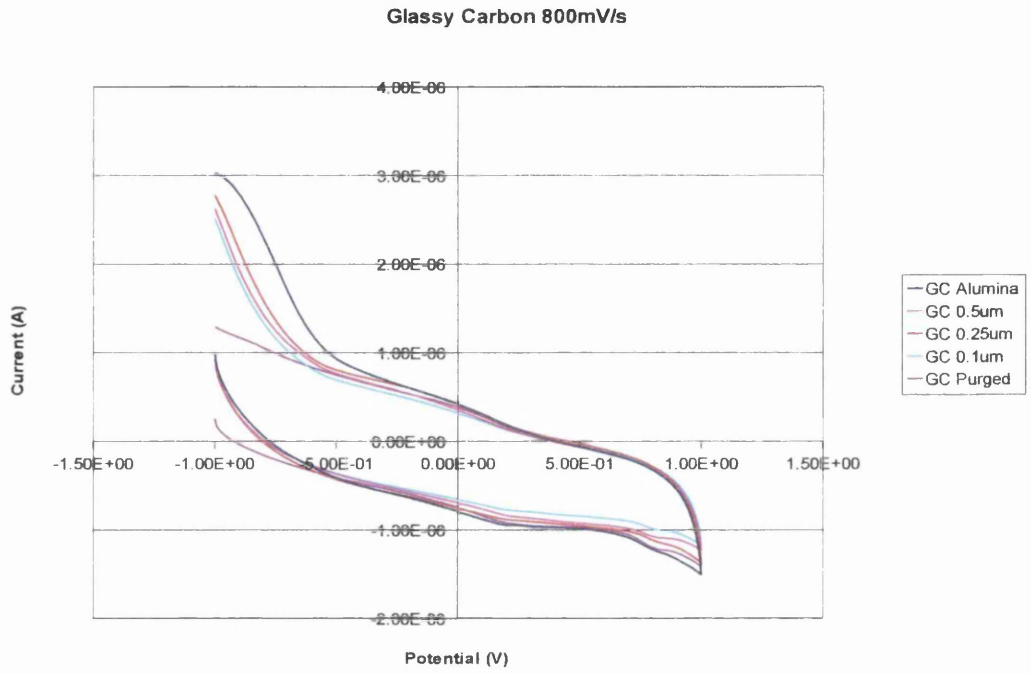

Figure 3.15- The effect polishing conditions on the CV of Oxygen at a polished GC electrode at 800 mV/s

Figure 3.15 shows that the diamond polishes all give similar results with the 0.25μm polishing having the greatest reaction. However the alumina slurry polishing results in an electrode that reacts at a lower potential and has a higher reactivity.

By contrast the PGE electrode's responses in figure 3.16 show that all the polishes have a similar response with the exception of the 0.5μm diamond polish, whose peak is at a greater negative potential and lower.

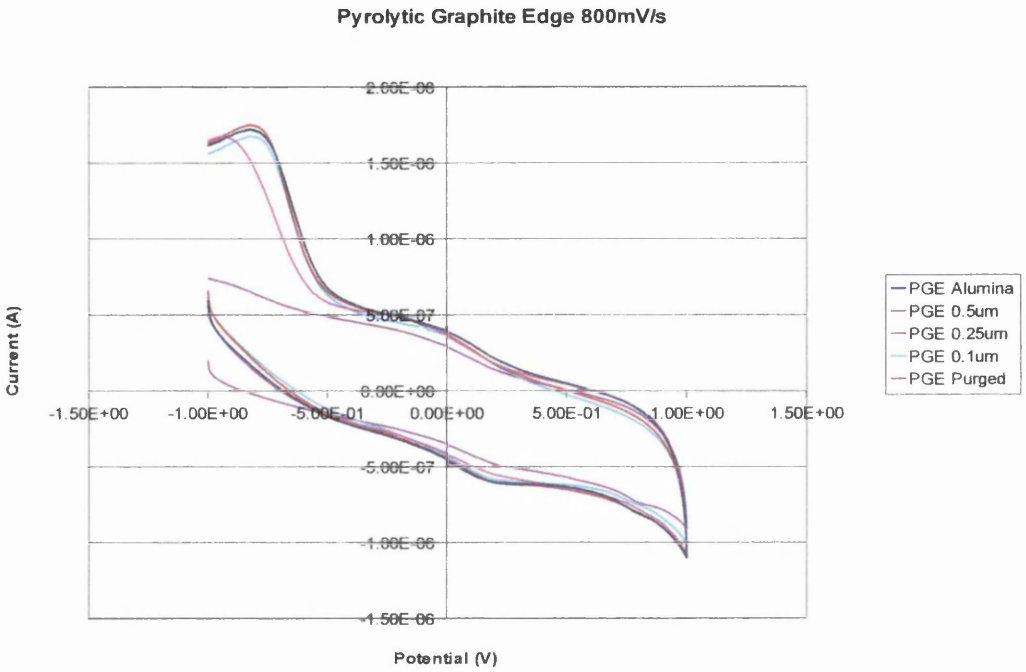

Figure 3.16- The effect polishing conditions on the CV of Oxygen at a polished PGE electrode at 800 mV/s

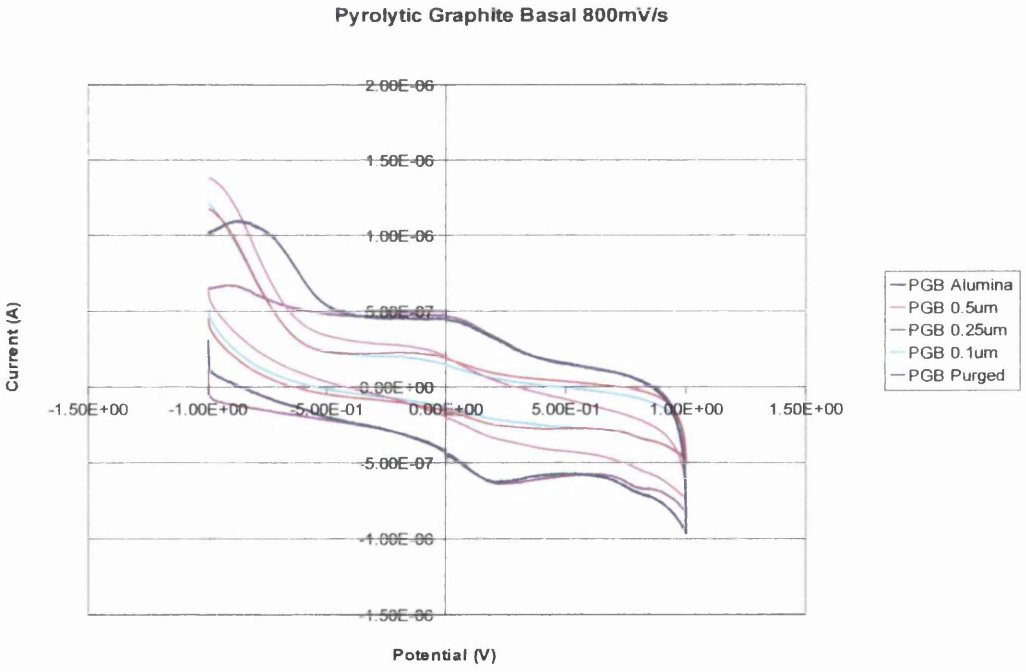

Figure 3.17- The effect polishing conditions on the CV of Oxygen at a polished PGB electrode at 800 mV/s

The reaction of the PGB electrode, as seen in figure 3.17, contradicts the results of both the other electrodes by getting the greatest reaction from the 0.5μm diamond polished electrode. However the alumina has its reduction peak at a lower negative potential and a lower peak.

Comparing the three sets of results for the electrodes it is clear that the PGB electrode shows the lowest peaks, with the PGE electrode having the second highest and the GC electrode giving the greatest peaks. In contrast to this result, the PGE electrodes reduction peaks occur at the lowest negative potential of the three, at around -820mV for alumina, 0.25 and 0.1 μm diamond polishes and -930mV for 0.5μm diamond polish. This would imply that the PGE electrode has the fastest electron transfer characteristic with oxygen. Interestingly, the alumina polished PGB also has a reduction peak at a lower negative potential than the diamond polished electrodes, around -870mV. This implies that in this case polishing greatly modifies the surface's properties, which is not seen in the same way on the other electrodes.

3.1.4. Discussion

Through the investigation of methyl viologen and oxygen it is possible to see the differences in the electrode and finishes for a solid and a gas in solution. The results have shown that there is no one electrode or polishing compound that stands out as the best. It varies depending upon the conditions and the chemical being tested.

The clearest result from the tests was that for the affect of pH on the reaction of methyl viologen. There is an optimum pH level around 7.0 for the reaction, as above and below this the peaks are lower at both higher and lower scan rates.

Another result is that in all cases, particularly as scan rates increase, mass transport is a limiting factor. Stirring the cell during the experiment gave greater reduction peaks as the product is cleared from the electrode surface reducing the boundary.

3.1.4.1. Comparing electrode materials

Comparing all the electrode materials polished with alumina slurry gives contrasting results for the oxygen and methyl viologen experiments. With methyl viologen, the PGE electrode gave the greatest current peaks, followed by the GC electrode and the PGB electrode gave the lowest. However, for oxygen the GC electrode gave the greatest current peaks, then the PGE electrode and finally the PGB electrode. So with regards to the size of the current peaks, the PGB electrode gave the lowest peaks for both experiments. The PGE and GC electrodes each gave a greater peak for one reactant. This gives no clear indication of which is the most reactive.

Bringing the electron transfer characteristics and the potential at which the reaction occurs into the picture gives a different result about which electrode is the most reactive. For methyl viologen, the PGB electrode has the fastest electron transfer and the GC electrode the slowest, but for oxygen the PGE electrode is the fastest and the PGB the slowest.

Thus with all electrodes polished with alumina, it is not possible to declare one electrode the "most reactive". Likewise it is not possible to declare one the most reactive for methyl viologen and another for oxygen. The only firm conclusion to draw is that the PGB electrode is the least reactive with oxygen.

3.1.4.2. Comparing polishing compounds

Once again there is no clear winner when comparing the polishing compounds. Each electrode behaves differently to each polishing compound. The GC electrode is clearly the most reactive when polished with the alumina slurry, which gave both the greatest peaks and the lowest potential for the peak. The PGE electrode has a very similar response for the alumina. 0.25 and 0.1 μm diamond polished surfaces, only the 0.5 μm stands out as having the lowest peak and highest potential for the peak. PGB then has a different response again, with alumina giving the peak at the lowest potential, but also having the smallest peak. The 0.5 μm diamond polish gives the greatest peak and appears to be at a lower potential than the other diamond polishes, which are both very similar and have the middle height peak and the greatest potential needed.

From these results it is not possible to conclusively draw which finish gives the greatest peaks in all situations, but it should be stated that the alumina slurry gives the greatest peaks for the GC and PGE electrodes. Also across all three electrodes, the alumina polished electrodes produce their peaks at an equal or lower potential than those of the diamond polished finishes. This shows that polishing with the alumina slurry gives the best electron transfer characteristics. So whilst not being conclusive, the alumina slurry appears to give the most reactive finish.

The other observation worth making is that the 0.1 and 0.25 μm diamond polishes gave fairly similar results. This is not unexpected as they are the two closest polishes in size and material of the group.

3.1.4.3. Conclusion

The results do not give a conclusive best electrode material or best polishing compound. However, the alumina slurry certainly appears to be equally or more reactive in the majority of cases.

As for the best electrode material, there is also no conclusive answer. It comes down to the dynamics of the reaction. As noted in the discussion, electrodes can produce low current peaks but still have fast electron transfer. So ultimately the conclusion of which is the most reactive electrode will be based upon which characteristic is more important in the interaction with proteins at the electrode surface, the peak current or the speed of electron transfer.

3.2. AFM

3.2.1. Introduction

The atomic force microscope can bring to the experiments an insight into the roughness of the electrode surface, an image of an electrode's topology and, using advanced techniques, an indication of its reactivity.

3.2.2. AFM

As discussed in the introduction, the AFM scans the surface on an atomic level giving fine detail of the surface. The fact that it can be used in air and fluid is a

characteristic of the AFM that sets it apart from the other microscopes used in nanotechnology.

Also discussed in the introduction are the different techniques that can be used, in the following sections, contact and tapping modes were used. Unfortunately the GC electrode would not fit under the AFM head, so only the PGB and PGE electrodes could be scanned as these had been designed for this purpose.

3.2.2.1. AFM imaging of electrode surfaces in air

AFM in air is the best method of getting accurate images and topographic data of the electrode surface. The two methods of imaging, tapping and contact are discussed in the introduction.

Figures 3.18 through to 3.25 are a series of scans taken using tapping mode in air showing height and phase images of the different polished finishes on both PGE and PGB.

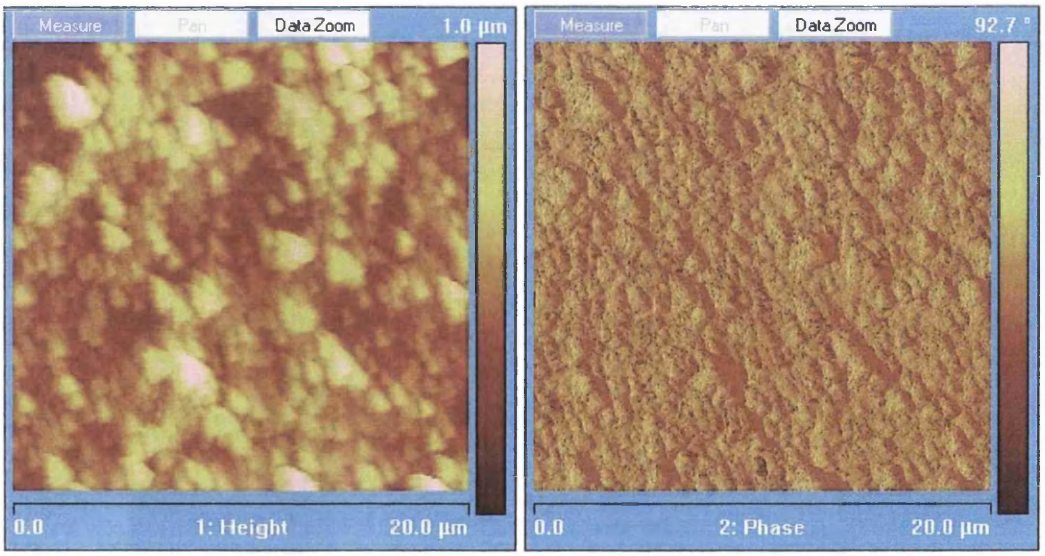

Figure 3.18- Tapping mode AFM images of pyrolytic graphite basal plane polished with alumina slurry

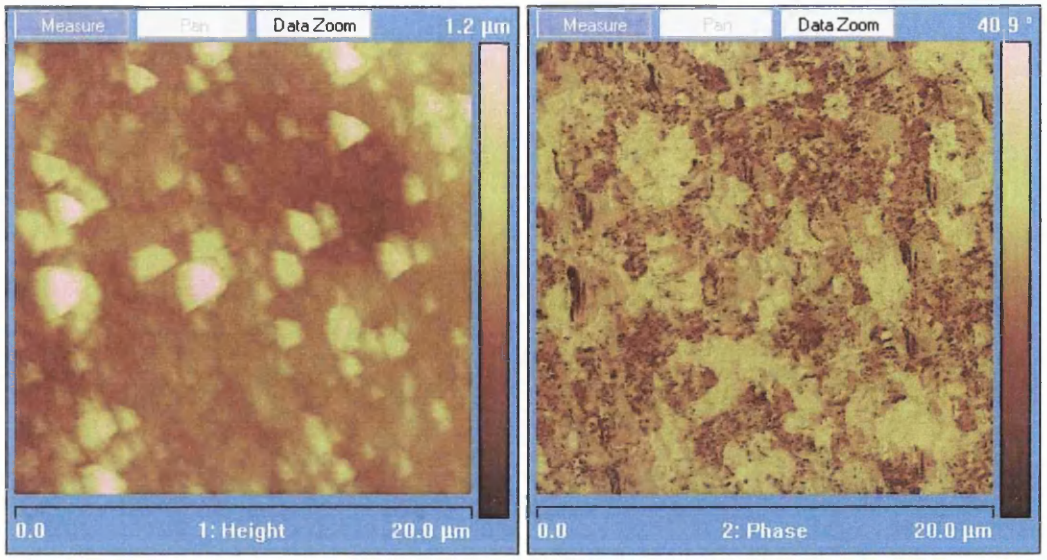

Figure 3.19- Tapping mode AFM images of pyrolytic graphite basal plane polished with 0.5µm diamond paste

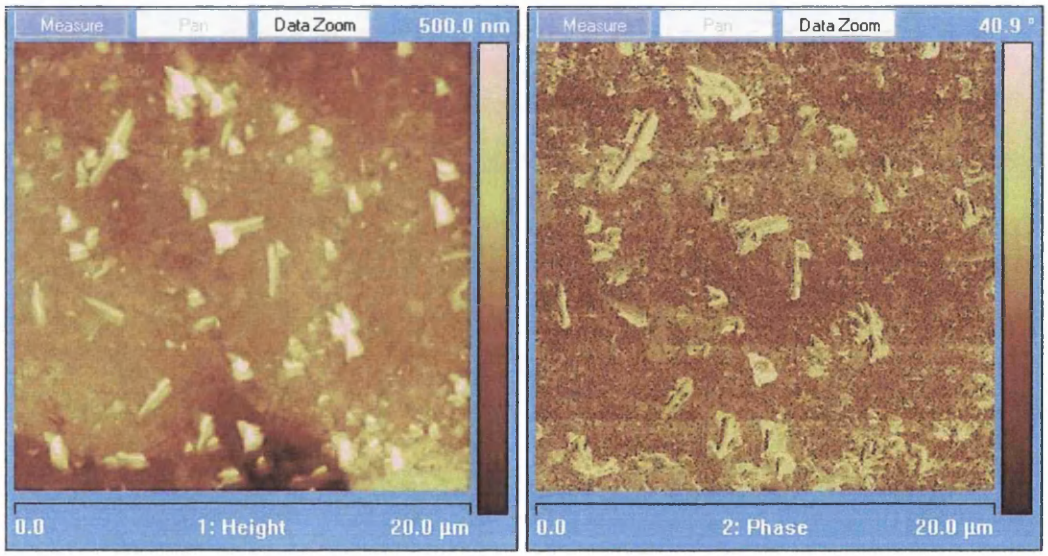

Figure 3.20- Tapping mode AFM images of pyrolytic graphite basal plane polished with 0.25µm diamond paste

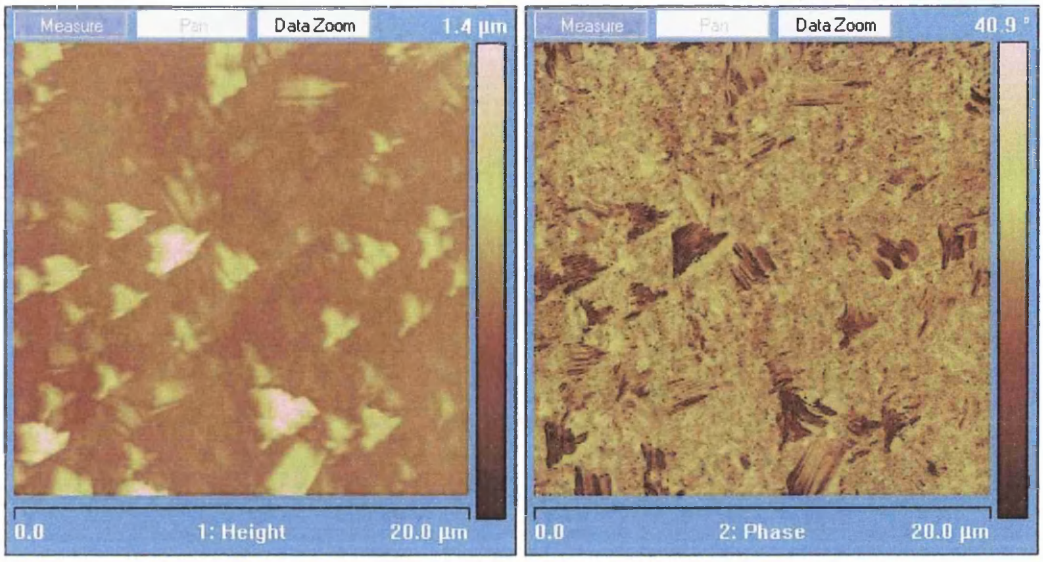

Figure 3.21- Tapping mode AFM images of pyrolytic graphite basal plane polished with 0.1µm diamond paste

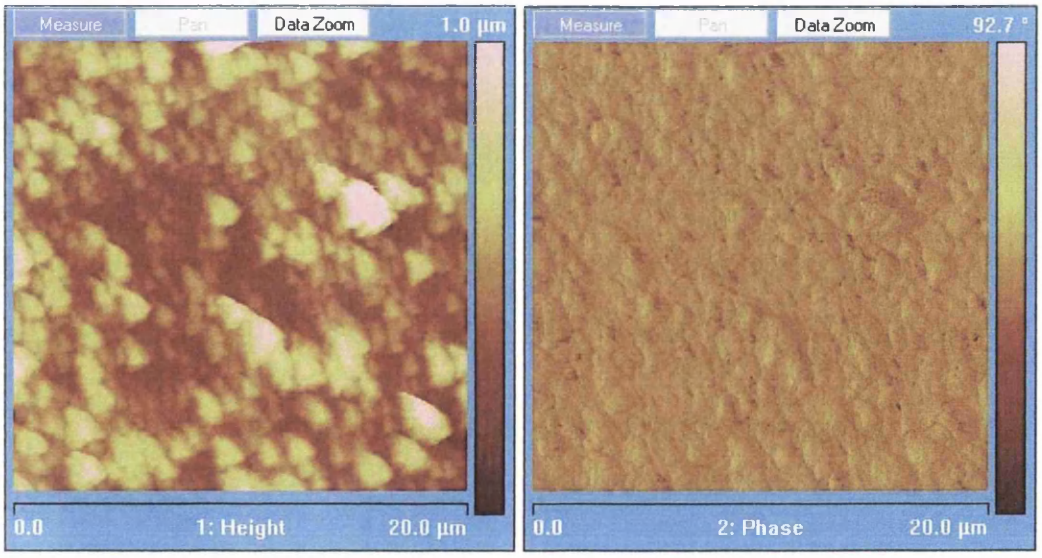

Figure 3.22- Tapping mode AFM images of pyrolytic graphite edge plane polished with alumina slurry

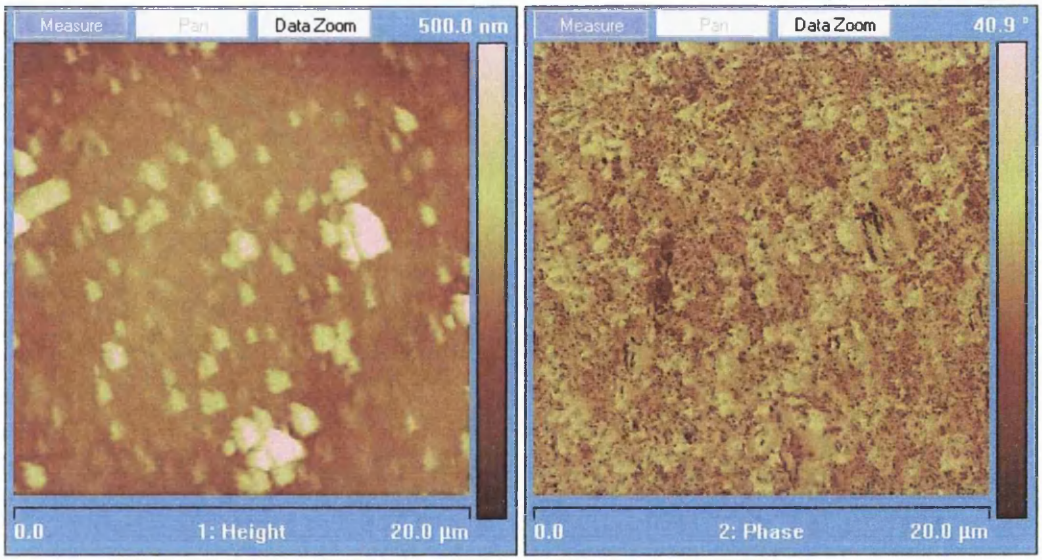

Figure 3.23- Tapping mode AFM images of pyrolytic graphite edge plane polished with 0.5µm diamond paste

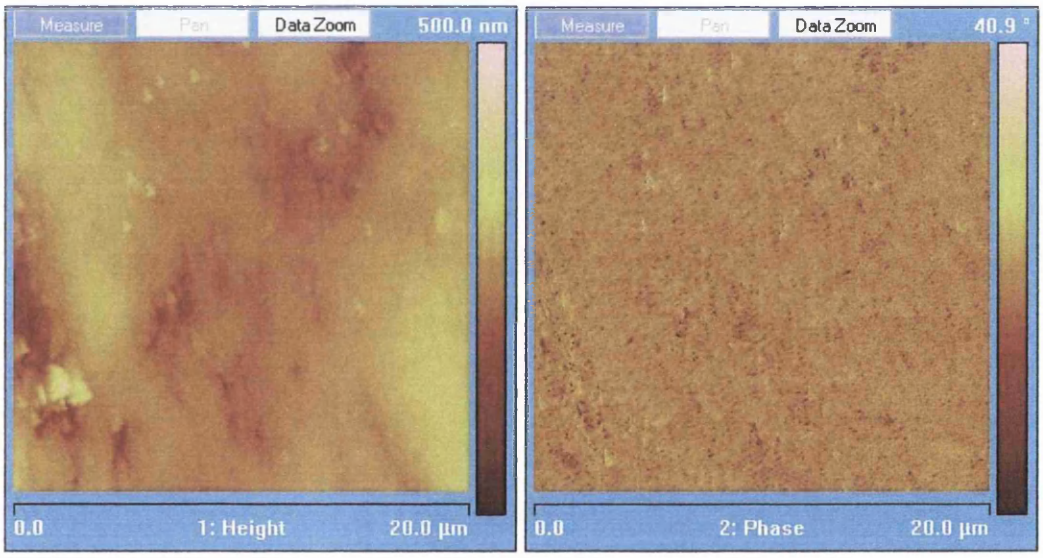

Figure 3.24- Tapping mode AFM images of pyrolytic graphite edge plane polished with 0.25µm diamond paste

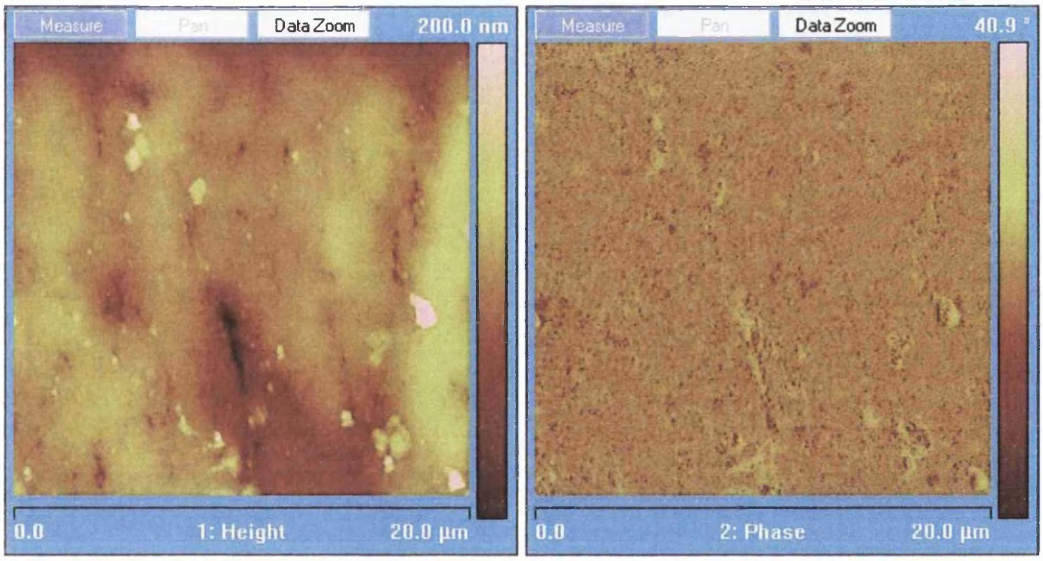

Figure 3.25- Tapping mode AFM images of pyrolytic graphite edge plane polished with 0.1µm diamond paste

Comparing the images, both of the alumina slurry polished electrodes stand out from the diamond polished electrodes as they have more rounded peaks and troughs on the surface. The diamond polishes by comparison seem to have smooth surfaces with irregularly shaped peaks dispersed more sparsely over the surface. As the electrodes were flushed and thoroughly sonicated before the scans, there should be little debris on the surface, so these peaks could be graphite crystals left on the surface after polishing, or deeply embedded clumps of the diamond from the polishes. Figures 3.26 to 3.33 below are 3D representations of the height scans shown in figures 3.18 to 3.25.

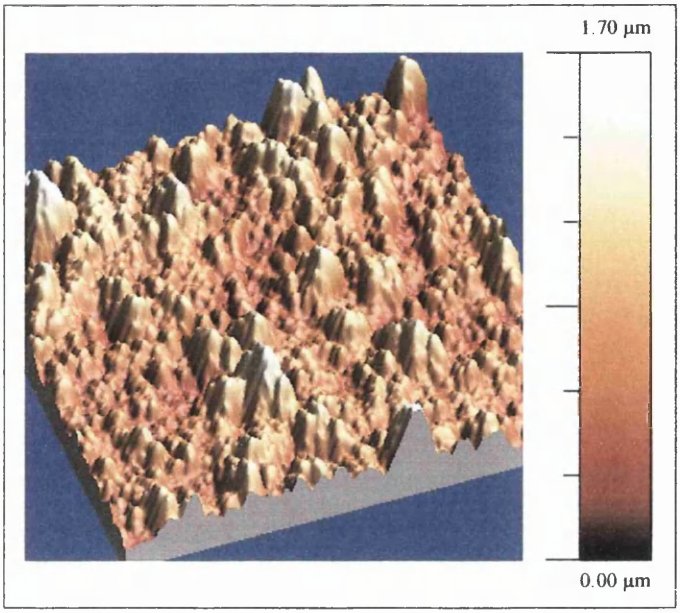

Figure 3.26- 3D representation of an AFM scan of pyrolytic graphite basal plane polished with alumina slurry

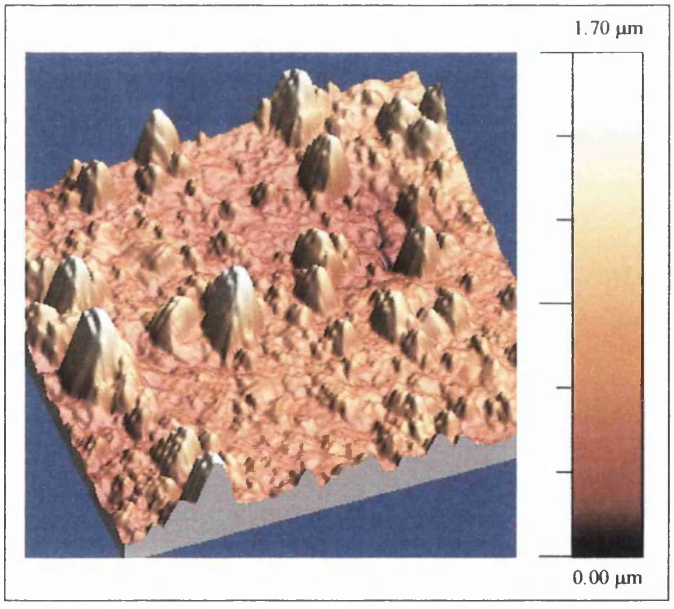

Figure 3.27- 3D representation of an AFM scan of pyrolytic graphite basal plane polished with 0.5µm diamond paste

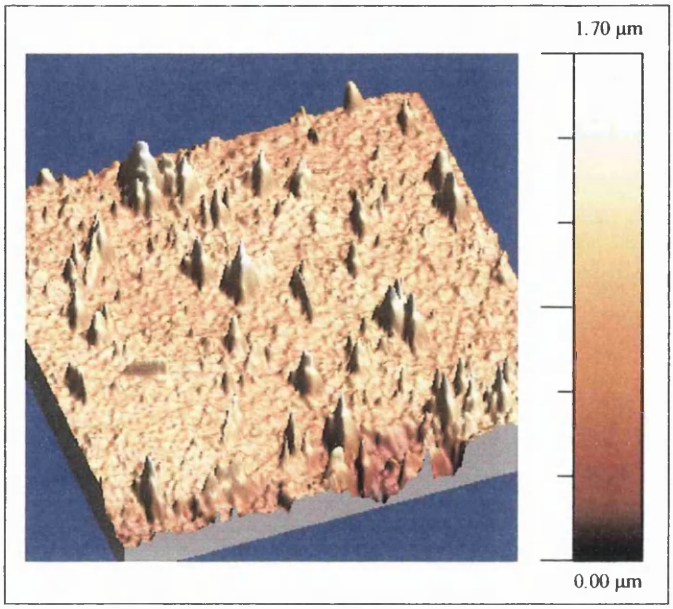

Figure 3.28- 3D representation of an AFM scan of pyrolytic graphite basal plane polished with 0.25µm diamond paste

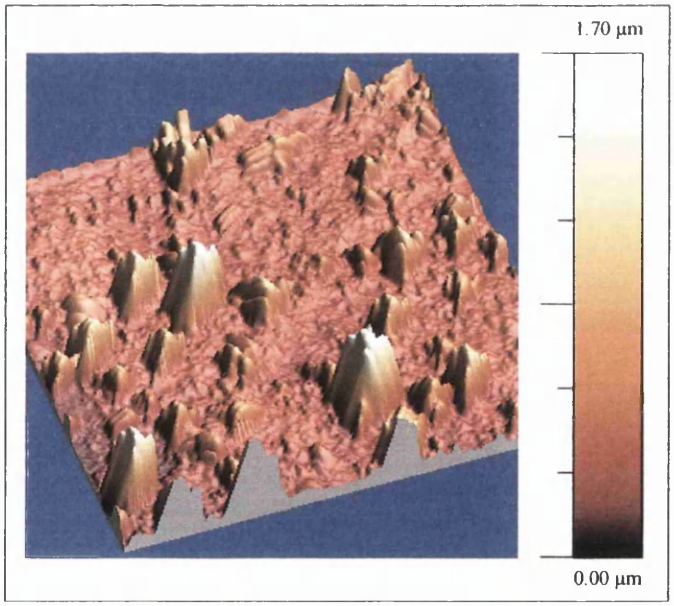

Figure 3.29- 3D representation of an AFM scan of pyrolytic graphite basal plane polished with 0.1µm diamond paste

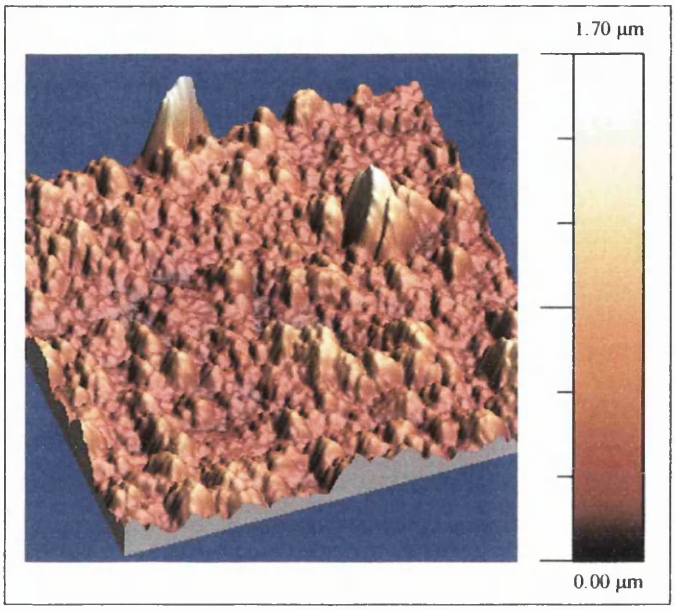

Figure 3.30- 3D representation of an AFM scan of pyrolytic graphite edge plane polished with alumina slurry

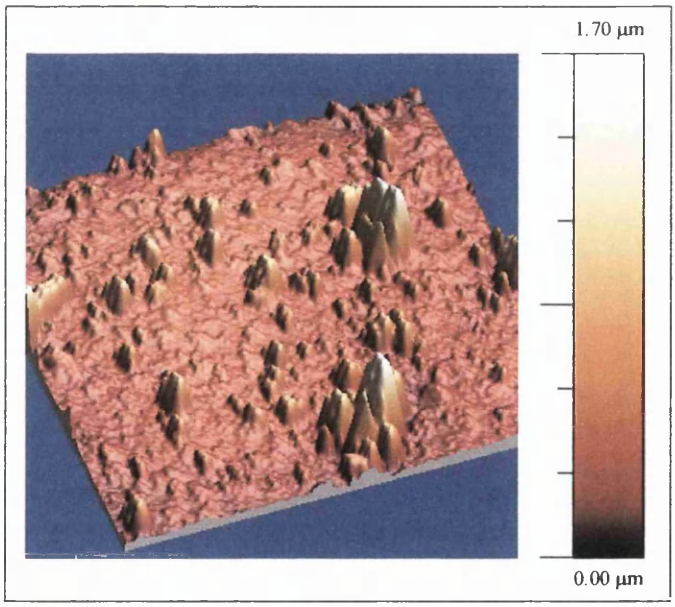

Figure 3.31- 3D representation of an AFM scan of pyrolytic graphite edge plane polished with 0.5µm diamond paste

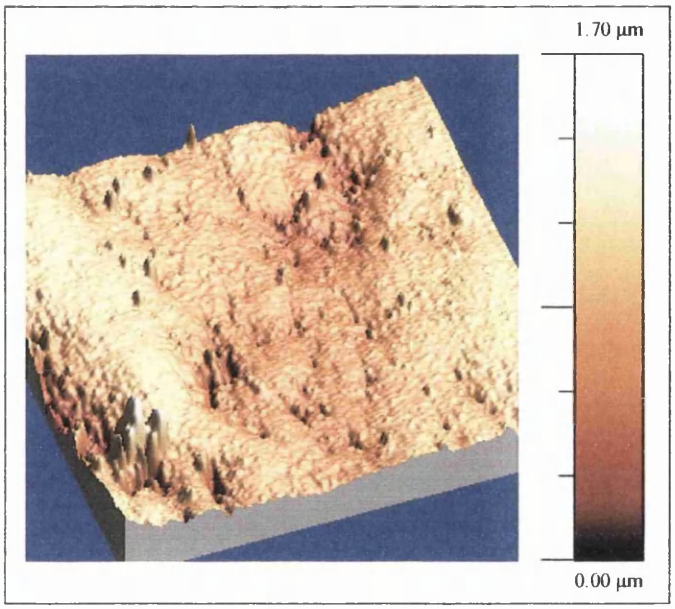

Figure 3.32- 3D representation of an AFM scan of pyrolytic graphite edge plane polished with 0.25µm diamond paste

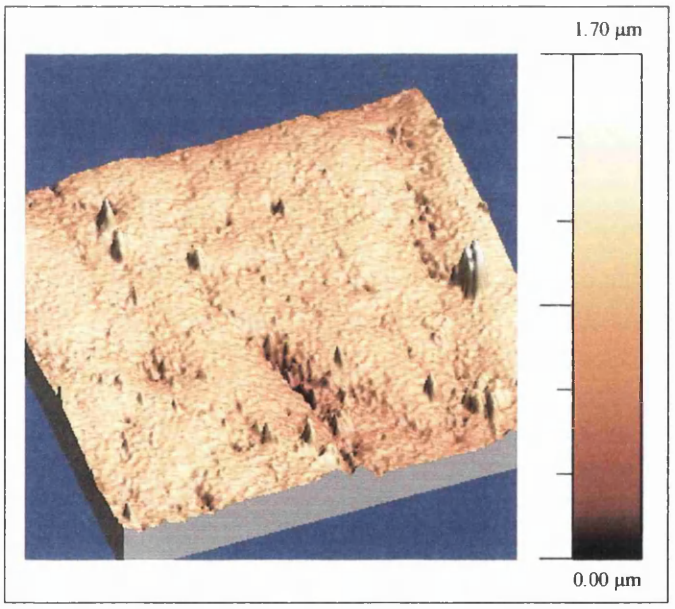

Figure 3.33- 3D representation of an AFM scan of pyrolytic graphite edge plane polished with 0.1µm diamond paste

The 3D images make it clear to see that PGB has a rougher finish than the PGE for every polish. The alumina has the most peaks and troughs but as stated above they are more rounded than the diamond polish. Also as stated above the diamond has fewer peaks, but they are sharper.

Each polish on each electrode results in a different finish, as was hoped. As the grade of the polish gets finer fewer peaks on the surface are apparent. The only similar finishes appear to be that of the 0.25 and 0.1μm diamond polishes on the PGE electrode, otherwise every finish looks different.

3.2.3. Statistical Analysis of pyrolytic graphite electrode surfaces

Polishing the electrodes may give different electrochemical reactions, but what difference does the polishing make to the topology of the electrode? As the AFM creates a picture of the surface from height measurements, these measurements can also be analysed for roughness data. Within the DI software there are options to calculate the roughness for the images. The software calculates the maximum range, the average height and surface area. The surface area is calculated by sum of the area of all of the triangles formed by three adjacent data points in the scan data. It also makes two average roughness measurements, the RMS roughness and the Ra. The RMS is calculated as:

$$Roughness = \sqrt{\frac{\sum Z_i^2}{N}}$$

Equation 3.3.1- RMS roughness

Where Z_i is the height measurements taken in the AFM scan and N is the number of measurements (or samples) taken.

R_a is the mean roughness taken as the arithmetic mean of modulus of the height measurements:

$$R_a = \frac{1}{N}\sum_{j=1}^{N}|Z_j|$$

Equation 3.3.2- Ra, mean roughness

Thus between these measurements it is possible to build up roughness detail of the surface and see how the different finishes change the values.

All scans were taken in tapping mode at arbitrary points on the electrode surface after the electrode has been polished, or coated, flushed with deionised water and allowed to dry. The scans are all 10μm by 10μm except the one set of scans done over 50μm by 50μm for investigating how different scan sizes affect the roughness statistics. The alumina polished PGE was used without re-polishing for the 10μm, 50μm and PDL coated scans. All scans were levelled before the roughness calculations carried out. All average values were calculated as the mean value from at least 10 scans. The error was calculated as the percentage change from the average up to the previous scan, to the average including the last scan.

Table 3.3- The effect of surface finishing methods on RMS roughness of pyrolytic graphite electrodes

Electrode	Surface finish	Average RMS Roughness / nm	Error / %
PGE	Alumina polished (50μm scan)	61.9	1.0
PGE	Alumina polished	45.8	0.2
PGE	0.5μm Diamond polished	39.2	2.4
PGE	0.25μm Diamond polished	12.2	0.3
PGE	0.1μm Diamond polished	24.7	1.3
PGB	Alumina polished	95.8	0.5
PGE	Alumina polished, PDL coated	49.3	2.1

PGE = Pyrolytic Graphite Edge Plane, PGB = Pyrolytic Graphite Basal Plane

Starting with the RMS roughness, shown in table 3.3, comparing a 50μm to a 10μm scan gives a different roughness. This is perhaps not surprising as a larger scan is more likely to pick up more imperfections, but it does show that larger scans could give more accurate results, unfortunately due to time constraints it was not possible to take every scan at a larger size.

Comparing the polished finishes of the PGE electrode, the alumina slurry gives the roughest finish, followed by the 0.5μm diamond polish, surprisingly the 0.1μm diamond polish gave the 3rd roughest and the 0.25μm diamond polish gave the smoothest finish. As the 0.1μm polish was used after the 0.25μm the difference could either be down to the positions at which the samples were taken being rougher, but as the values were all fairly similar it is more likely the polish gives a rougher finish.

Comparing the PGB to the PGE, the PGB gives a rougher finish. PDL coating the electrode also gives a slightly rougher finish.

Table 3.4- The effect of surface finishing methods on Ra roughness of pyrolytic graphite electrodes

Electrode	Surface finish	Average Ra / nm	Error / %
PGE	Alumina polished (50μm scan)	43.7	0.8
PGE	Alumina polished	31.7	0.5
PGE	0.5μm Diamond polished	17.4	1.4
PGE	0.25μm Diamond polished	7	1.6
PGE	0.1μm Diamond polished	14.2	3.8
PGB	Alumina polished	70.1	0.7
PGE	Alumina polished, PDL coated	36	2.0

PGE = Pyrolytic Graphite Edge Plane, PGB = Pyrolytic Graphite Basal Plane

As might be expected, the R_a calculations give different results for the roughness, but the pattern of the results is the same as the RMS roughness. Comparing table 3.4 and 3.3, once again the 50μm scan is rougher than the 10μm. The polishes are ordered alumina, 0.5μm, 0.1μm 0.25μm diamond, from roughest to smoothest and both PGB and PDL coated PGE have a rougher finish that the alumina polished PGE.

Table 3.5- the effect of surface finish on the surface area of scans of pyrolytic graphite electrodes

Electrode	Surface finish	Average Surface Area / μm²	Error / %
PGE	Alumina polished (50μm scan)	2704	0.19
PGE	Alumina polished	122.7	0.3
PGE	0.5μm Diamond polished	110.8	0.08
PGE	0.25μm Diamond polished	102.3	0.04
PGE	0.1μm Diamond polished	105.4	0.06
PGB	Alumina polished	137	0.24
PGE	Alumina polished, PDL coated	110.6	0.39

PGE = Pyrolytic Graphite Edge Plane, PGB = Pyrolytic Graphite Basal Plane

The surface area of the electrode could be an important factor, as the greater the area, the more protein could potentially attach to the electrode. When considering the size of scan, in this case 10μm by 10μm or 50μm by 50μm, the projected area is considered which does not take into account the vertical variations in the surface. Comparing the size of the actual surface area to the projected area you can get a percentage increase in area. Considering the data in table 3.5, the 50μm

scan the projected area is 2500μm^2, the increase in the real surface area over the projected area is 8.2%, which is much less than the 22.7% increase of the 10μm scan. This is at odds with the roughness data, which shows the larger scan to be rougher and would imply that the larger scan would have the larger area increase. Thus the key is to consider the roughness and surface area differently.

Comparing the polished finishes, the alumina has the greatest surface area, with a 22.7μm^2 increase over the 100μm^2 of the projected area. The 0.5μm diamond polish is the second greatest area with a 10.8μm^2 increase, 0.1μm is the third with a 5.4μm^2 increase and once again 0.25 has the lowest value with just a 2.3μm^2 increase. This pattern does follow the roughness data above, despite the two apparently not being directly linked.

The PGB has a surface area increase of 37μm^2, the greatest by some margin, giving the greatest surface area of all the electrode finishes. The PDL coating on the electrode, which has an increase in 10.6μm^2 over the projected area, actually has an area 12.1μm^2 less than that of the alumina surface that is coated, this is despite having a rougher finish. This would seem to imply that the PDL fills some of the topographic features on the surface of the electrode, resulting in a flatter surface, but the PDL coating is in itself rougher than the surface of the electrode.

Not considering the actual data, but the accuracy of the data for a minute, it should be noted that the variation between one scan and the next is considerably less than for the roughness measurements. The surface area seems to fluctuate far less and hence might be considered to be a more accurate measurement.

Table 3.6- the effect of surface finish on average height measurements for scans of pyrolytic graphite electrodes

Electrode	Surface finish	Average Height / nm	Error / %
PGE	Alumina polished (50μm scan)	299	1.8
PGE	Alumina polished	214.4	0.2
PGE	0.5μm Diamond polished	223.1	4.0
PGE	0.25μm Diamond polished	61.4	1.9
PGE	0.1μm Diamond polished	136.6	19.8
PGB	Alumina polished	346.5	0.1
PGE	Alumina polished, PDL coated	239.2	8.2

PGE = Pyrolytic Graphite Edge Plane, PGB = Pyrolytic Graphite Basal Plane

The average height measurements, shown in table 3.6, follow the same patterns as the roughness, which makes sense as the measurements are both based on the height. Two notable points are that the average height of the PDL scan is 15.9nm higher as the surface has been coated and that whilst in the cases of the alumina polished PGE and PGB the measurements are accurate with a difference of a fraction of a percent, in the case of the 0.1μm diamond polished PGE the measurement there is almost a 20% variation to the previous measurement. This would imply that the measurements vary greatly from one scan to another requiring a much greater sample for accurate data.

Table 3.7- Maximum range of scans of pyrolytic graphite electrodes

Electrode	Surface finish	Average Max Range /nm	Error / %
PGE	Alumina polished (50μm scan)	1015	1.4
PGE	Alumina polished	562.4	0.03
PGE	0.5μm Diamond polished	729.6	2.1
PGE	0.25μm Diamond polished	233.2	0.4
PGE	0.1μm Diamond polished	412.1	3.5
PGB	Alumina polished	917.3	0.98
PGE	Alumina polished, PDL coated	546.5	6.3

PGE = Pyrolytic Graphite Edge Plane, PGB = Pyrolytic Graphite Basal Plane

The maximum range data in table 3.7 follows some of the same patterns of results seen above in the other data, but also shows some differences. The 50μm scans show a much greater range than 10μm, this makes sense as the larger scan is more likely to pick up a higher peak or lower trough that a smaller scan. Interestingly the 0.5μm diamond polish has a larger max range than the alumina polish. As all the other measurements in some way average out the data, this is the only one to pick the raw peak and trough heights and compare them. Thus it can be theorised that the 0.5μm polished surface has a low number of sharp peaks, which gives the greater range, whilst averaging over the larger area these features are not apparent as most of the surface is flat.

In agreement with the other data, the 0.1μm diamond polish has a greater range than the 0.25μm and the PGB has a greater range than the PGE.

The PDL coating has a lower maximum range than the uncoated alumina polished sample, once again supporting the theory that the PDL is filling in some of the

topographical features. This result should come with an attached warning though as the error of 6.3% on the range of 546.5nm gives a range of 512.1 to 580.9, which makes the alumina polished result within the range of the results for the PDL coated surface.

3.2.3.1. Statistical analysis of laccase on the a PGE electrode

Following the statistical analysis of the electrodes, another set was carried out this time with and without a coating of laccase on the surface of the PGE electrode. The electrode was polished, flushed with deionised water and left to dry. Then the electrode was scanned with the Explorer AFM, compiling the polished results. The electrode was then covered with a solution of 10mg/ml laccase from *Rhus vernificera* in phosphate buffer (50mM, pH 7.0) and left to dry for 20 minutes. The electrode was then gently flushed with deionised water and allowed to dry again. The AFM scans were then repeated for the coated electrode. The conditions were as above for the statistical analysis.

Table 3.8- Comparison of RMS roughness between polished PGE electrode and laccase coated electrode

Electrode	Surface finish	Average RMS Roughness / nm	Error / %
PGE	0.5μm Diamond polished	25.1	0.28
PGE	0.5μm Diamond polished, Laccase coated	35.3	7

PGE = Pyrolytic Graphite Edge Plane

Table 3.9- Comparison of R_a roughness between polished PGE electrode and laccase coated electrode

Electrode	Surface finish	Average Ra / nm	Error / %
PGE	0.5μm Diamond polished	14.6	1.1
PGE	0.5μm Diamond polished, Laccase coated	23.4	5.1

PGE = Pyrolytic Graphite Edge Plane

Both the RMS and R_a roughness measurements show that the electrode is rougher after being coated with the laccase. Hence it may be deduced that at least some of the protein has attached to the surface.

Table 3.10- Comparison of surface area between polished PGE electrode and laccase coated electrode

Electrode	Surface finish	Average Surface Area / μm²	Error / %
PGE	0.5μm Diamond polished	109.5	0.17
PGE	0.5μm Diamond polished, Laccase coated	116.8	0.1

PGE = Pyrolytic Graphite Edge Plane

The surface area also increases with the laccase coating, also implying that the laccase may have attached to the surface of the electrode.

Table 3.11- Comparison of average height between polished PGE electrode and laccase coated electrode

Electrode	Surface finish	Average Height / nm	Error / %
PGE	0.5μm Diamond polished	219.2	1.6
PGE	0.5μm Diamond polished, Laccase coated	175	7.2

PGE = Pyrolytic Graphite Edge Plane

Table 3.12- Comparison of maximum range between polished PGE electrode and laccase coated electrode

Electrode	Surface finish	Average Max Range /nm	Error / %
PGE	0.5μm Diamond polished	510.2	2.2
PGE	0.5μm Diamond polished, Laccase coated	471	6.3

PGE = Pyrolytic Graphite Edge Plane

Both the average height and max range decrease. So assuming the laccase has attached to the surface of the electrode, it appears to have done so in the troughs on the surface, decreasing the range of measurements taken, although more studies would need to be done to confirm this.

3.2.4. Other AFM techniques

During the work with the AFM some other techniques were investigated, but were not used in the ultimate set of experiments. However, it is felt they should be included in this study for completeness. The techniques, Conducting AFM and Electromagnetic Force Microscopy, involve the charging of the electrode so could be suitable areas for further investigation

3.2.4.1. Conducting AFM (C-AFM)

As described in the introduction C-AFM involves the charging of the surface or tip during a contact scan. The current is then measured at each sample point of the scan as well as the height and friction data.

Figure 3.34 shows all three scans for a section of a pyrolytic graphite edge plane electrode. Although the height scan is not the clearest of images, it can be seen that there is a relatively flat plane in the upper right half of the image and a rough area in the bottom left. When analysing the height with the C-AFM current image, it is possible to see that the plane is conducting and the rough area is only conducting in some areas, mostly around the edge of the peaks. Perhaps more interesting is when comparing the current and friction images. The areas where current flows tend to match the areas of higher friction, this can be more clearly seen in figure 3.35 where the current has been subtracted from the friction scan to form an overlay.

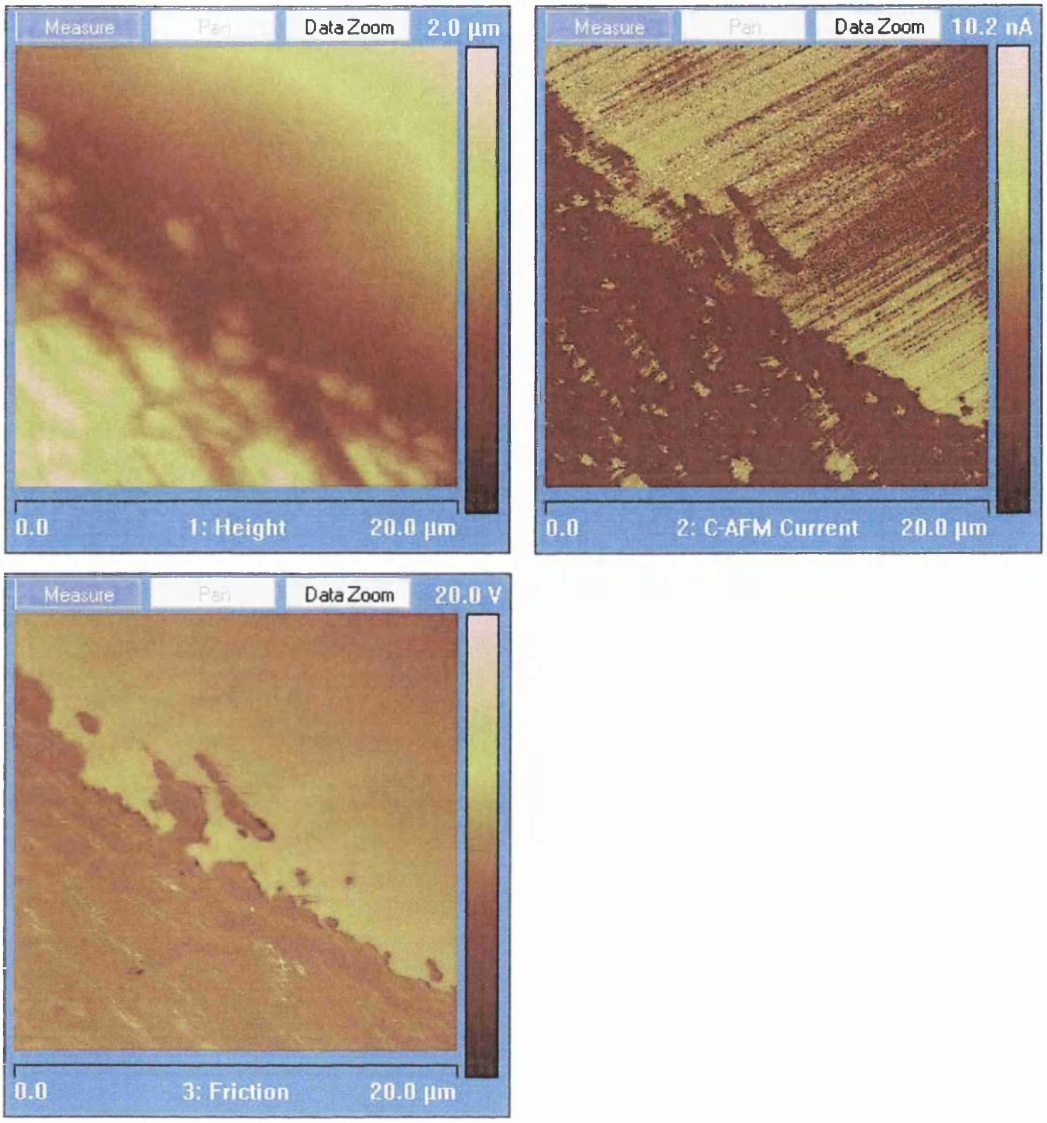

Figure 3.34- Conducting AFM scans of a pyrolytic graphite edge plane electrode showing height, current and friction

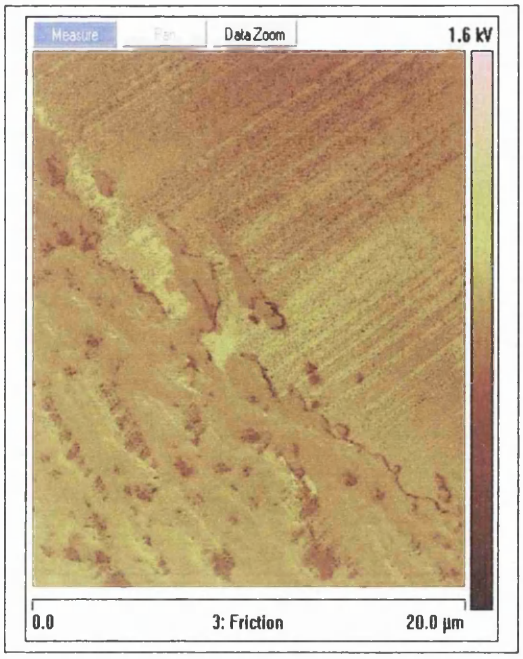

Figure 3.35- Conducting AFM friction scan with current scan subtracted (factor of 0.5 applied to current)

Another scan to show the C-AFM was across the boundary of PGE and the non-conduction epoxy mounting the electrode was set in, this is shown in figure 3.36. In this image the PGE is on the left of the image and the epoxy on the right. Once again the current is the overlaid, but this time over the height, in figure 3.37.

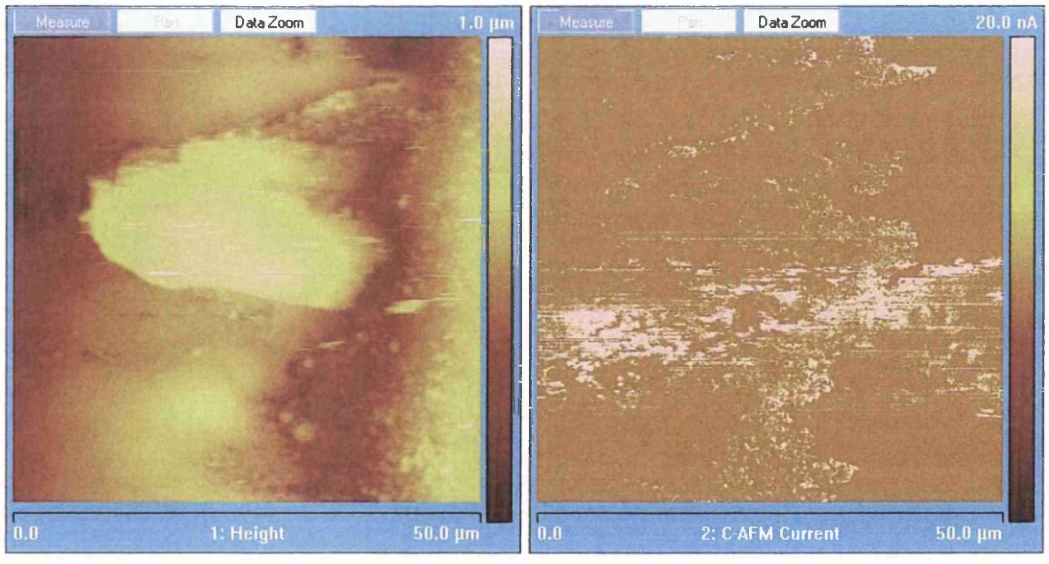

Figure 3.36- Conducting AFM scan of a pyrolytic graphite edge plane electrode's boundary with epoxy resin

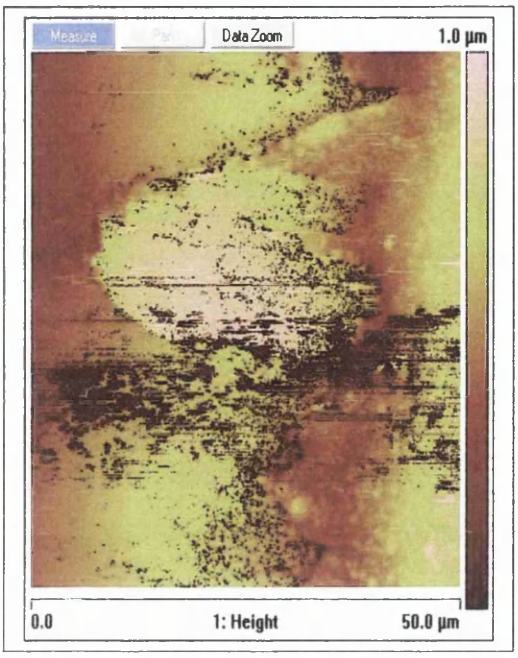

Figure 3.37- Conducting AFM height scan with current scan subtracted (factor of 2 applied to current)

The areas of current, on the whole, follow the edge of the electrode and around the higher area, which may be a pyrolytic graphite crystal. However, around 30µm down the image, current can be seen all across the image and into the epoxy, which is an insulator, so potentially this could be caused by external noise. Thus, any scans taken with the C-AFM should be carefully analysed before being taken as accurate.

Another issue with the C-AFM was that it could only measure small currents, hence needing a sample to have a resistance of over 1 kΩ, making it unsuitable for use with electrodes without them first being modified.

3.2.4.2. Electromagnetic Force Microscopy (EFM)

In a similar way to C-AFM, EFM uses a special cantilever and charges the sample. However in EFM there is no contact or current flow, instead the cantilever is vibrated above the sample and phase analysed. So to get an image of the underlying topology the AFM is run in interleave mode, a line of the surface is scanned and then the tip raised and the line rescanned for the EFM.

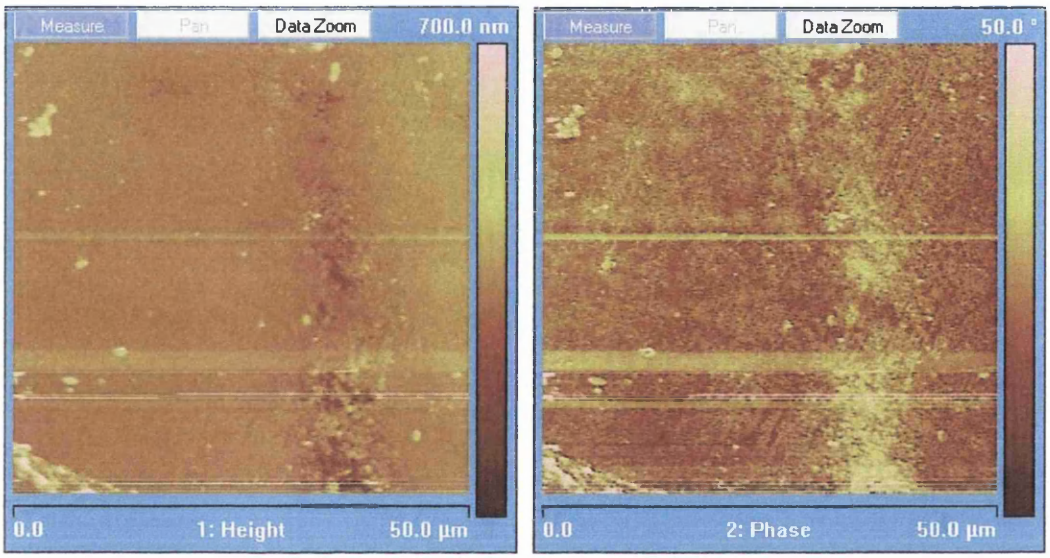

Figure 3.38- Electrostatic Force Microscopy scan of a pyrolytic graphite edge plane electrode

In figure 3.38 the height image shows the height surface and the phase image shows the EFM scan, the phase above the image. What can be seen is that field is strongest around the faults on the surface. The main flat surface of the electrode gives little field, areas with peaks and troughs give a stronger field signified by the greater phase change.

3.2.5. Discussion

The AFM proves a powerful tool when investigating the properties of a surface. Not only can you see in detail the topology, but also can find out more about the surfaces properties.

Through both subjective viewing of topology images and statistical analysis, PGB has shown itself to be the rougher of the two electrodes. Each different polish has been shown to give a different surface finish too.

Alumina slurry has proved to give the roughest surface, covered with peaks and troughs. Then 0.5μm diamond polish is the next roughest, not having peaks all over like the alumina slurry, but having fewer and sharper peaks. Surprisingly, the 0.25μm diamond polish gives a smoother finish than the 0.1μm, but both show similar topology on PGE and have the closest statistics. This similarity is also seen in the electrochemical responses in chapter 3.1, where the responses are similar for both the 0.25 and 0.1μm diamond polishes.

Although not used in detail, both C-AFM and EFM have shown that current appears to flow, and the greatest electromagnetic fields are around the edges of surface defects, be they the edge of a crystal, a peak or a scratch. C-AFM has also shown the current to flow in areas where the friction is higher, this would imply that these areas are more reactive and hence would be the sites where any electrochemical reaction and protein bonding may occur.

If these are the areas that the reactions take place at, then it would follow that the alumina slurry would give the best electrochemical response as it has the most peaks and troughs hence the most "edges". This corresponds to section 3.1 also, in which, despite not being a clear winner, the alumina had shown itself to be at least as good as all the diamond polishes.

The interesting result is that despite the PGB being the rougher electrode when polished with the same compound, and hence has more peaks and troughs, it was not as reactive in the electrochemistry. It did however have fast electron transfer characteristics with the methyl viologen. So, this could be attributed to the basal plane being the less reactive of the two materials, even after modification.

The statistical analysis of laccase on the surface has shown that reduces the maximum range of the peak to trough heights was reduced, implying that the laccase bonds in the trough. If this is the case then once again the alumina finish could prove to be the best, as these are potentially more sites for the protein to attach itself to the electrode.

Whilst not being used within the context of this work on the electrodes, the use of the AFM to image double layers also has the potential to be a powerful tool in the investigation of electrodes, see appendix IV. The double layers can be seen to exert a force in relation to the ionic strength of the solution used, thus charging the electrode could also grow or collapse the double layers, which will show up as sharper or less sharp images. The charging of the electrode could be fairly easily achieved using a simple potentiostat, such as the one designed and constructed in appendix III The possibilities of future work with double layers will be discussed further in chapter 4.

3.2.6. Conclusion

The results of the work on the AFM back up the results of the electrochemistry. Although the surface finish has proved to be important to reactivity of an electrode, it is not as important as the electrode material in the first place, PGB has shown this with having the roughest finish, but poor electrochemical responses.

Alumina slurry has shown itself to be the roughest finish, which when coupled to the findings of the C-AFM and EFM, would show it to be the most reactive and potentially have the greatest number of sites for proteins to attach.

3.3. Proteins on the electrodes

3.3.1. Introduction

Up to this point, PGE polished with alumina has shown itself to be the most reactive electrode, but reactivity in electrochemistry, while potentially being an indicator, does not necessarily translate into a good level of reactivity with proteins. So despite hydrogenase being ruled out because of extraction problems, the testing of proteins continued with other samples.

3.3.2. Proteins

In this study laccase and azurin were chosen to show bioelectrochemical responses and react on the electrode, whilst bovine serum albumin (BSA) was chosen block the electrode and stop the reaction with methyl viologen. All three proteins were sourced from Sigma already extracted. The laccase was from *Rhus vernificera* and the azurin from *Pseudomonas aeruginosa*.

Hydrogenase from *Clostridium pasteurianum* was also going to investigated in this study. However, due to issues with growing the cells and harvesting the hydrogenase in an active state it could not be tested in an electrochemical cell, see appendix II.

All experiments in this section are carried out using the 50mM pH 7.0 phosphate buffer as described in chapter 2.

3.3.2.1. Electrode Blocking with BSA

The theory behind the experiment was that the BSA would attach to the electrode and block the reaction with methyl viologen.

The first experiment was carried out as described in section 2.3.1.6. Where following the test with methyl viologen, BSA was added to the cell and the electrode then allowed to soak for a period of 5 minutes before testing and then a further 20 minutes before retesting. This experiment was carried out with the GC, PGE and PGB electrodes, all polished with alumina slurry. Once again all results were normalised to an area of 1mm^2.

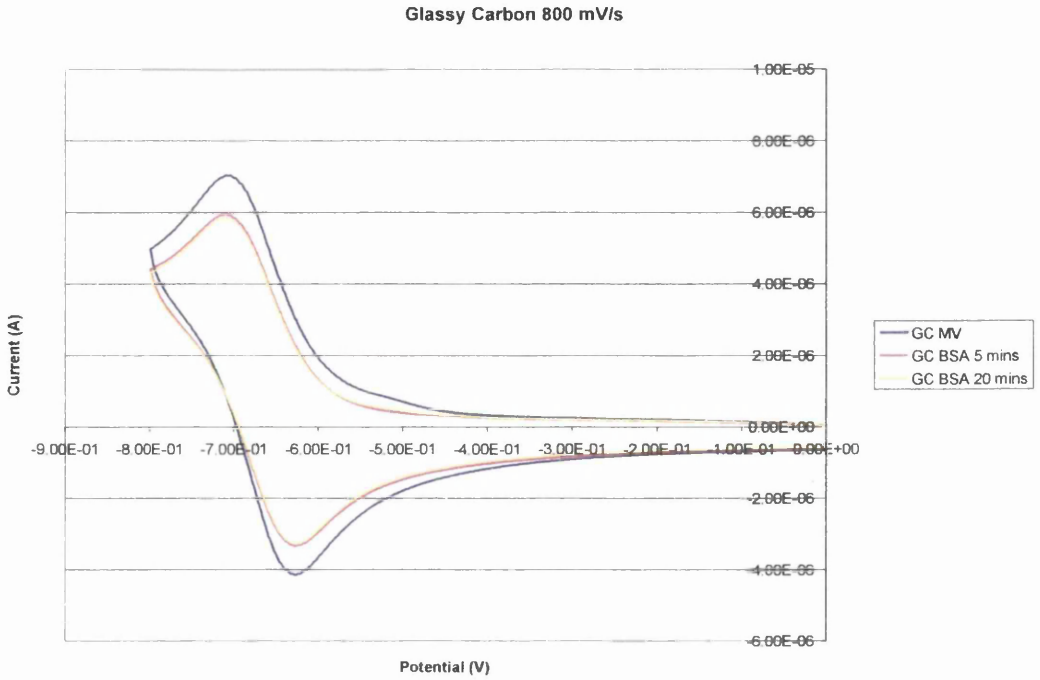

Figure 3.39- CV scan of methyl viologen at a GC electrode, showing the effect of soaking in a BSA solution

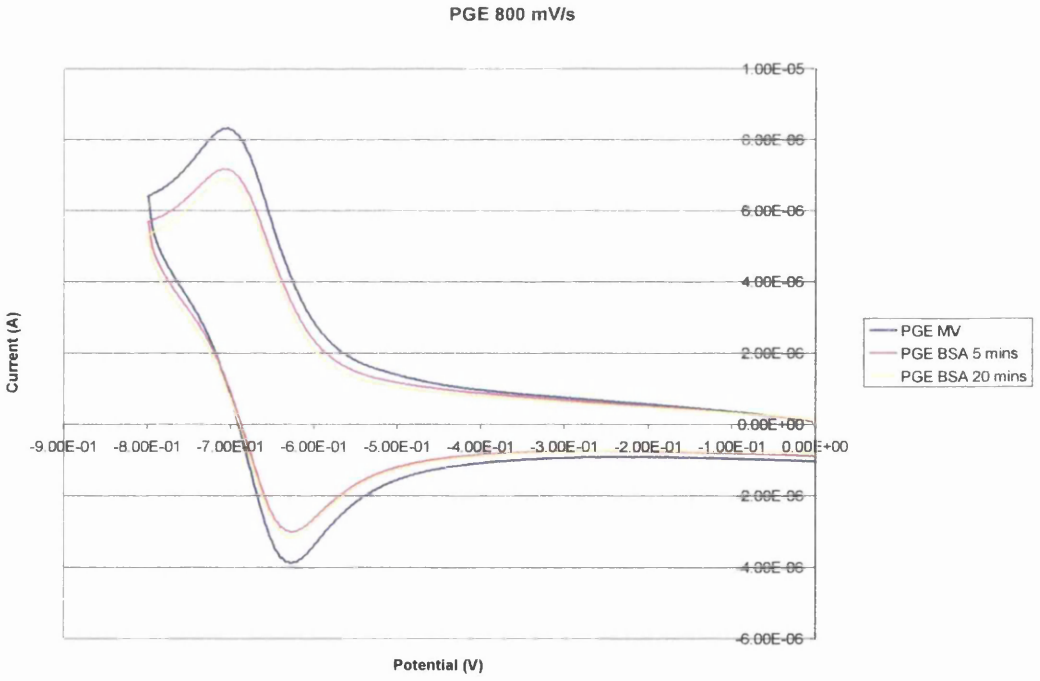

Figure 3.40- CV scan of methyl viologen at a PGE electrode,showing the effect of soaking in a BSA solution

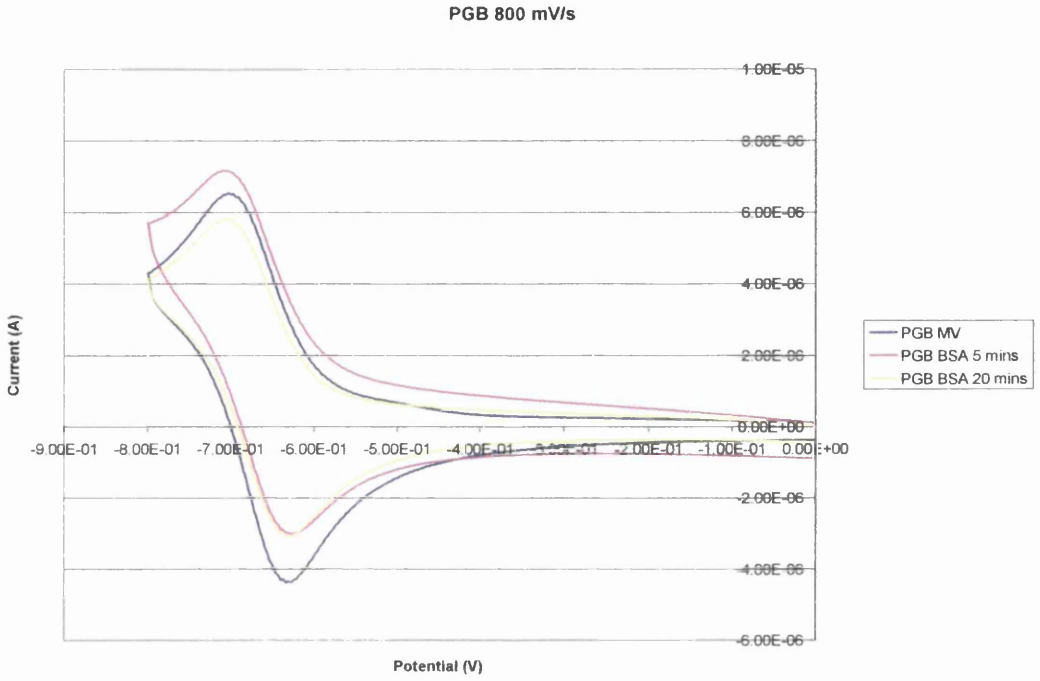

Figure 3.41- CV scan of methyl viologen at a PGB electrode, showing the effect of soaking in a BSA solution

As can be seen in figures 3.39, 3.40 and 3.41, particularly obviously with the GC and PGE, the BSA blocks the reduction and oxidation of the methyl viologen reducing the height of the peaks. Despite having a higher current, the peak current of the PGB soaked in BSA for 5 minutes is actually lower than that of the methyl viologen, around 4.1μA and 4.7μA respectively. This positive current offset was present in repetitions of the experiment, always only on the PGB after soaking for 5 minutes. Reduction of peak heights can be seen in table 3.13.

Table 3.13- Reduction peak heights of methyl viologen with and without BSA blocking the electrode

	Peak currents per mm^2 (μA)		
Electrode	GC	PGE	PGB
Methyl viologen	5.5	5.9	4.7
5 minutes BSA	5.0	4.8	4.1
20 minutes BSA	4.8	4.5	4.6

The further soaking of the electrode for 20 minutes appears to have a small effect on the blocking of the reaction. In the case of PGB, the peak is actually higher after the 20 minutes, around 4.6μA. Thus it appears that the reaction between the BSA and electrode happens within the first 5 minutes.

Looking at the peak separation in figures 3.39, 3.40 and 3.41, the peaks can be seen to separate slightly when the BSA has been added. This is the result of slower electron transfer from the electrode to the methyl viologen, caused either by the electron having to pass through, or along the BSA, or by the fastest and most reactive sites on the electron being blocked, hence the reaction only taking place at less reactive sites.

Comparing the three electrodes, it is clear that PGE not only has the greatest reduction peak for the methyl viologen, but also that the drop in peak is the greatest, both in current and proportionally to the methyl viologen only peak. This would imply that the PGE not only is the most reactive, but also exhibits the best interaction with BSA.

From this experiment it is clear to see that BSA will block the reaction with methyl viologen, but it is not clear if the BSA has attached to the electrode or is staying in solution. So a further set of experiments were run soaking the electrode for a period of 5 minutes, 20 minutes and finally 1 hour, each time allowed to dry and then being tested. The experiment now relies on the BSA bonding to the electrode in order to block it.

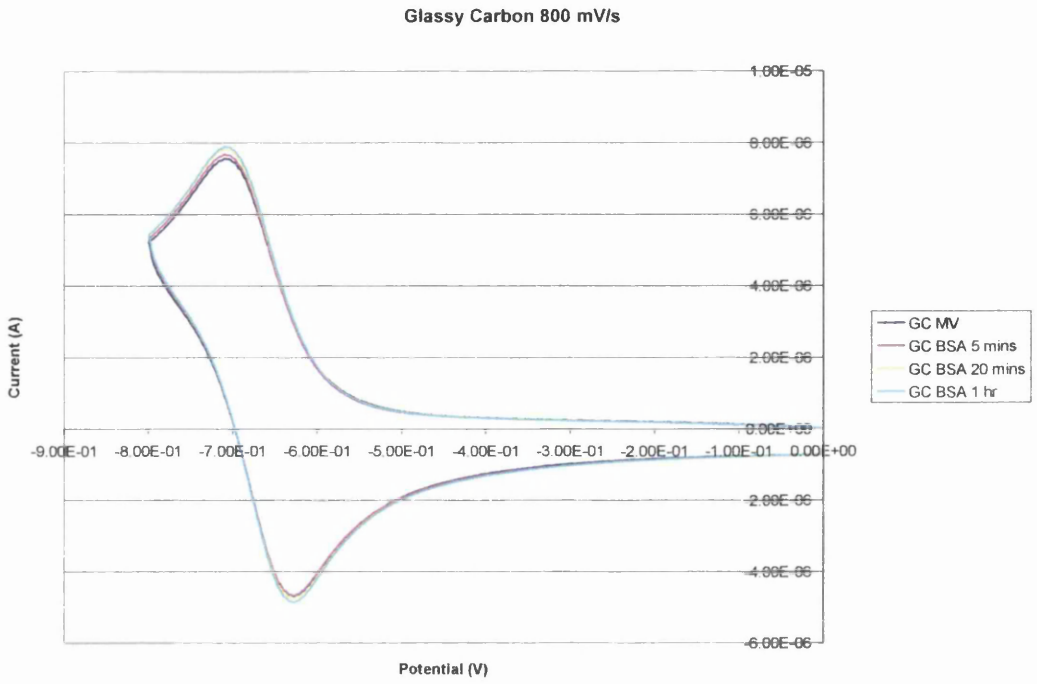

Figure 3.42- CV scan of methyl viologen at a GC electrode, showing the effect of BSA film

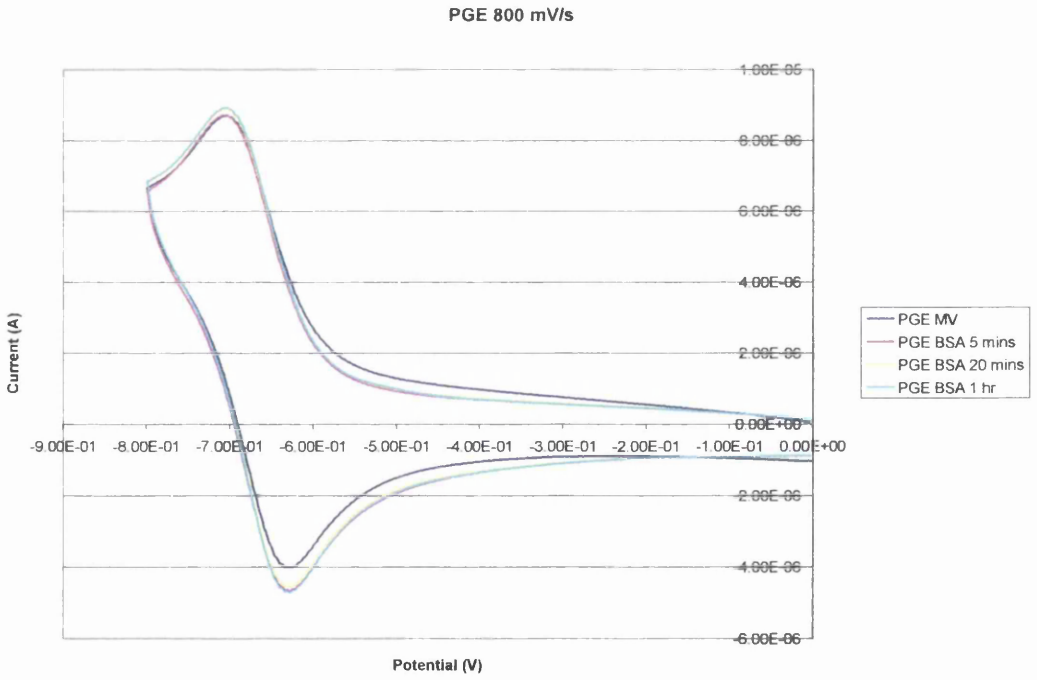

Figure 3.43- CV scan of methyl viologen at a PGE electrode, showing the effect of BSA film

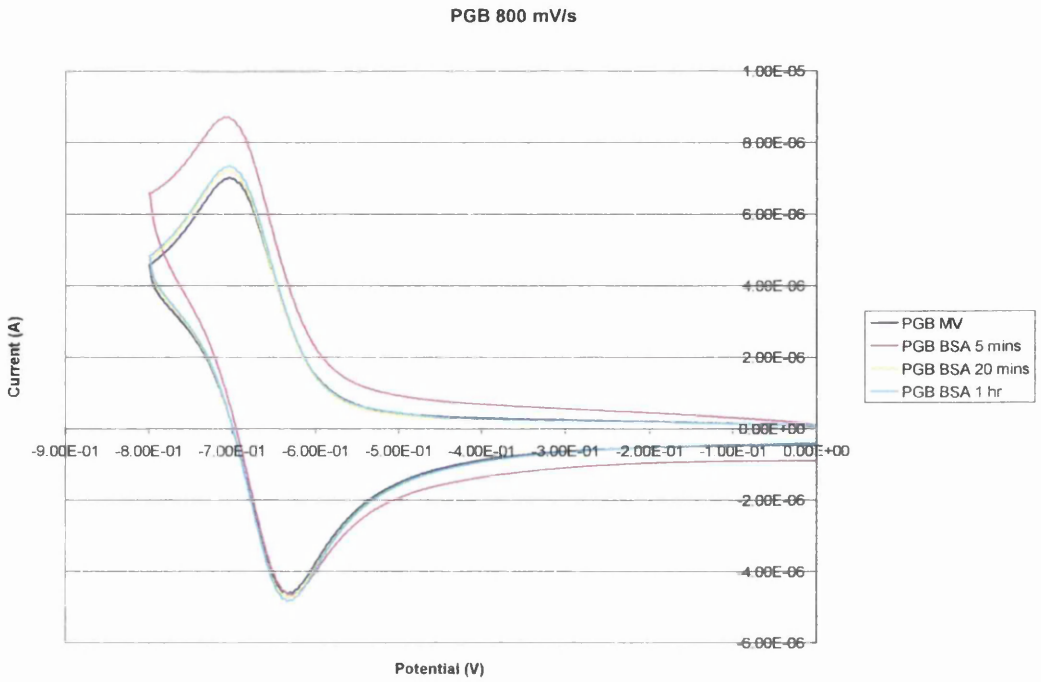

Figure 3.44- CV scan of methyl viologen at a PGB electrode, showing the effect of BSA film

From the results seen for this second experiment, figures 3.42, 3.43 and 3.44, it is clear that the BSA does not stay attached to the electrode. In fact the peaks are similar or greater for all the BSA dipped scans.

So whilst BSA will block the electrode in solution, it will not bond to the electrode. To improve the bonding of the BSA to the electrode a coating of Poly-D-Lysine was investigated.

3.3.2.1.1. Poly-D-Lysine Films and BSA

Poly-D-Lysine (PDL) creates a layer on the surface of the electrode which the BSA can then attach to, so despite not being in direct contact with the electrode it would be held close to the surface. The coating of course acts as another barrier to the electron transfer, so the experiment was run as above for the BSA, but an extra stage was added to apply and test the PDL layer, as described in section 2.3.1.7, before the electrode was dipped into the BSA.

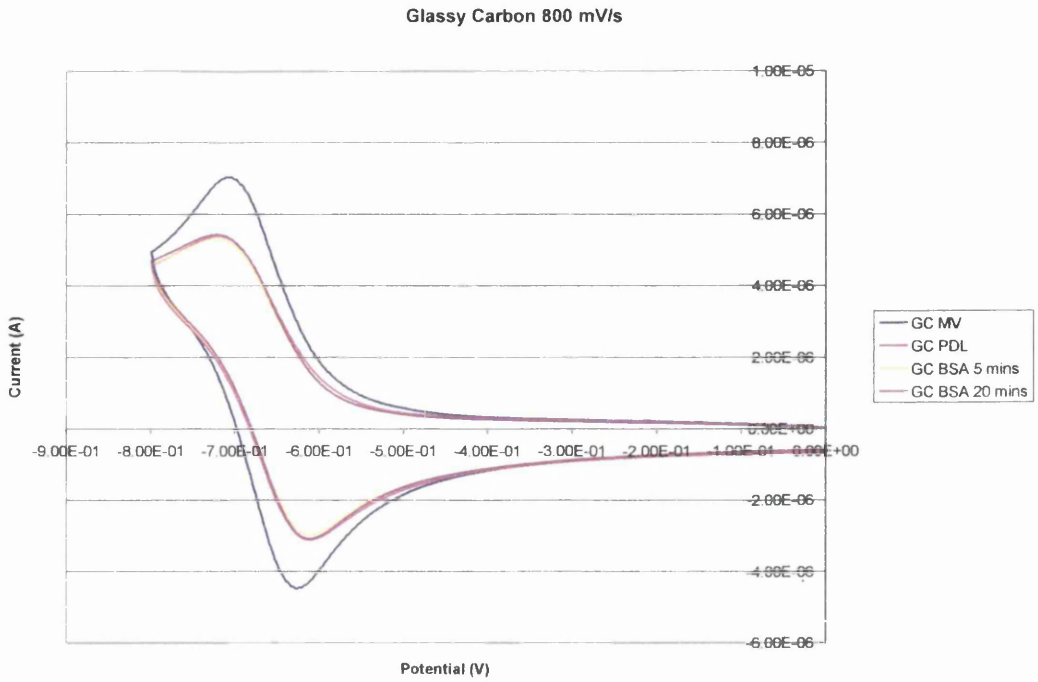

Figure 3.45- CV scan of methyl viologen at a GC electrode, showing the effects of PDL and BSA coatings

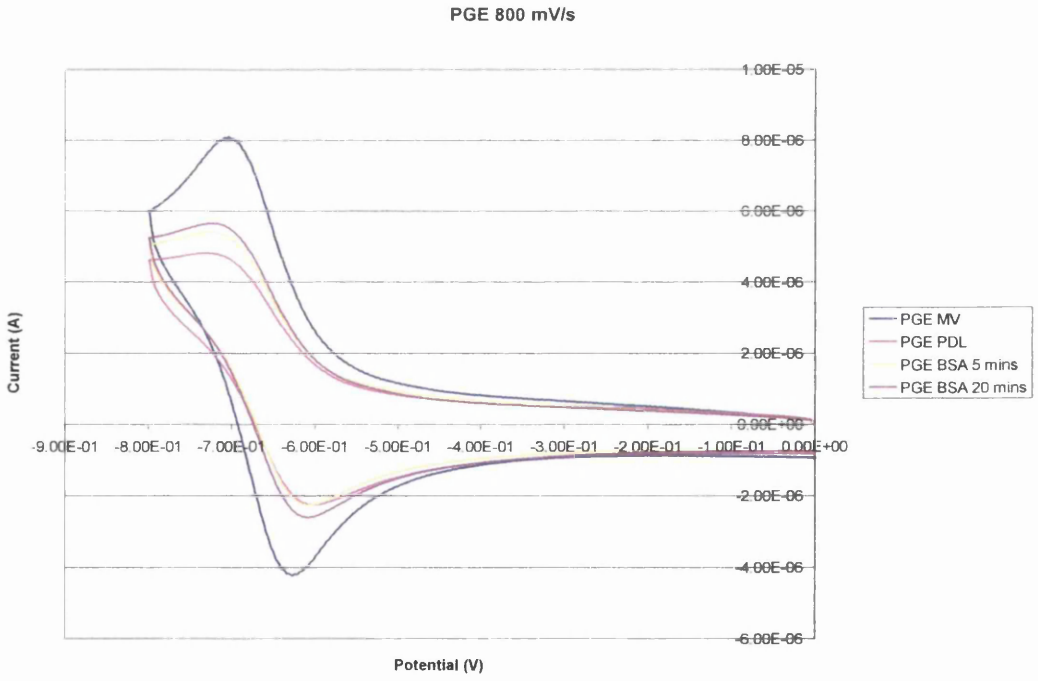

Figure 3.46- CV scan of methyl viologen at a PGE electrode, showing the effects of PDL and BSA coatings

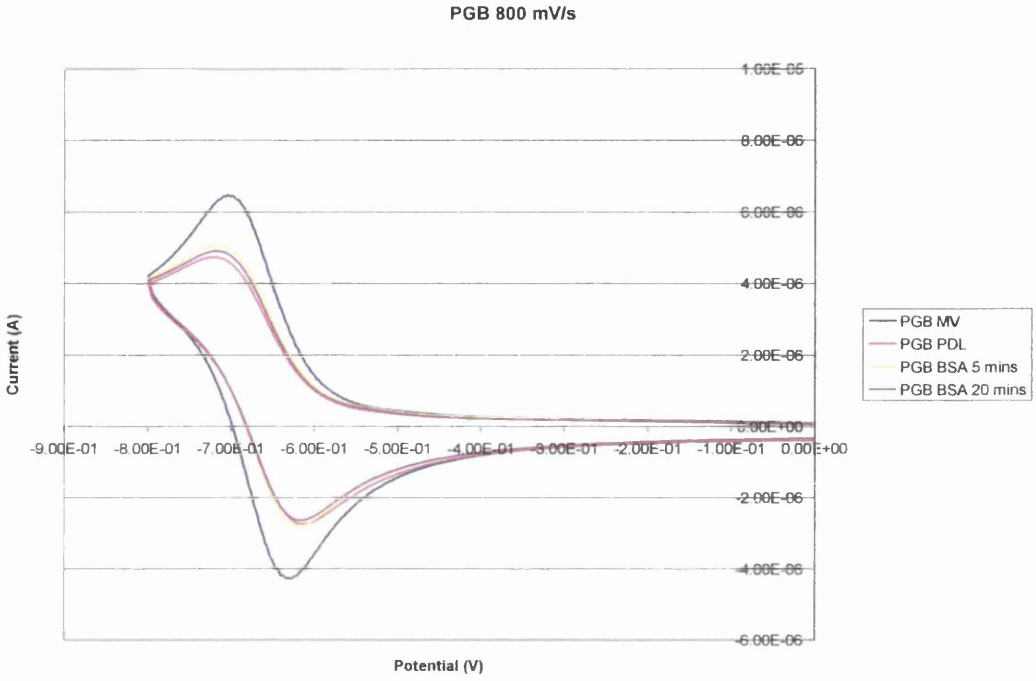

Figure 3.47- CV scan of methyl viologen at a PGB electrode, showing the effects of PDL and BSA coatings

Applying the PDL layer reduces and separates the peaks for all three electrodes, displaying less of a reaction and slower electron transfer as would be expected. Adding the BSA to the electrode on top of the PDL layer has almost no effect. In figure 3.45, the GC electrodes response stays almost exactly the same. Figures 3.46 and 3.47 show that for the PGE and PGB electrode, the response actually improves following the soaking in BSA solution, perhaps as a result of the PDL being washed off the surface. Thus in this instance, it is conclusive that PDL did not improve the bonding of BSA to the electrode.

3.3.2.2. Laccase

In contrast to the electrode blocking of the BSA, laccase is electrochemically active on an electrode in the presence of oxygen. Once again, the experiment was carried out as described in section 2.3.1.6 using a 10mg/ml solution of laccase. The first preliminary test used only the alumina slurry polished electrode to check that a peak was found.

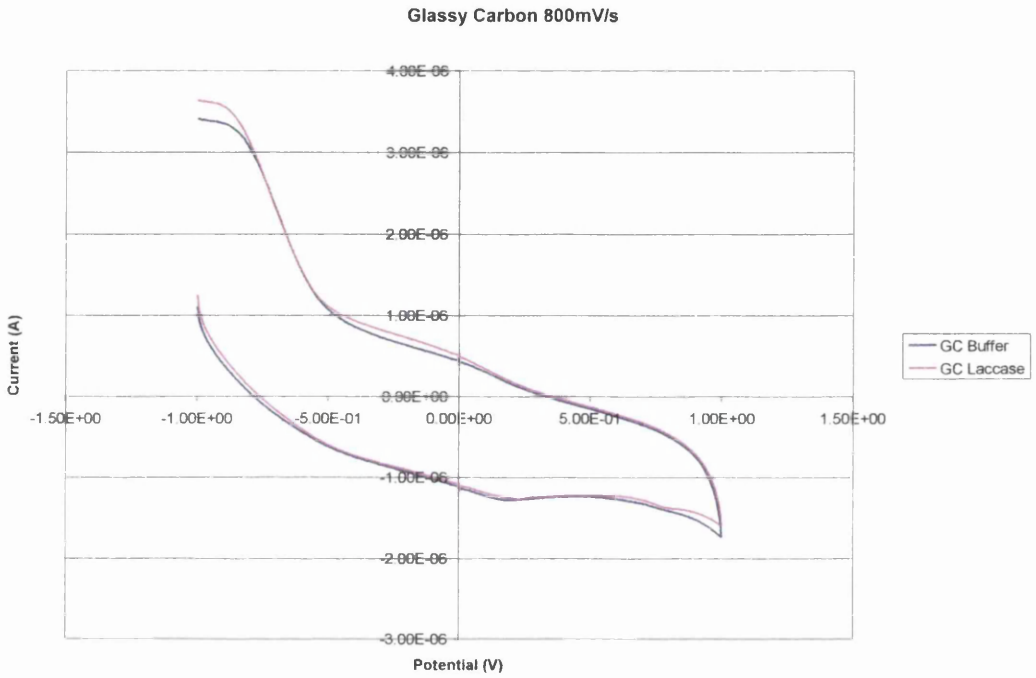

Figure 3.48- CV scans of laccase on a GC electrode

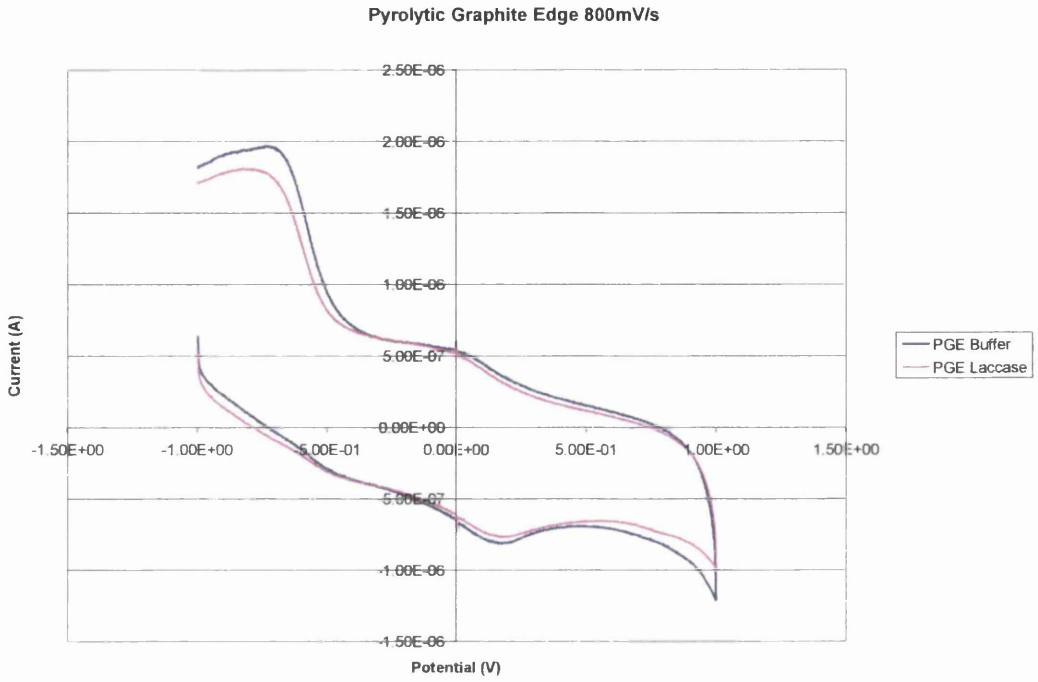

Figure 3.49-CV scans of laccase on a PGE electrode

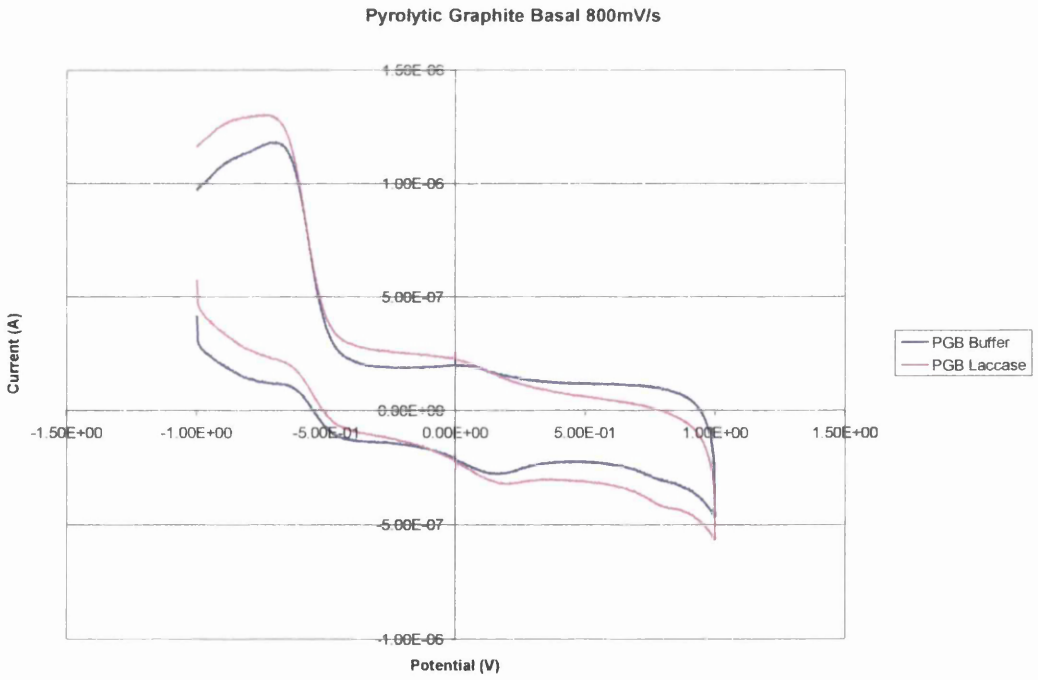

Figure 3.50- CV scans of laccase on a PGB electrode

From these preliminary scans of laccase on the three electrodes, figures 3.48, 3.49 and 3.50, it is possible to see a small oxidation peak around 800 mV, this is more pronounced as a peak with the GC and PGB electrodes and less so with the PGE, which does not follow the theory that the PGE is the most reactive. So the experiment was repeated comparing the four polishes.

Once again the peaks were present in the GC and PGB scans, figures 3.51 and 3.53, but not in the PGE scan, figure 3.52. Interestingly, all electrodes again showed alumina slurry to give the greatest oxygen peaks and where present "laccase" peaks too.

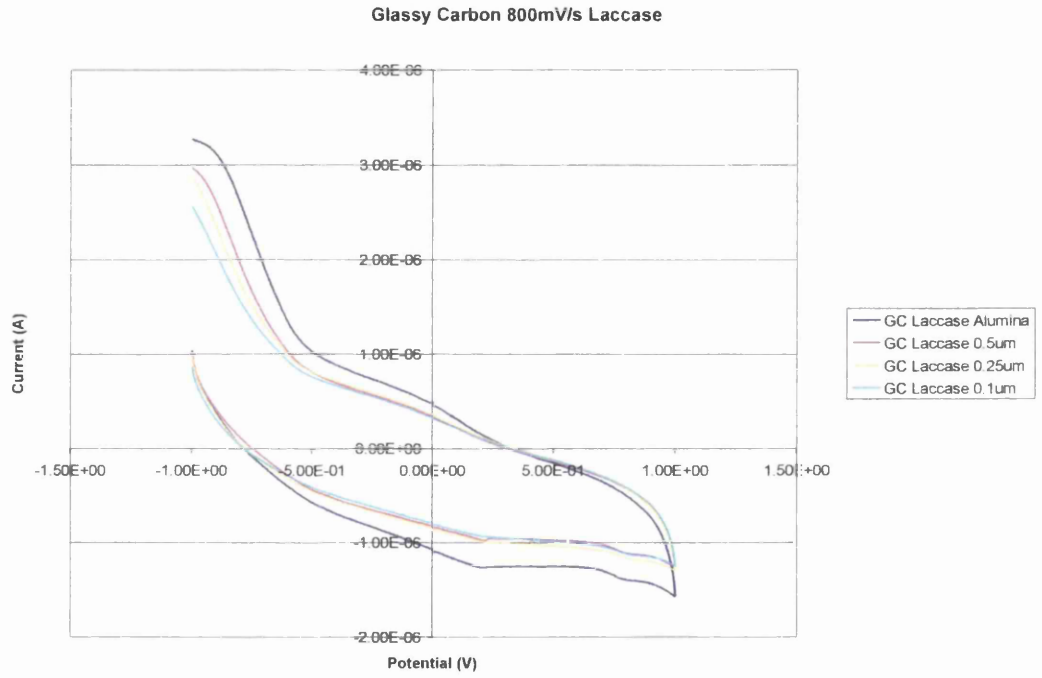

Figure 3.51- The effect of polishing with alumina slurry and diamond polishes on CV scans of laccase on a GC electrode

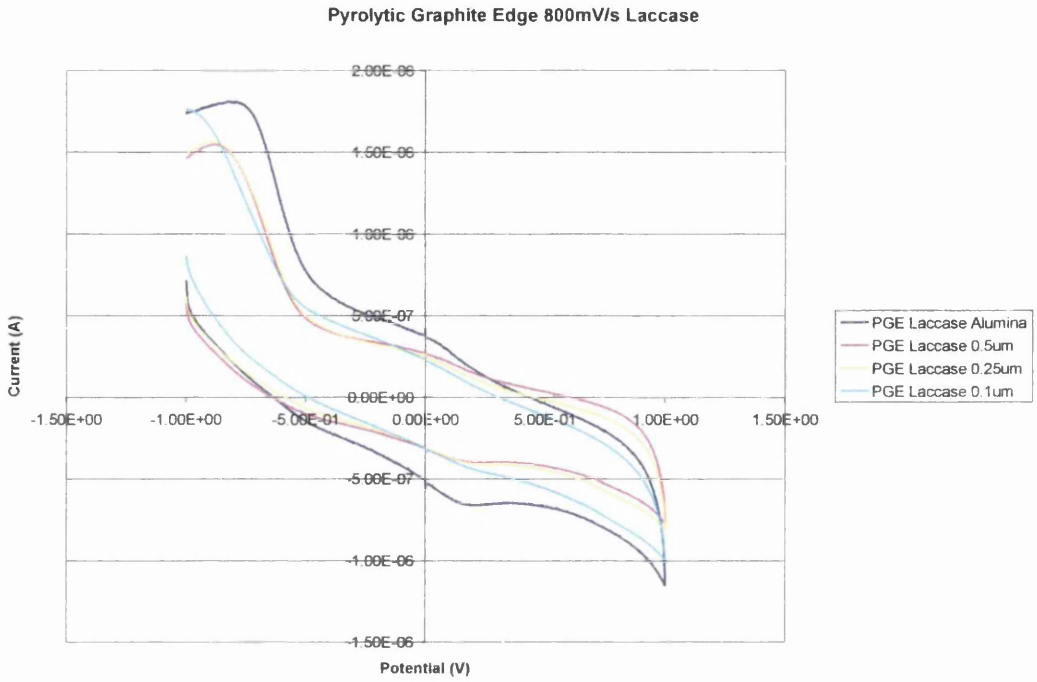

Figure 3.52- The effect of polishing with alumina slurry and diamond polishes on CV scans of laccase on a PGE electrode

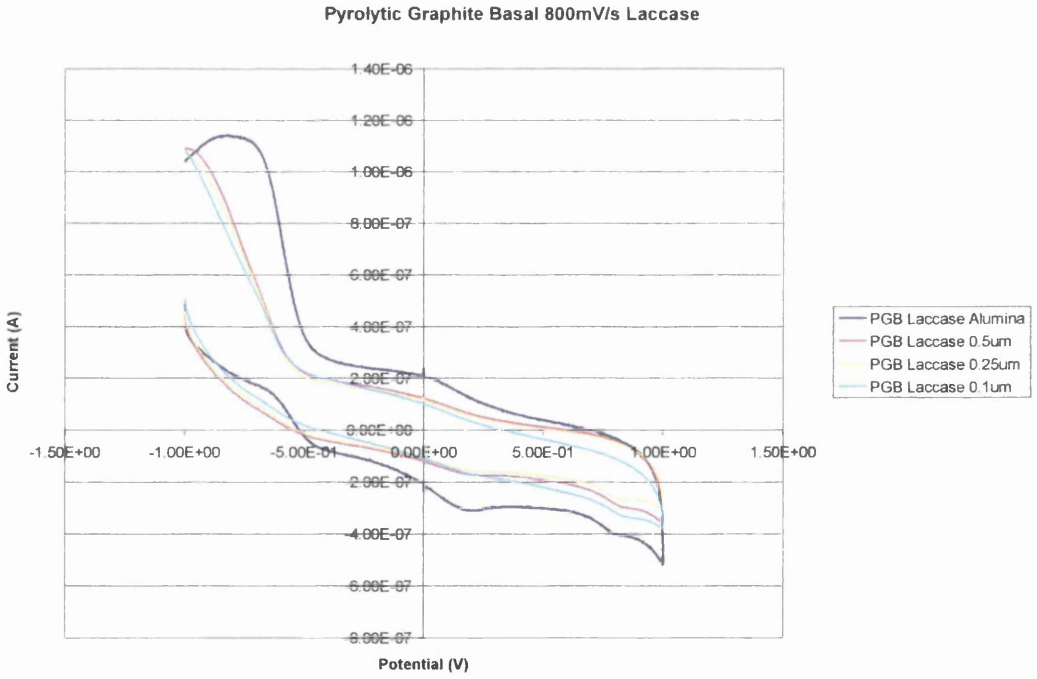

Figure 3.53- The effect of polishing with alumina slurry and diamond polishes on CV scans of laccase on a PGB electrode

Despite repetition of the experiment, with all three electrodes and all polished finishes, the PGE electrode continued to show the smallest peak of the three electrodes. In order to qualify this result the experiment was repeated, just using the alumina slurry polished electrodes, and then the cell thoroughly purged and the experiment repeated. By removal of the oxygen, the peak should disappear.

It is clear from the scans 3.54, 3.55 and 3.56, that on purging the peaks grow rather than disappear. This means that the peaks are not caused by the laccase, but by another electrochemical reaction. Changing of the buffer and retesting did not remove this peak, hence the contamination causing the peak is either a material present in the buffer, or in the laccase compound. Seeing a peak in the buffer only scans appears to imply the buffer, but the contamination may come from the electrodes despite thorough cleaning, polishing and flushing between tests.

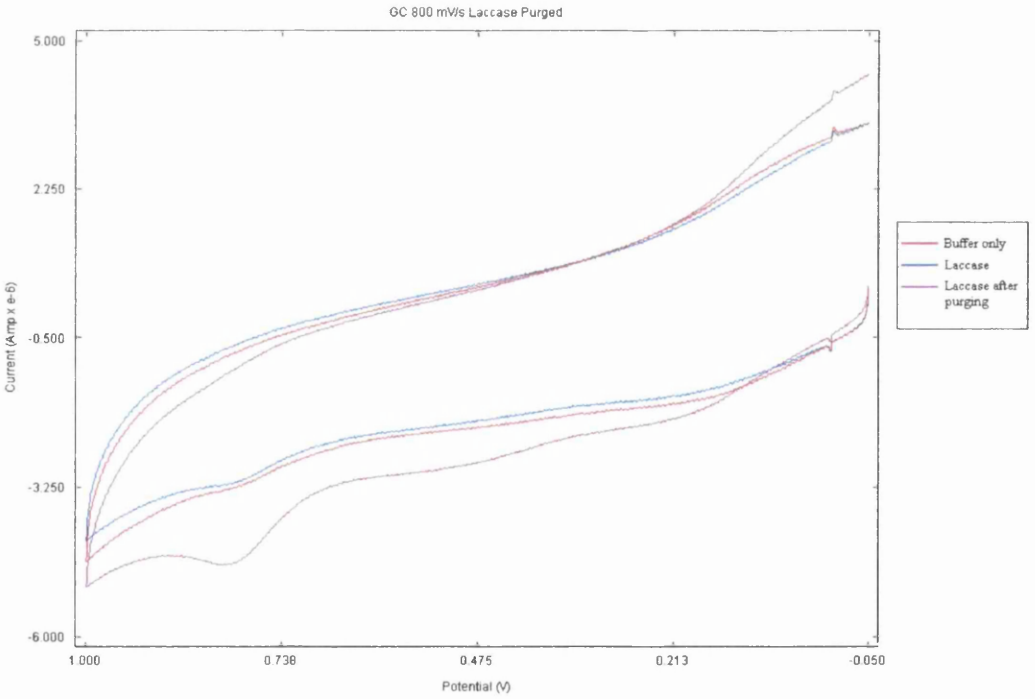

Figure 3.54- The effects of purging on CV scans of laccase on a GC electrode polished with alumina slurry

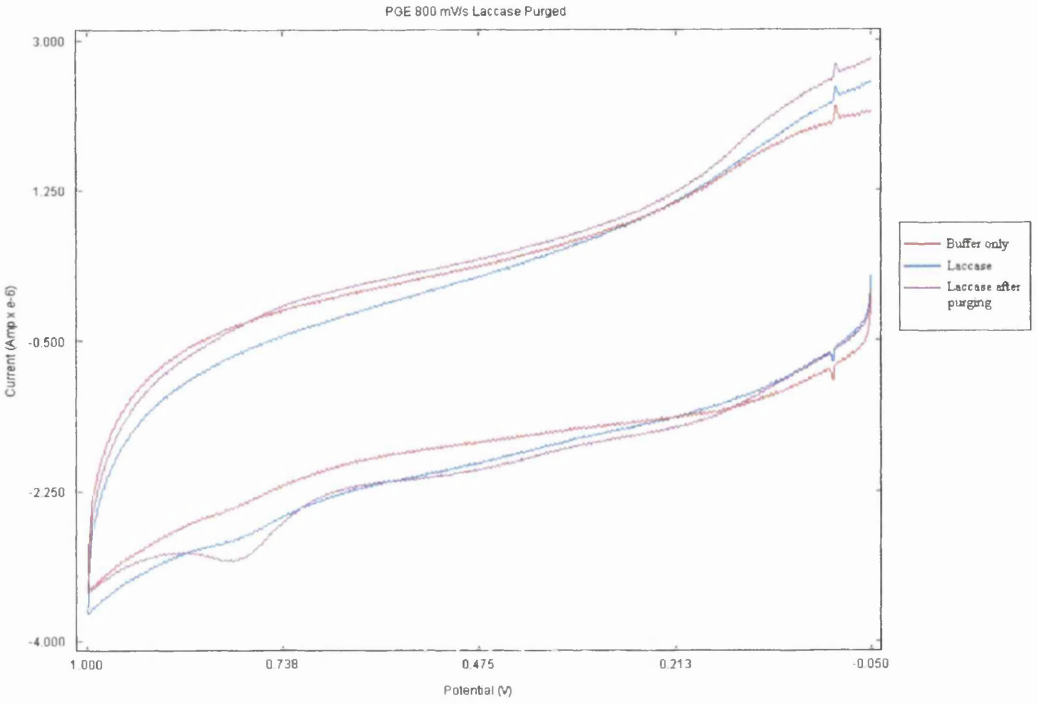

Figure 3.55- The effects of purging on CV scans of laccase on a PGE electrode polished with alumina slurry

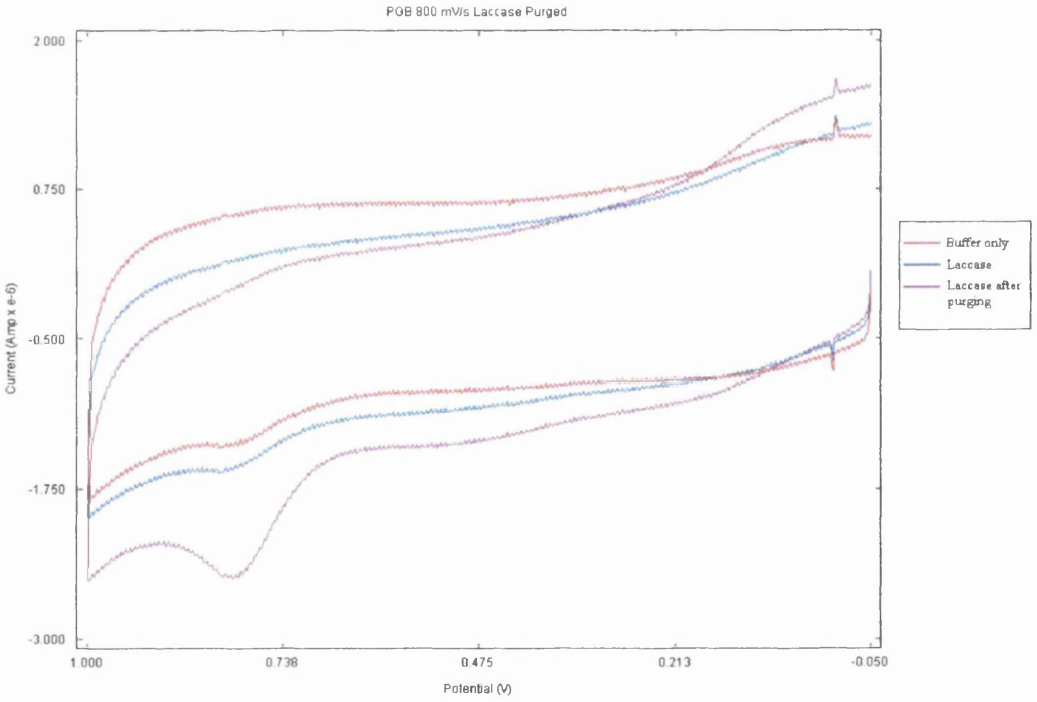

Figure 3.56- The effects of purging on CV scans of laccase on a PGB electrode polished with alumina slurry

3.3.2.2.1. Laccase and pyrocatechol

As the laccase was not reacting at the electrode during the CV scans, it was decided to introduce a substrate to the cell and retest. By adding the substrate, the laccase should become active, giving the best chance of getting a positive test result.

Pyrocatechol was chosen as the substrate and the experiment carried out as stated in section 2.3.1.6. Figures 3.57, 3.58 and 3.59 show the results.

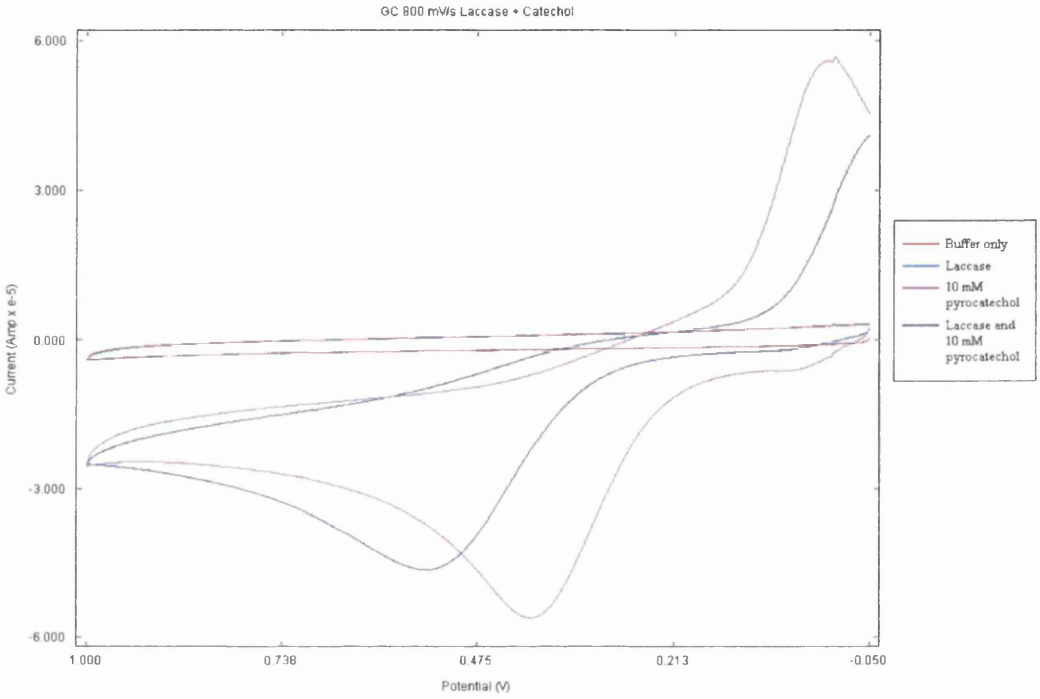

Figure 3.57- The effects of pyrocatechol on CV scans of laccase on a GC electrode

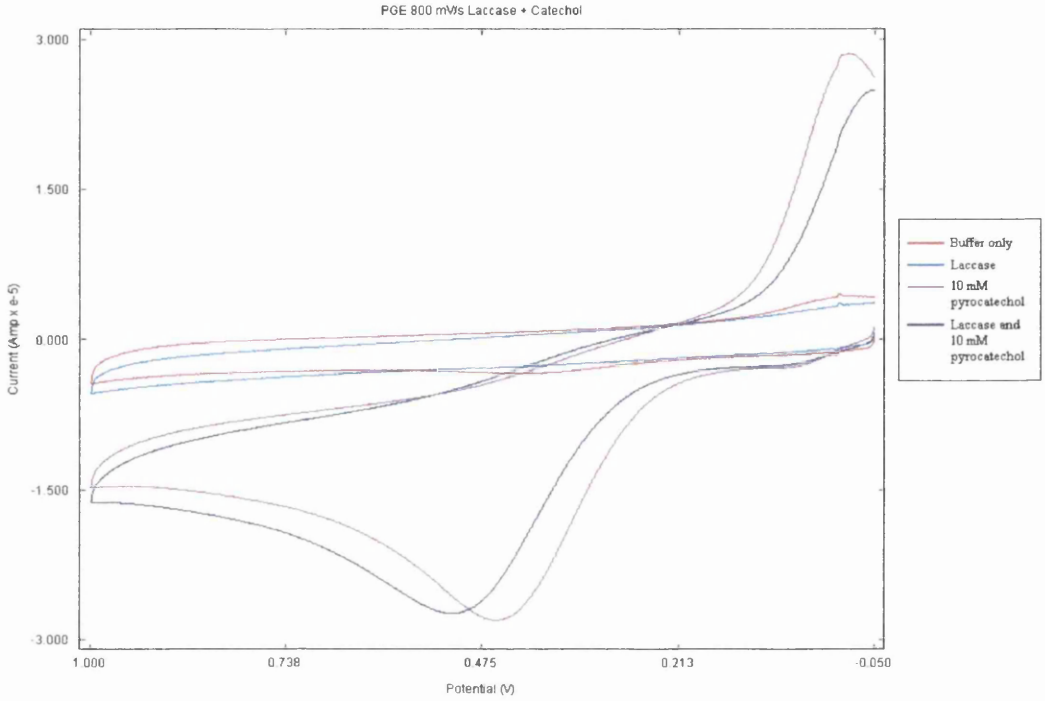

Figure 3.58- The effects of pyrocatechol on CV scans of laccase on a PGE electrode

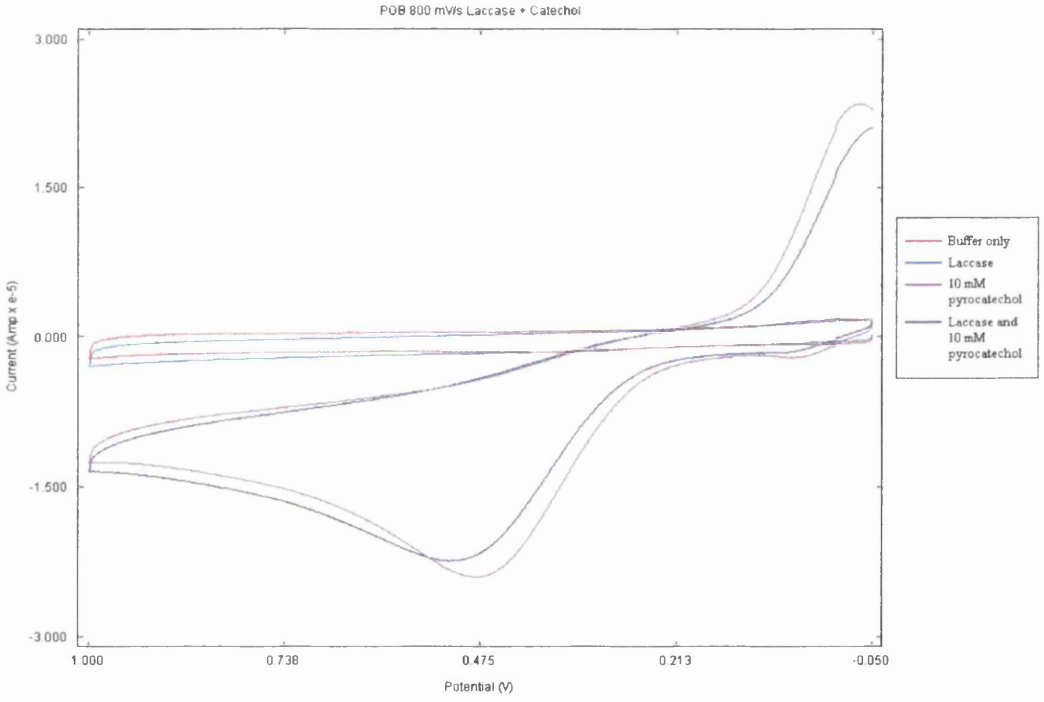

Figure 3.59- The effects of pyrocatechol on CV scans of laccase on a PGB electrode

It is clear that pyrocatechol itself is electrochemically active and the redox characteristics are clearly seen for all three electrodes. With the laccase coating, there is no peak for the laccase, but it can be seen that the peaks for the pyrocatechol are both reduced in height and separated, implying that there is a coating blocking the electrode. Retests showed similar results.

From these experiments, it is clear that there is no activity from the laccase, even with a substrate, thus the enzyme appears to be inactive or denatured.

3.3.2.3. Azurin

Following the problems with laccase not showing an electrochemical response, azurin was tried. Azurin has been shown in literature to be electrochemically active, plus it has the benefit over laccase of the experiment needing to be anaerobic, hence not having the issue of large oxygen peaks hiding any smaller peaks.

A preliminary run was made using just the GC electrode and two periods of soaking of the electrode, 5 and 20 minutes, otherwise the test case was as described in section 2.3.1.6.

This preliminary test showed no response from the azurin, as seen in figure 3.60. As seen before, the coating of the electrode resulted in less reaction with the buffer, implying the electrode is being blocked or impaired.

Following the preliminary result, the experiment was run in full, soaking the electrodes for 20 minutes. Once again, as can be seen in figures 3.61 and 3.62 there was no electrochemical response from the azurin. Also, the reaction with the buffer was reduced after coating.

Following no response from either the GC or PGE electrode, it was decided not to test the PGB, but to save the small quantity of azurin for another experiment.

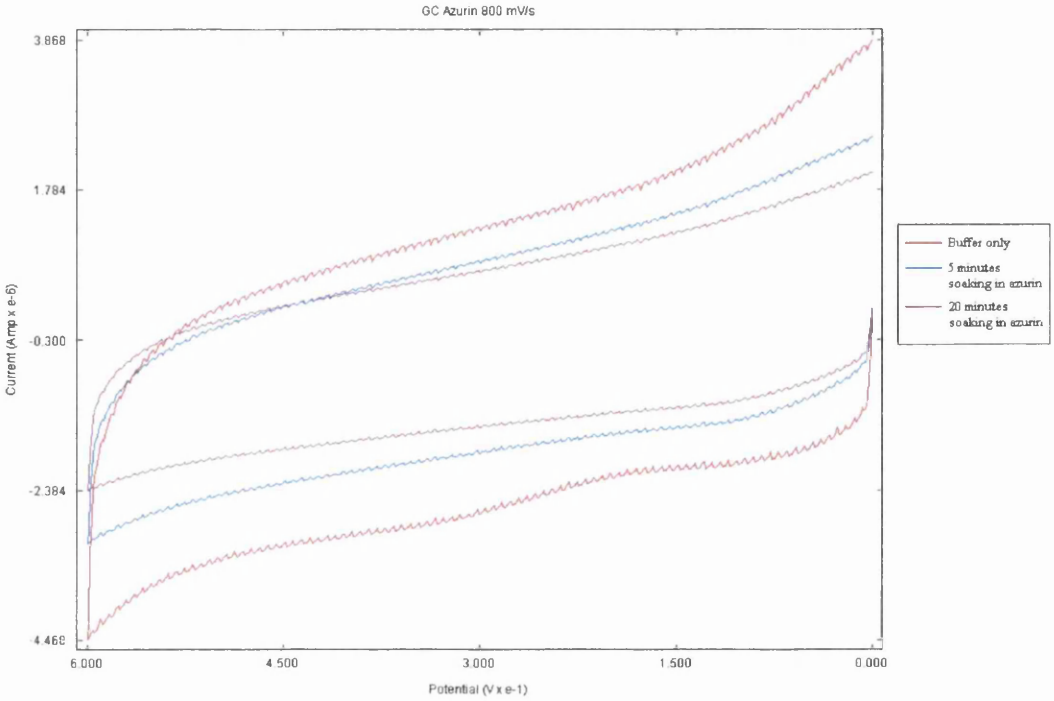

Figure 3.60- A preliminary run of azurin on a GC electrode

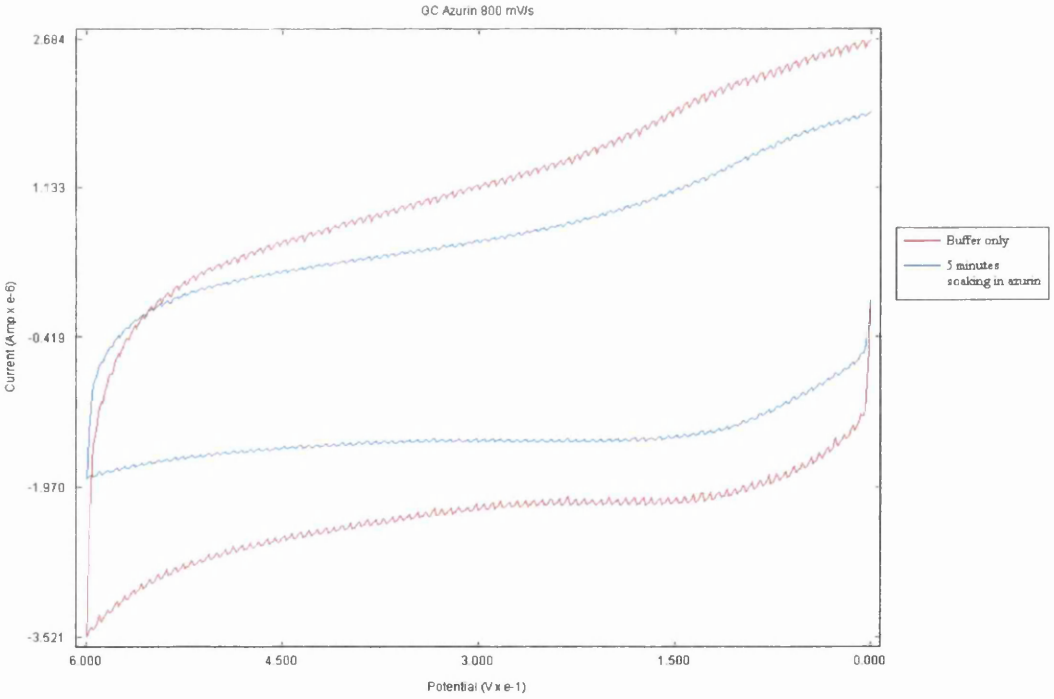

Figure 3.61- A CV scan of azurin on a GC electrode

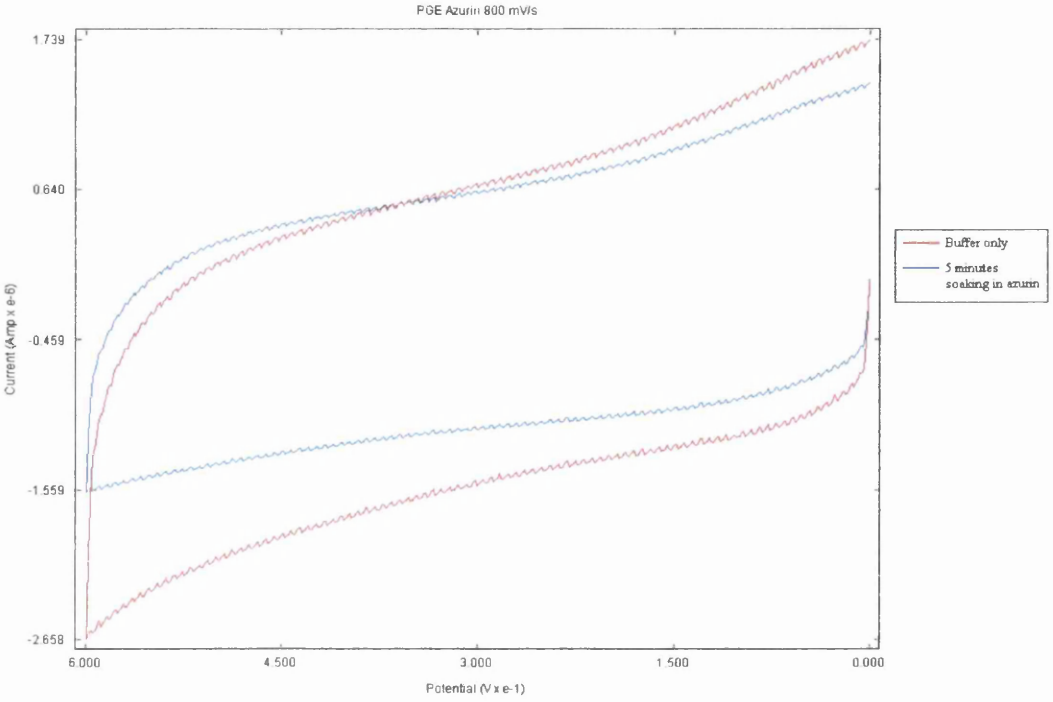

Figure 3.62- A CV scan of azurin on a PGE electrode

With no response from either of the previous experiments, one final technique was tested. This time, following the coating of the electrode with the azurin, the electrode was charged, in one test to 600 mV and in a second to 300 mV and held for 5 minutes before the start of the test. This was done in an attempt to activate the azurin. This experiment was carried out only on the GC electrode and the results can be seen in figure 3.63.

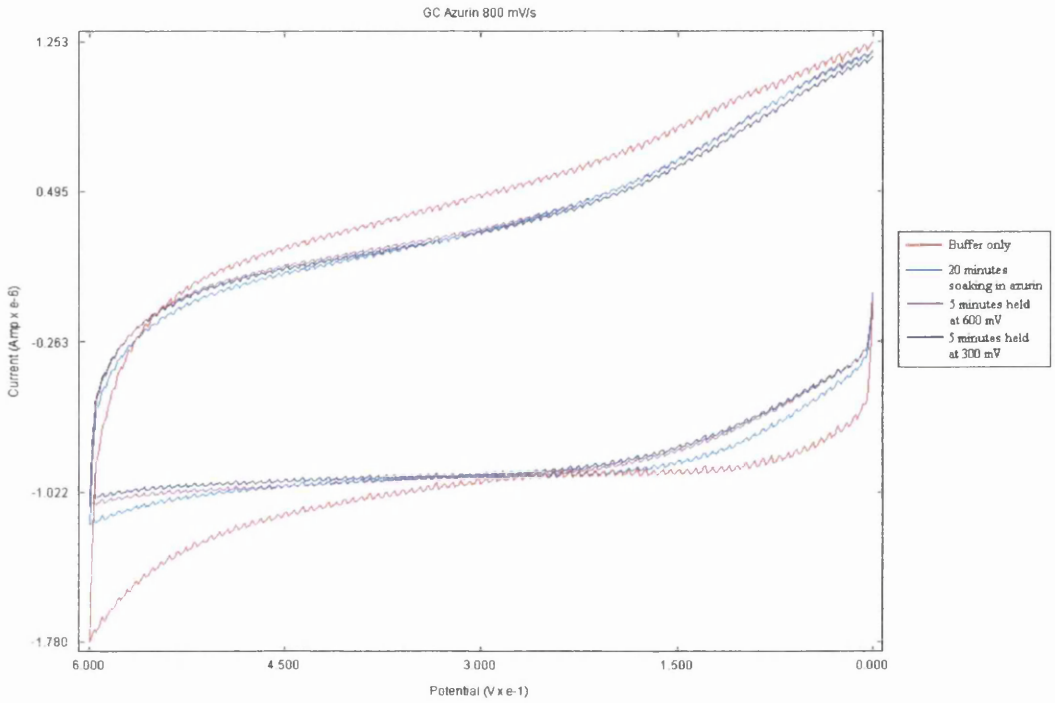

Figure 3.63- The effects of poising the electrode at 600mV and 300mV potentials prior to running the CV scans of azurin on a GC electrode

Despite the holding of the charged electrode, there was no electrochemical response from the azurin. Once again it was decided that the sample was inactive or denatured.

3.3.3. Discussion

The BSA proved to be successful, to a point, as there was no electrochemical response expected from it. Whilst in solution the BSA would block the redox reaction of methyl viologen, but clearly the BSA was staying in solution and not binding to any of the electrodes as shown by dipping the electrode. Adding a layer of PDL did not improve the bonding of the BSA to the electrode, but the PDL did block the methyl viologen reaction itself and slowed the electron transfer.

Laccase and azurin were both inactive when tested, despite having been bought in and carefully handled. The laccase at first appeared to give a reaction, but this was proved to be a contaminant as the peak increased when the cell was made anaerobic, instead of disappearing as would be the case with the oxidation of

laccase. Even with fresh buffer the contaminant was still present, thus it may be concluded that the contaminant was part of the supplied laccase compound. With more time available, it would have been possible and preferable to purify the laccase, as the supplied powder was crude and contained only around 120 units/mg. However, even after purification, it is unlikely that any reaction would have been seen from the laccase. The laccase was inactive, even in the presence of a substrate, thus even pure laccase would not have produced a reaction. For this reason, with more time available, carrying out a laccase assay, such as using syringaldazine (Harkin & Obst 1973), would be preferable before starting experiments to prove the activity of the laccase and save running CV tests with an inactive enzyme. In addition to these further steps, a further control should be added to the experiment, so not only is the buffer tested, but also an anaerobic test run to ensure peaks found are in fact from laccase.

Whilst the azurin was also inactive, it did not show the presence of contamination. The original sample was more pure than the laccase, containing only azurin and buffer salts. So whilst it may not be necessary to purify the azurin, running an assay to check for activity would have been preferable with more time.

Despite care being taken during the experiments with enzymes to ensure that conditions were kept as close to ideal as possible and everything was thoroughly cleaned and sterilised, it is still be possible take more precautions. For instance, working in an anaerobic glove box would ensure no oxygen was to reach the azurin.

In the CV scans of BSA in solution, it should be noted that the PGE electrode showed greatest response with methyl viologen, again supporting the theory that it is the most reactive electrode. Perhaps more importantly in the context of this work, when the BSA was added to the cell, the PGE electrode showed the greatest drop in reaction, this shows that the PGE electrode reacts most strongly with the protein, although it does not bond to the electrode.

Whilst this section has not delivered the results it was hoped it would, it has once again shown that PGE is the most reactive of the electrodes. It has also provided some important lessons and given pointers to ensure more successful experiments in the future.

In addition to the work carried out on BSA, laccase and azurin in this study, work was also carried out on to harvest hydrogenase from *Clostridium pasteurianum* to allow the investigation of another enzyme. However, as this was not successful it has been added as appendix II. Likewise investigation into cytochrome c as an oxygen sensor was also thought to be not directly relevant for this investigation and hence is included as appendix I.

4. Conclusions

Throughout this investigation there have been successes and, unfortunately, also some difficulties that could not be overcome. Despite this some useful lessons have been learnt and will give direction for further investigations into electrodes and electrode protein interactions.

4.1. General Discussion of results

4.1.1. Investigation of electrochemical properties of electrode materials and finishes

The study started properly with the investigation of the electrochemical responses of the electrodes and their different finishes, but the results did not come clear until the data was compared with the statistical analysis of the electrode surfaces by AFM.

As might be expected, investigating methyl viologen and oxygen gave different results for the performance on the electrodes. Investigating the cyclic voltammetry of oxygen, showed GC to give the greatest peaks and PGB smallest, methyl viologen also showed PGB to have the smallest current peaks, but PGE to give the greatest. Bringing the speed of electron transfer into the equation confuses results further by PGE the fastest for oxygen and PGB the slowest. Despite this result PGB proved to the fastest for methyl viologen and GC the slowest.

Polishing of the electrodes, once again gave no clear result for the "best" finish, however the alumina slurry did prove itself to either be either similar or better than the other finishes, particularly on the GC and PGE, with large peaks and fast electron transfer characteristics.

Once the AFM results were brought together with the electrochemical results, the results began to make more sense. The alumina polished PGE proved to be the roughest surface, followed by the 0.5μm diamond polish, then very similar results for the 0.1μm and 0.25μm diamond polishes. This tallied with the electron

transfer characteristics of the PGE electrode. Considering the PGB electrode, it was shown to have the roughest surface, hence following this line of the rougher the surface the better the electron transfer rate holds true in the case of methyl viologen. With the rough surface and good electron transfer characteristics it would follow that PGB should give the largest peaks in the cyclic voltammetry experiments, but this is not the case, probably down to the material. As stated in the introduction, PGB is known to be the least reactive of the materials and because of the structure of material it has a higher resistance. This could be interpreted that the rough surface exposes many of the edge sites, hence the good electron transfer, but the material itself limits the number and size of the sites of reactivity and the current that can flow through these areas. Thus it may be concluded that the underlying material is important to the reactivity level as well as the electrode finish.

Although not investigated in detail, C-AFM and EFM both supported the theory that it is the rough edge areas around peaks that provide the areas with the greatest current flow, electromagnetic field strength and highest friction, implying these are the most reactive areas. It is unfortunate that these technologies were not studied further in this investigation, but they do offer great potential for further investigations.

When combined, the AFM and CV results pointed towards alumina polished PGE being the most likely to give good results with proteins.

Also key in getting the best results out of the reaction is to overcome the problem of mass transport. Whenever the cell was stirred, the current peaks were seen to grow, implying that mass transport was slowing the turnover at the electrode. In order to get the response of the electrode without the mass transport limitation, it would be necessary to introduce a spinning plane electrode, or a flow of solution through the cell.

4.1.2. Investigation of proteins on the electrodes

Complications with the enzymes studied resulted in no electrochemical response from either laccase or azurin. However the results of the azurin test supported those of the BSA tests. In both cases, when the electrode was coated with azurin,

or the solution contained BSA, smaller electrochemical responses were seen at the electrodes. Particularly in the case of BSA, the PGE electrode was shown to give the best methyl viologen response and the greatest reduction in peak height, showing it to be blocked, or fouled, by the BSA to a greater degree than the other electrodes.

Whilst this does not prove conclusively that the alumina polished PGE is the "best electrode" for interfacing to proteins, when the CV and AFM results are brought into consideration, a convincing argument can be made worthy of further investigation.

Despite not getting a bioelectrochemical response from the laccase, the AFM roughness statistics results show that whilst the roughness of the electrodes increased, the height differences reduced, implying that laccase had attached to the surface, possibly in the troughs on the surface, hence the difference from peak to trough.

4.1.3. Difficulties encountered and how them avoid in future work

The inactivity of the laccase and azurin is of greater mystery as great care was taken in preparation of both enzymes for use. In the case of the laccase the supplied powder was a crude extract, thus it could be the case that there was a strong enough concentration of laccase in solution. It can also be seen from the CV scans that the laccase contained a contaminant which produced a current peak on the scans, even after changing of the buffer and making a fresh laccase solution. Thus if the experiment was to be repeated in future the laccase should be purified and concentrated to alleviate these possible problems. It would also be advisable to carry out a laccase assay as discussed in section 3.3.3 to check the activity of the enzyme.

The issue with azurin is less clear, thus the only advice that could be given is to work in sterile and anaerobic environment to ensure the environment is as favourable as possible.

4.2. Summary

Whilst this study was not successful in finding the best electrode and electrode surface for electrochemical responses with laccase and azurin, it has given a strong indication that the most promising carbon based electrode is pyrolytic graphite edge plane polished with alumina slurry. However, as the study of oxygen and methyl viologen has proved the electrode that is best for one reaction, is not necessarily best for another.

Most importantly, this study has discovered some of the difficulties in working with proteins on electrodes and suggested some other techniques to be investigated in future studies. It has also touched on areas that could be used to gather more information about electrodes in future work, namely Conducting AFM, Electromagnetic Force Analysis and the investigation of double layers on an electrode through the use of AFM in fluid (see appendix IV).

4.3. Future Work

Whilst this study has not given any definitive results, it has found some of the difficulties in carrying out bioelectrochemistry with proteins. The study has also touched on areas that could be used for more in depth studies of electrodes through the use of the AFM. These areas and others are discussed below as ideas of where this work can lead.

4.3.1. Electrochemistry and electrodes and their properties

Within this study carbon based electrodes were used, with platinum being used for one test. This is only a small sample of all the materials that can be used, for instance highly oriented pyrolytic graphite, carbon filament and numerous metallic electrodes. All are going to have a different effect on the electrochemistry and are worthy of investigation.

As well as the different materials there are also all the different finishes. Polishing can be done with different compounds and emery cloth, all of which will also give different results. These were not studied here as a fairly smooth surface was

needed to allow imaging with the AFM but the results of this study indicate that a rougher surface may be better for interacting with proteins. Modification is also possible by cleaving the electrode, by razor blade or tape, in the case of a PGB electrode giving a very smooth plane. The surface can also be accurately modified by laser or etching using the AFM. By combining this accurate surface etching with a freshly cleaved basal plane, it may be possible to discover the electrochemically active areas of the electrode and accurately tailor the reactivity of the electrode.

The other key part of the electrode response is the chemical being tested. In this study methyl viologen and oxygen gave different results at the same electrodes with the same preparation. Thus it follows that other chemicals will have different results again.

Through the different electrode materials, finishes and chemicals there are many different combinations to try and optimise for the greatest peaks, or fastest electron transfer.

Also within this study, it was noted that mass transport limited the potential peaks in the cyclic voltammetry experiments. Spinning disk electrodes have been shown to help to remove the influence of mass transport and could be used in any of these experiments to gain higher turnover rates.

4.3.2. AFM

During this experiment the AFM has started to show its strengths both as a topographic microscope and for investigating the other properties of the surface.

Firstly and simply the AFM could be used to carry out a larger statistical investigation of the roughness of different electrodes and different finishes. Combining these results with electrochemistry will help to understand more about optimising the electrode surfaces and which features are important.

The AFM could also be used to image the proteins on an electrode to understand more about where they attach to the electrode and hence what features are necessary for the best coverage and bioelectrochemical activity.

Other techniques used in this study, but are not yet widely used, include C-AFM, EFM and double layer imaging in fluid. Each of these has shown promise in this study, but could be an investigation in its own right.

Within this study C-AFM showed that it was the edges of peaks and troughs that most current flows through, these areas coincided with the areas of greatest friction. This study could be continued from here to investigate different electrodes, electrode surfaces and different features on the surfaces. However, as mentioned in the results, C-AFM does have a limit on the current that can flow, and hence needs a resistance of around 1kΩ for potentials around 1V. As a result, it might be necessary to build a resistive stage that could be used on the AFM to increase the resistance to a suitable level before undertaking the study. If this study is combined with one of imaging proteins on an electrode, it could be determined if the proteins are attracted to these areas of higher current and even to image the proteins and find there areas of conduction.

Likewise EFM, showed similar results to the C-AFM, that it is the surface defects that have the strongest fields. As a result, the EFM could be used for a similar study to the C-AFM, or in conjunction with the AFM.

Imaging double layers was briefly touched on in this work, appedix IV, and not used on an electrode. However, the images showed that it is possible to see the double layers change with ionic strength, hence charging the electrode could have the same effect, and this could be imaged with AFM, leading to a better understanding of the charged areas of the electrode.

4.3.3. Electrochemistry of proteins

The issues with laccase and azurin and possible solutions were discussed in the conclusions, but will be repeated here for completeness.

The laccase powder from Sigma was a crude extract, so as to ensure that contamination does not occur again, and to ensure there is a high enough concentration of laccase, the laccase should be purified and concentrated. Hopefully this will result in the laccase producing an electrochemical response. If not then the process should be revised to ensure that the laccase is kept as pure as possible and is not exposed to anything that may inactivate or denature it.

The reason for the lack of activity of the azurin is unknown. Therefore it is difficult to give any alternatives except ensuring that a sterile and anaerobic environment is used at all times.

Obviously there are many more redox proteins which could also be investigated, such as hydrogenase (Adams & Stiefel 1998; Guiral-Brugna et al. 2001; Jones et al. 2002; Karyakin et al. 2002; Karyakin et al. 2005; Leger & Bertrand 2008; Leger, Jones, Roseboom, et al. 2002; Mertens & Liese 2004; Morozov, Karyakina, Zadvornyi, et al. 2002; Morozov, Karyakina, Zorin, et al. 2002; Morozov, Vignais, et al. 2002; Morozov et al. 2006; Vincent, Cracknell, et al. 2005), ferredoxin and plastocyanin, which have been investigated and known to give an electrochemical response (Armstrong, Bond, Hill, Oliver, et al. 1989). Each different protein comes from a different environment, so may need different conditions to function at its best and hence a different electrode and electrode finish to be tested for each redox protein.

Another area only briefly investigated in this work is that of self assembled monolayers used to coat the electrode to promote the bonding of the protein to the electrode and a more favourable environment for the protein, for instance LB films of lysines. Once again this is probably an area where each protein will work best with a different linker molecule, so a great deal of investigation can be carried out to find the best in each situation.

4.3.4. Carbon Nanotubes

Carbon nanotubes potentially have a lot to bring to both electrochemistry and bioelectrochemistry. As discussed in the introduction (sections 1.3.3 and 1.3.6) they can both be formed into electrodes or used on an underlying electrode. Carbon nanotubes have been used as electrodes in electrochemistry (Gong et al. 2005) and bioelectrochemistry (Gong et al. 2005; Yang et al. 2007), but have also been shown to work as electrocatalysts in their own right (Gong et al. 2005)

Using carbon nanotubes for direct electron transfer has been achieved with glucose oxidase, cytochrome c, horseradish peroxidase, hemoglobin, myglobin and catalase (Gong et al. 2005), so they are certainly worth investigating for

improving electron transfer, increasing the stability of electrodes and improving the sensitivity of biosensors (Yang et al. 2007).

A particularly interesting concept is that of using carbon nanotubes to get access inside large enzymes to improve the electron transfer to inner active sites, hence increasing turnover rates (Yang et al. 2007). Or even reconstituting proteins on the end of carbon nanotubes to directly wire into them as has been achieved with glucose oxidase (Gong et al. 2005; Leger & Bertrand 2008).

However, despite the interest in carbon nanotubes, there are still questions over their toxicity (Yang et al. 2007) and in many cases their use brings no benefit (Yang et al. 2007).

4.3.5. A biological hydrogen fuel cell

Following on from successful investigations into hydrogenase and laccase, it would be possible to create a biological fuel cell with a hydrogenase anode to catalyse the reduction of hydrogen, and a laccase cathode to oxidise oxygen. This process would create a flow of electrons and hence produce electricity. This work has already been carried out by Vincent et al (Vincent, Cracknell, et al. 2005), but so far in only a basic form, there is still a great deal of work to be carried out on optimisation of the process.

4.3.6. Synthesis of redox protein active sites

On a different route from this work, the ultimate goal could be considered to be the synthesis of the redox proteins active sites, thus not needing to harvest and purify the proteins at all. For instance, the synthesis of hydrogenase and laccase active sites could give a hydrogen fuel cell with no need for precious metals, a high turnover rate and clean power. Surely that is one of mankind's greatest goals at this point in time.

5. References

Adams, M.W.W. & Stiefel, E.I., 1998. Biochemistry - Biological hydrogen production: Not so elementary. *Science*, 282(5395), pp.1842–1843.

Ahmed, M.U., Hossain, M.M. & Tamiya, E., 2008. Electrochemical Biosensors for Medical and Food Applications. *Electroanalysis*, 20(6), pp.616–626.

Allen, M.J., 1966. Symposium on bioelectrochemistry of microorganisms. II. Electrochemical aspects of metabolism. *Microbiol. Mol. Biol. Rev.*, 30(1), pp.80–93.

Andolfi, L., Bizzarri, A.R. & Cannistraro, S., 2006. Assembling of redox proteins on Au(111) surfaces: A scanning probe microscopy investigation for application in bio-nanodevices. *Thin Solid Films*, 515(1), pp.212–219.

Armstrong, F.A., Bond, A.M., Hill, H.A.O., Psalti, I.S.M., et al., 1989. A Microscopic Model of Electron Transfer at Electroactive Sites of Molecular Dimensions for Reduction of Cytochrome c at Basal- and Edge-Plane Graphite Electrodes. *Journal of Physical Chemistry*, 93, pp.6485–6493.

Armstrong, F.A., Bond, A.M., Hill, H.A.O., Oliver, N., et al., 1989. Electrochemistry of Cytochrome c, Plastocyanin, and Ferredoxin at Edge- and Basal-Plane Graphite Electrodes Interpreted via a Model Based on Electron Transfer at Electroactive Sites of Microscopic Dimensions in Size. *Journal of the American Chemical Society*, 111, pp.9185–9189.

Armstrong, F.A., 2002. Insights from protein film voltammetry into mechanisms of complex biological electron-transfer reactions. *Journal of the Chemical Society-Dalton Transactions*, (5), pp.661–671.

Armstrong, F.A., Heering, H.A. & Hirst, J., 1997. Reactions of complex metalloproteins studied by protein-film voltammetry. *Chemical Society Reviews*, 26(3), pp.169–179.

Armstrong, F.A., Hill, H.A.O. & Walton, N.J., 1988. Direct Electrochemistry of Redox Proteins. *Accounts of Chemical Research*, 21, pp.407–413.

Banks, C.E. et al., 2005. Electrocatalysis at graphite and carbon nanotube modified electrodes: edge-plane sites and tube ends are the reactive sites. *Chemical Communications*, (7), pp.829–841.

Bartlett, P.N., 1990. Modified Electrode Surface in Amperometric Biosensors. *Medical & Biological Engineering & Computing*, 28(3), pp.B10–B17.

Blanford, C.F. & Armstrong, F.A., 2006. The pyrolytic graphite surface as an enzyme substrate: microscopic and spectroscopic studies. *Journal of Solid State Electrochemistry*, 10(10), pp.826–832.

Bowen, W.R. et al., 1997. Atomic force microscope studies of membranes: Force measurement and imaging in electrolyte solutions. *Journal of Membrane Science*, 126(1), pp.77–89.

Cahan, D. et al., 2002. Fuel Cells.

Chi, Q.J. et al., 1999. Electrochemistry of self-assembled monolayers of the blue copper protein Pseudomonas aeruginosa azurin on Au(111). *Electrochemistry Communications*, 1(3-4), pp.91–96.

Chu, X. & Kinoshita, K., 1997. Surface modification of carbons for enhanced electrochemical activity. *Materials Science and Engineering B-Solid State Materials for Advanced Technology*, 49(1), pp.53–60.

Doelling, R., 2000. Potentiostats.

Gong, K.P. et al., 2005. Electrochemistry and electroanalytical applications of carbon nanotubes: A review. *Analytical Sciences*, 21(12), pp.1383–1393.

Gosser, D.K., 1993. *Cyclic Voltammetry*, VCH.

Guiral-Brugna, M. et al., 2001. Electrocatalysis of the hydrogen production by Fe hydrogenase from Desulfovibrio vulgaris Hildenborough. *Journal of Electroanalytical Chemistry*, 510(1-2), pp.136–143.

Hallenbeck, P.C. & Benemann, J.R., 2002. Biological hydrogen production; fundamentals and limiting processes. *International Journal of Hydrogen Energy*, 27(11-12), pp.1185–1193.

Hansma, P.K. et al., 1994. TAPPING MODE ATOMIC-FORCE MICROSCOPY IN LIQUIDS. *Applied Physics Letters*, 64(13), pp.1738–1740.

Harkin, J.M. & Obst, J.R., 1973. Syringaldazine, an Effective Reagent for Detecting Laccase and Peroxidase in Fungi. *Experientia*, 29(4), pp.381–387.

Hill, H.A.O., 1996. The development of bioelectrochemistry. *Coordination Chemistry Reviews*, 151, pp.115–123.

Hirst, J. & Armstrong, F.A., 1998. Fast-scan cyclic voltammetry of protein films on pyrolytic graphite edge electrodes: Characteristics of electron exchange. *Analytical Chemistry*, 70(23), pp.5062–5071.

Hurth, C., Li, C. & Bard, A.J., 2007. Direct Probing of Electrical Double Layers by Scanning Electrochemical Potential Microscopy. *Journal of Physical Chemistry*, 111, pp.4620–4627.

Jeuken, L.J.C., Jones, A.K., et al., 2002. Electron-transfer mechanisms through biological redox chains in multicenter enzymes. *Journal of the American Chemical Society*, 124(20), pp.5702–5713.

Jeuken, L.J.C. & Armstrong, F.A., 2001. Electrochemical origin of hysteresis in the electron-transfer reactions of adsorbed proteins: Contrasting behavior of the 'blue' copper protein, azurin, adsorbed on pyrolytic graphite and modified gold electrodes. *Journal of Physical Chemistry B*, 105(22), pp.5271–5282.

Jeuken, L.J.C., McEvoy, J.P. & Armstrong, F.A., 2002. Insights into gated electron-transfer kinetics at the electrode-protein interface: A square wave voltammetry study of the blue copper protein azurin. *Journal of Physical Chemistry B*, 106(9), pp.2304–2313.

Jones, A.K. et al., 2002. Direct comparison of the electrocatalytic oxidation of hydrogen by an enzyme and a platinum catalyst. *Chemical Communications*, (8), pp.866–867.

Jones, A.K. et al., 2003. Enzyme electrokinetics: Electrochemical studies of the anaerobic interconversions between active and inactive states of Allochromatium vinosum NiFe -hydrogenase. *Journal of the American Chemical Society*, 125(28), pp.8505–8514.

Karyakin, A.A. et al., 2002. Hydrogen fuel electrode based on bioelectrocatalysis by the enzyme hydrogenase. *Electrochemistry Communications*, 4(5), pp.417–420.

Karyakin, A.A. et al., 2005. Hydrogenase electrodes for fuel cells. *Biochemical Society Transactions*, 33, pp.73–75.

Kim, C.H., Pyun, S. & Kim, J.H., 2003. An investigation of the capacitance dispersion on the fractal carbon electrode with edge and basal orientations. *Electrochimica Acta*, 48(23), pp.3455–3463.

Kovacs, K.L., Maroti, G. & Rakhely, G., 2006. A novel approach for biohydrogen production. *International Journal of Hydrogen Energy*, 31(11), pp.1460–1468.

KSV Instruments Ltd, Langmuir and Langmuir-Blodgett Films.

de Lacey, A.L., Fernandez, V.M. & Rousset, M., 2005. Native and mutant nickel-iron hydrogenases: Unravelling structure and function. , 249(15-16), pp.1596–1608.

Leger, C., Jones, A.K., Albracht, S.P.J., et al., 2002. Effect of a dispersion of interfacial electron transfer rates on steady state catalytic electron transport in NiFe -hydrogenase and other enzymes. *Journal of Physical Chemistry B*, 106(50), pp.13058–13063.

Leger, C., Jones, A.K., Roseboom, W., et al., 2002. Enzyme electrokinetics: Hydrogen evolution and oxidation by Allochromatium vinosum NiFe -hydrogenase. *Biochemistry*, 41(52), pp.15736–15746.

Leger, C. & Bertrand, P., 2008. Direct electrochemistry of redox enzymes as a tool for mechanistic studies. *Chemical Reviews*, 108(7), pp.2379–2438.

Lindsay, S., The Scanning Probe Microscope in Biology.

Lyon, E.J. et al., 2004. UV-A/blue-light inactivation of the 'metal-free' hydrogenase (Hmd) from methanogenic archaea - The enzyme contains functional iron after all. *European Journal of Biochemistry*, 271(1), pp.195–204.

Maness, P.-C. et al., 2002. Characterization of Oxygen Tolerance of a Hydrogenase Linked to a Carbon Monoxide Pathway in Rubrivivax gelatinosus. *Applied and Environmental Microbiology*, 68(6), pp.2633–2636.

Mechler, A. et al., 1998. Cantilever flexure, adhesive/attractive and lateral force measurements on highly-oriented pyrolytic graphite by scanning force microscopy. *Vacuum*, 50(3-4), pp.281–287.

Mertens, R. & Liese, A., 2004. Biotechnological applications of hydrogenases. *Current Opinion in Biotechnology*, 15, pp.343–348.

Morozov, S.V., Karyakina, E.E., Zadvornyi, O.A., et al., 2002. Bioelectrocatalysis by hydrogenase Th. roseopersicina immobilized on carbon materials. *Russian Journal of Electrochemistry*, 38(1), pp.97–102.

Morozov, S.V., Vignais, P.M., et al., 2002. Bioelectrocatalytic hydrogen production by hydrogenase electrodes. *International Journal of Hydrogen Energy*, 27(11-12), pp.1501–1505.

Morozov, S.V., Karyakina, E.E., Zorin, N.A., et al., 2002. Direct and electrically wired bioelectrocatalysis by hydrogenase from Thiocapsa roseopersicina. *Bioelectrochemistry*, 55(1-2), pp.169–171.

Morozov, S.V. et al., 2006. Tolerance to oxygen of hydrogen enzyme electrodes. *Electrochemistry Communications*, 8(5), pp.851–854.

Muller, D.J. et al., 1997. The bacteriophage phi 29 head-tail connector imaged at high resolution with the atomic force microscope in buffer solution. *Embo Journal*, 16(10), pp.2547–2553.

Murphy, L., 2006. Biosensors and bioelectrochemistry. *Current Opinion in Chemical Biology Bioinorganic chemistry / Biocatalysis and biotransformation*, 10(2), pp.177–184.

Padeste, C., Grubelnik, A. & Tiefenauer, L., 1998. Amperometric immunosensing using microperoxidase MP-11 antibody conjugates. *Analytica Chimica Acta*, 374(2-3), pp.167–176.

Pascher, T. et al., 1992. Reduction potentials and their pH dependence in site-directed-mutant forms of azurin from Pseudomonas aeruginosa. *European Journal of Biochemistry*, 212(2), pp.289–296.

Pershad, H.R. et al., 1999. Catalytic electron transport in Chromatium vinosum NiFe -hydrogenase: Application of voltammetry in detecting redox-active centers and establishing that hydrogen oxidation is very fast even at potentials close to the reversible H+/H-2 value. *Biochemistry*, 38(28), pp.8992–8999.

Pita, M. et al., 2006. Direct heterogeneous electron transfer reactions of fungal laccases at bare and thiol-modified gold electrodes. *Electrochemistry Communications*, 8(5), pp.747–753.

Portaccio, M. et al., 2006. Biosensors for phenolic compounds: The catechol as a substrate model. *Journal of Molecular Catalysis B-Enzymatic*, 41(3-4), pp.97–102.

Rief, M., Gautel, M., et al., 1997. Reversible unfolding of individual titin immunoglobulin domains by AFM. *Science*, 276(5315), pp.1109–1112.

Rief, M., Oesterhelt, F., et al., 1997. Single molecule force spectroscopy on polysaccharides by atomic force microscopy. *Science*, 275(5304), pp.1295–1297.

Shleev, S. et al., 2005. Direct electron transfer reactions of laccases from different origins on carbon electrodes. *Bioelectrochemistry*, 67(1), pp.115–124.

Solomon, E.I., Sundaram, U.M. & Machonkin, T.E., 1996. Multicopper oxidases and oxygenases. *Chemical Reviews*, 96(7), pp.2563–2605.

Vincent, K.A., Cracknell, J.A., et al., 2005. Electrocatalytic hydrogen oxidation by an enzyme at high carbon monoxide or oxygen levels 10.1073/pnas.0504499102. *Proceedings of the National Academy of Sciences of the United States of America*, 102(47), pp.16951–16954.

Vincent, K.A., Parkin, A., et al., 2005. Electrochemical definitions of O-2 sensitivity and oxidative inactivation in hydrogenases. *Journal of the American Chemical Society*, 127(51), pp.18179–18189.

Wright, M. & Revenko, I., 2004. Tapping Mode Atomic Force Microscopy Operation in Fluid.

Xiao, Z.G. et al., 1999. The dependence of reversible potentials on the form of modification of edge plane pyrolytic graphite electrodes in voltammetric studies on rubredoxin and ferredoxin from Clostridium pasteurianum. *Electrochemistry Communications*, 1(8), pp.309–314.

Xu, F. et al., 1996. A study of a series of recombinant fungal laccases and bilirubin oxidase that exhibit significant differences in redox potential, substrate specificity, and stability. *Biochimica Et Biophysica Acta-Protein Structure and Molecular Enzymology*, 1292(2), pp.303–311.

Yang, F. et al., 2005. Characterization of Purified c-Type Heme-Containing Peptides and Identification of c-Type Heme-Attachment Sites in Shewanella oneidenis Cytochromes Using Mass Spectrometry. *Journal of Proteome Research*, 4, pp.846–854.

Yang, W.R. et al., 2007. Carbon nanotubes for biological and biomedical applications. *Nanotechnology*, 18. Available at: ://000249735600001.

Yue, H.J. et al., 2006. The effect of ionic strength on the electron-transfer rate of surface immobilized cytochrome c. *Journal of Physical Chemistry B*, 110(10), pp.5062–5072.

Yue, H.J. & Waldeck, D.H., 2005. Understanding interfacial electron transfer to monolayer protein assemblies. *Current Opinion in Solid State & Materials Science*, 9(1-2), pp.28–36.

Zhang, W.J. & Li, G.X., 2004. Third-generation biosensors based on the direct electron transfer of proteins. *Analytical Sciences*, 20(4), pp.603–609.

6. Appendices

6.1. Appendix I: Cytochrome C oxygen sensor

6.1.1. Introduction

Prior to the investigation of electrodes, a period of three months was spent at the Korea Institute of Science and Technology (KIST), investigating the use of cytochrome C from *Shewanella putrefaciens* as an oxygen sensor.

It had been noted that on exposing the cell to oxygen, the cytochrome would stop reacting and conducting electrons. On removal of the oxygen it would restart. Hence it was proposed that the cytochrome could be used as an oxygen sensor if the results could be recreated using extracted cytochrome C on an electrode.

6.1.2. Materials and Methods

6.1.2.1. Equipment

Whilst working at KIST, the following equipment was used for the experiments:

For cyclic voltammetry two systems were used, a Bioanalytical Systems CV-50W Voltammetric Analyser with a C2 Cell Stand and Bio Analytical Systems electrodes and a Princeton Applied Research Potentiostat/Galvanostat 273A.

Centrifuge was carried out with a Sorvall Instruments RC5C and ultracentrifuge with a Beckmann L-80.

A Jasco V-530 Spectrophotometer was used for all measurements.

6.1.2.2. Materials

6.1.2.2.1. Electrochemistry

The buffers used were the same as in section 2.2.2.

6.1.2.2.2. Growth Media for Shewanella

Two media were used in the growing of Shewanella, the first was Tryptic Soy Broth (TSB) and the second was Phosphate Buffered Basal Medium (PBBM). Both media were boiled and then purged with N_2 before being sealed and autoclaved. The vitamin solution was kept refrigerated and added just before inoculation.

Table 6.1- Tryptic Soy Broth composition

Substance	Concentration
Tryptic Soy Broth	30 g per litre of water
Sodium lactate solution	30mM
Sodium fumerate dibasic	60mM

Table 6.2- Phosphate buffered basal medium composition

Substance	Quantity
NaCl	0.9g
$MgSO_4 \cdot 2H_2O$	0.2g
$CaCl_2 \cdot 2H_2O$	0.2g
NH_4Cl	1.0g
$Na_2S \cdot 9H_2O$ (2.5%)	25ml
Resazurin (0.02%)	1ml
Yeast extract	1.0g
Distilled water	944ml
Trace mineral solution (see below)	10ml
Vitamin solution	10ml
Phosphate buffer (1M, pH 7.0)	10ml
PH	7.0

Table 6.3- Trace mineral solution composition

Substance	Quantity (g/l)
Nitrilo triacetic Acid (NTA)	1.5
$FeSO_4 \cdot 7H_2O$	0.1
$MnCl_2 \cdot 4H_2O$	0.1
$CoCl_2 \cdot 6H_2O$	0.17
$ZnCl_2$	0.1
$CaCl_2 \cdot 2H_2O$	0.1
$CuCl_2 \cdot 2H_2O$	0.1
H_3BO_3	0.01
Na_2MoO_3	0.01
Na_2SeO_3	0.017
$NiSO_4 \cdot 6H_2O$	0.026
NaCl	1.0

Table 6.4- Vitamin solution composition

Substance	Quantity (g/l)
Biotin	2.0
Folic Acid	2.0
Pyridoxine HCl	10.0
Thiamine HCl	5.0
Riboflavin	5.0
Nicotinic Acid	5.0
Pantothenic Acid	5.0
Cyanocobalamine	0.1
P-aminobenzoic Acid	5.0
Lipoic Acid	5.0

6.1.2.3. Methods

6.1.2.3.1. Cytochrome C extraction using EDTA

The Shewanella cells were cultivated and harvested by centrifuging at 8000rpm for 10 minutes. They were then washed twice using Tris-HCl buffer (pH7.0, 50mM) and centrifuged at 8500rpm for 10 minutes for each wash. The cells were then resuspended in Tris-HCl buffer (50mM, pH9.0) containing 50mM EDTA and placed in a water bath at 37°C for 30 minutes, then placed in ice for 30 minutes. Following the heat cycle the tubes were centrifuged at 8000rpm for 10 minutes,

and then the supernatant was filtered off by using a 0.2μm PES membrane. The filtered supernatant was then ultracentrifuged for 90 minutes at 132,000 x *g*. Finally the resultant pellet was resuspended in Tris-HCl buffer (pH 7.5, 50mM) containing 15mM Z3-12 detergent for storage or use.

6.1.2.3.2. CV test protocol

The cells were cultivated and then harvested by centrifuging at 10,000 x *g* for 30 minutes. The cells were then three times using anaerobic phosphate buffer (pH 7.0, 50mM) containing 0.1M NaCl. Following washing the cells were resuspended in anaerobic phosphate buffer and the cell concentration adjusted to give an OD of 6 at 660nm. The CV equipment was then prepared, purged with nitrogen and the buffer tested before the cells were added and the test run. The cell was then aerated for 30 minutes and purged for 5 minutes to test the affect of oxygen on the cells without oxygen being present in the buffer. The cell was then purged for a further 20 minutes to check for reactivation of the cytochrome c when anaerobic conditions were restored.

The testing of whole cells disrupted by EDTA was carried out as above, but the CV scans were run on the whole cell and then disrupted cells. Following the test of the whole cell, EDTA was added and the cell placed in a water bath at 37°C for 30 minutes before the test was re-run with the disrupted cells.

Testing of the cytochrome C was carried out by creating a layer of the cytochrome solution on the surface of the electrode and allowing to dry.

All tests were carried out using Bio Analytical Systems CV-50W with cell stand C2. The electrodes used were a pyrolytic graphite electrode, silver silver chloride reference electrode and platinum wire counter electrode, all also from Bio Analytical Systems.

6.1.2.3.3. Creating a Langmuir-Blodgett film

The film is created by floating a single layer of the lipid on the surface of water. The area is then reduced to pack the lipid molecules close together. Then the surface is dipped in to the water through the layer of lipid, which creates the first

layer. As it is then removed, the second layer is formed on top of the first. This process is illustrated in figure 6.1.

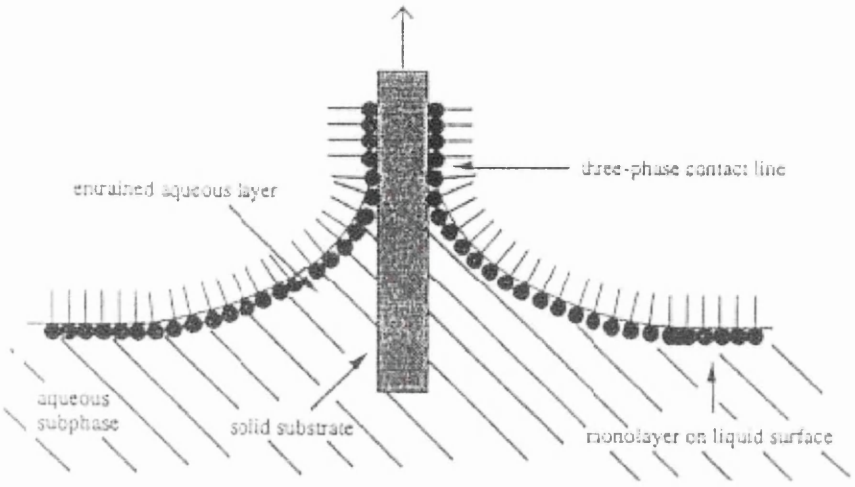

Figure 6.1- Making an LB film

6.1.3. Shewanella putrefaciens IR-1 and Cytochrome C

A hypothesis had been formed by the group, prior to my arrival, that the heme group containing redox proteins on the outer membrane provided the electrochemical activity, i.e. cytochrome c. When exposed to oxygen, the cytochrome c would rotate in the outer membrane to hide its heme group and become inactive.

Thus in order to get the same reaction on an electrode and produce a working sensor, the cytochrome c would need to be able to behave in the same way on the electrode.

6.1.4. Electrochemistry

The first experiment involved the use of whole IR-1 cells and disrupting the outer membrane with EDTA. This would keep the cytochrome c within the fragments of the membrane. As the electrode surface and the membrane fragments are hydrophobic, they should attach together.

The experiment was carried out as described in section 6.1.2.3.2 by disrupting the cells in solution within the electrochemical cell.

The initial runs before nitrogen purging or aeration showed large reduction and oxidation peaks at around -350mV as can be seen in figure 6.2.

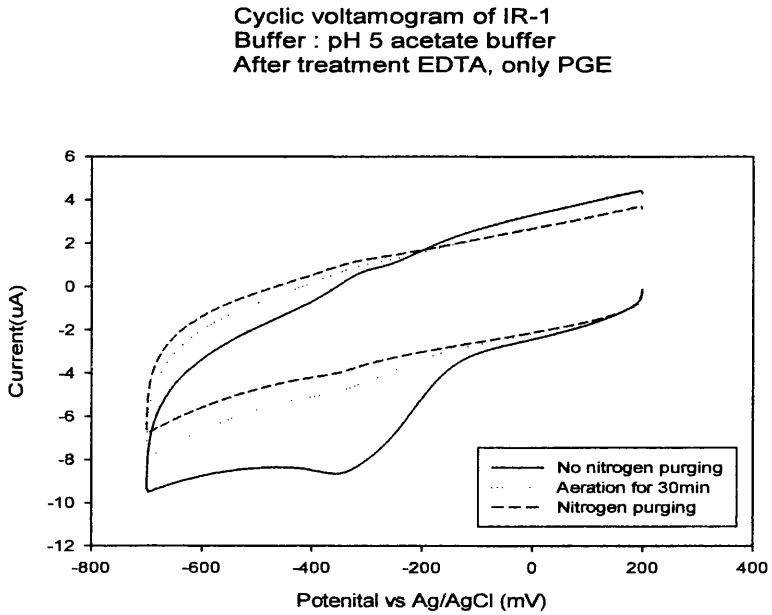

Figure 6.2- Cyclic voltammogram of EDTA extracted outer membrane on pyrolytic graphite electrode (Scan rate: 200mV/s, pH 5.0)

After aerating the cell for 30 minutes with the electrode soaking in the buffer, the peaks reduced, showing decreased activity as would be expected. After purging the system for 20 minutes with nitrogen again with the electrode soaking in the buffer, the peaks were not restored, but stayed at a similar level to that after the aeration. The reason for the peaks not returning to their original size has been put down to the aeration making the membrane fragments detach from the electrode. The other option was that the cytochrome is inactivated by the oxygen, but this has been shown not to be the case by Kyung Shik Kim's earlier work (not shown here).

6.1.5. LB Films

A Langmuir-Blodgett (LB) film consists of a bi-layer of lipids on a surface. The lipids used are molecules with a hydrophobic and a hydrophilic part. Thus when

placed on a surface, if the surface is hydrophilic, the hydrophilic ends of the first layer will be attracted to the surface and the hydrophobic ends will stick out. Then the second layer will have the hydrophobic end towards the first layer and the hydrophilic ends out. This creates a hydrophobic area between the layers. Likewise if the surface is hydrophobic, the area created will be hydrophilic.

By using the LB film the cytochrome c will hopefully sit inside the bilayer, which will simulate the outer membrane. The cytochrome c could then behave as it would in the outer membrane and the LB film will keep the cytochrome in close proximity to the electrode.

The first attempt to make an LB layer gave the results seen in figure 6.3.

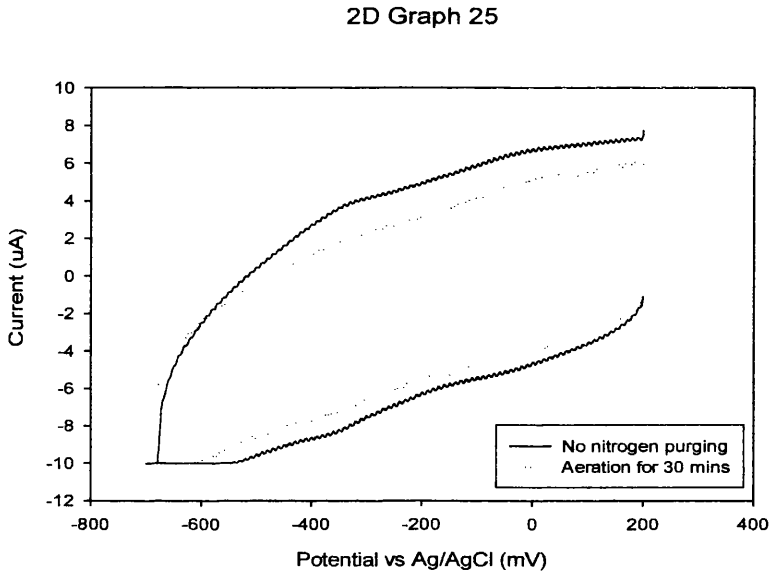

Figure 6.3- Cyclic voltammogram of EDTA extract on pyrolytic graphite electrode (Scan rate: 600mV/s, pH 5.0)

From the cyclic voltammogram it is possible to see, firstly that the peaks at around -350 mV and -400 mV are very small, and secondly that the change in peak size by aeration is also very small. The reason for this is that due to the manual method of making the film creates a very thick layer of the lipid. This reduces how quickly the reaction can occur, as electrons and the chemicals must first get through the lipid layers before the reaction can take place. The thick layer of lipid also exerts a strong force on the cytochrome c, not letting it rotate when it is exposed to oxygen.

6.1.6. Discussion

Although a successful oxygen sensor was not made, these steps have eliminated some possible methods. The technique that looks most promising is the LB film made by a LB machine. The apparatus was not available at KIST, so this work was undertaken at Department of Chemical and Biomolecular Engineering, Sogang University, Seoul. An attempt was made at making an LB film, but was unsuccessful. In order to improve the technique, a literature review (not included here) was undertaken and showed that the temperature and pH levels are very important to the process and should be monitored more closely the next time the LB film is attempted.

6.2. Appendix II: Hydrogenase

6.2.1. Introduction

The original focus of this study was on hydrogenase and its interaction with electrodes. The hydrogenase used was from *Clostridium pasteurianum*, which contains two iron (Fe) hydrogenases, one considerably more reactive than the other.

6.2.2. Methods and Materials

6.2.2.1. Clostridium pasteurianum growth medium

The growth medium used for Clostridium pasteurianum is laid out in table 6.5. The medium was made using distilled or deionised water, then boiled and purged with oxygen free nitrogen to make it anaerobic, then autoclaved.

Table 6.5- Growth medium for Clostridium pasteurianum

Substance	Concentration
Yeast	0.5%
Peptone	0.5%
Glucose	1%
KH_2PO_4	0.5%
KOH	Added to pH 7.0

6.2.2.2. Folin Assay

Before the experiment, the reagents need to be prepared as in the table 6.6. Reagents A and B can be stored indefinitely, C and D were mixed and discarded on the day of use.

Table 6.6- Composition of reagents for folin assay

Reagent	Composition
Reagent A	20g sodium carbonate (Na_2CO_3) dissolved in 1l 0.1M sodium hydroxide (NaOH) solution
Reagent B	0.5g $CuSO_4$ dissolved in 100ml 1% (w/v) aqueous solution of sodium tartrate ($[CH(OH)COONa]_2$)
Reagent C	Reagent A mixed with Reagent B in the ratio 50:1
Reagent D	Folin reagent diluted 1:1 with distilled water

6.2.2.3. Hydrogenase Assay

The hydrogenase assay was prepared as show in table 6.7 in a suitable stoppered cuvette. The cuvette was thoroughly purged with oxygen free nitrogen followed by high purity hydrogen, both from BOC.

Table 6.7- Hydrogenase assay composition

Substance	Quantity
Tris HCl pH 7.8	0.5 ml
Methyl viologen 20 mM solution	50 µl
Sodium hydrosulfite 20 mM solution	Added until the solution turned slightly blue

6.2.2.4. Extraction of Hydrogenase from Clostridium pasteurianum

Clostridium pasteurianum was grown, in the growth medium described above in section 6.2.2.1, to a volume of 5 litres. The cells were then washed.

In order to keep the cells as anaerobic as possible, it was necessary to construct modified centrifuge tubes that could maintain an anaerobic atmosphere.

The original tubes were based upon the normal centrifuge tubes used in the laboratory, Fisher Brand code FB55960, these are constructed with polypropylene and suitable for up to 6000 x *g*. Into the cap, a 7mm hole was drilled and an 8mm neoprene stopper inserted. This setup would hold pressure of over 1 bar and vacuum of greater than 20mm mercury. With 1 bar N_2 in the tube, positive pressure was maintained for over one week.

The tubes were flushed with N_2 for 5 minutes then purged by 5 cycles of vacuum and flushing with N_2. They were then filled with 40 ml of cells in their medium using N_2 pressure. The tubes were then purged for another 5 cycles. The tubes are then centrifuged at 4000 x *g* for 15 minutes. The supernatant is then drained by pressuring the tube with N_2.

The cells were then washed by filling the tubes with 25 ml of anaerobic 50mM phosphate buffer (pH 7.0), mixed thoroughly and centrifuged again at 4000 x *g* for 15 minutes. The cells were then rewashed at least 2 more times, and the solution filtered to remove as much buffer as possible.

The cells were then centrifuged at 4000 x g for 10 minutes and the supernatant discarded. The pellets were then frozen.

To extract the hydrogenase, the C. pasteurianum was re-suspended in anaerobic phosphate buffer (50mM, pH 7.0). The cells were then passed twice through a cell disruptor at 2.5 kpsi. The solution was the re-purged with N_2 and centrifuged at 6000 x g for 10 minutes, the supernatant was removed and both supernatant and pellet were stored under H_2.

6.2.2.5. Folin Assay

Firstly a standard curve must be generated using Bovine Serum Albumin (BSA). The BSA was then mixed with distilled water to give a range of protein concentrations from 0 – 250 mg/l in 50 mg/l steps. All samples were made up to 0.5 ml using distilled water.

At the same time, the samples of cell extract were added at full strength, or diluted with distilled water to 1 in 2, 1 in 5 and 1 in 10. These samples were also made up to 0.5 ml.

2.5 ml of reagent C was the added and mixed well. The samples were then left to stand for 10 minutes at room temperature. After this time, 0.25 ml of reagent D was added, the solution mixed well again and left to stand for 30 minutes at room temperature.

The solution turns to a varying blue colour dependant on the concentration of protein in the sample. The colour was measured using a spectrophotometer at 750 nm.

All samples were conducted in duplicate and the average taken.

Once the standard curve has been derived, it is possible to obtain the equation of the line and hence calculate the concentration of the protein in the sample.

6.2.2.6. Hydrogenase Assay

A gas tight, stoppered cuvette was filled with 900 µl of 50 mM phosphate buffer. The cuvette was then made anaerobic through a number of cycles of vacuum and purging with nitrogen. 100 µl of 10 mM methyl viologen solution was added to the cuvette and it was made anaerobic again. Less than 10 µl of 10 mM sodium hydrosulfite was added to the cuvette to show a slight blue colour.

The headspace of the cuvette was then thoroughly flushed with hydrogen for a minimum of 15 minutes. 50µl of hydrogenase was added from an anaerobic solution and a spectrophotometer is used to measure the rate of change of colour.

The activity of the hydrogenase can be calculated from the molar extinction coefficient of methyl viologen $\varepsilon_{570} = 13.1\ mM^{-1}\ cm^{-1}$.

6.2.3. Extraction of hydrogenase

The *Clostridium pasteurianum* was bought in and grown up to a volume of five litres using the growth medium described in section 6.2.2.1, using vacuum bottles and demijohns the atmosphere was kept anaerobic using nitrogen.

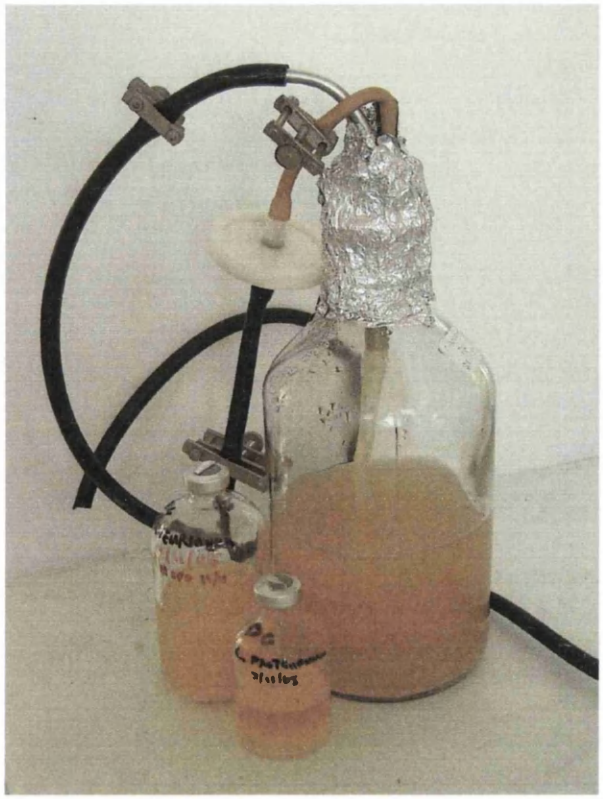

Figure 6.4- Apparatus used for the growth of *Clostridium pasteurianum*

Once the five litres was grown the cells were washed three times with phosphate buffer (50mM, pH 6.5), using filtration column. The cells were then disrupted by pressure and the resulting solution centrifuged at 6000 x *g* for 10 minutes to remove the cell material. A folin assay was then carried out to gain the concentration of protein.

6.2.3.1. Folin Assay

The Folin assay was carried out as described in section 6.2.2.5 using Bovine Serum Albumin (BSA) to create the standard curve.

Table 6.8 -Folin assay for BSA to create standard curve

Concentration mg/l	OD1	OD2	Average OD
250	0.434	0.434	0.434
200	0.325	0.376	0.3505
150	0.237	0.237	0.237
100	0.165	0.165	0.165
50	0.103	0.103	0.103
0	0.021	0.019	0.020

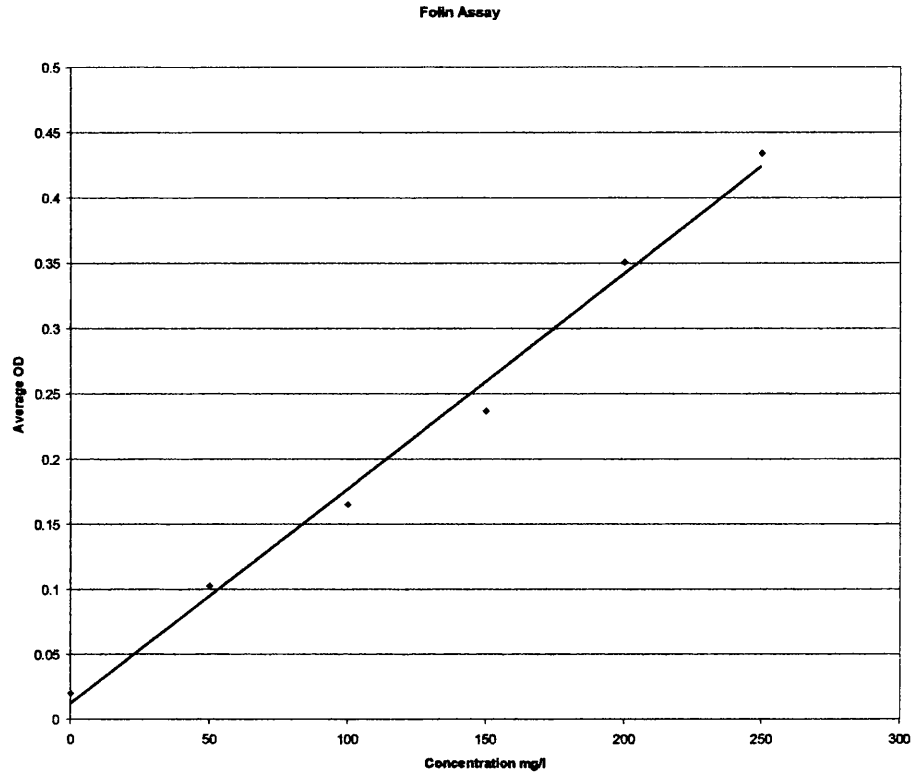

Figure 6.5- The standard curve

Having found the standard curve, figure 6.5, the equation 6.1 was established .

$$y = 0.0016x + 0.0122$$

Equation 6.1: Equation of the standard curve

Rearranging for x gave the equation 6.2

$$x = \frac{y - 0.0122}{0.0016}$$

Equation 6.2: Rearranging the stardard curve for x

Using this equation where y = the optical density at 750nm and x = the concentration of protein, the results in the following table could be calculated.

Table 6.9 - Folin assay of hydrogenase from *Clostridium pasteurianum*

Dilution of protein sample	OD1	OD2	Average OD	Protein Concentration mg/l	Protein Concentration at full strength mg/l
1	Off scale	Off scale	N/A	N/A	N/A
1:2	1.279	0.978	1.1285	697.7	1395
1:5	0.501	0.580	0.5405	330.2	1650
1:10	0.237	0.237	0.237	140.5	1405

From the results in table 6.9, it is can be simply calculated that the average protein concentration of the full strength sample is 1480 mg/l.

6.2.3.2. Hydrogenase Assay

Having found the concentration of protein from the disrupted cell, it is then necessary to carry out a hydrogenase assay to find the activity of the hydrogenase. The assay was carried out as described in section 6.2.2.6, however there was no colour change to the solution. The assay was repeated with increasing quantities of the hydrogenase solution but with no success, there was no activity from the hydrogenase.

6.2.3.3. Making the process anaerobic

Although *Clostridium pasteurianum* can survive exposure to air, hydrogenase is known to be susceptible to exposure to oxygen. Thus it was deduced that the exposure to oxygen during the washing and cell disruption was causing the deactivation of the hydrogenase.

In order to reduce the exposure to oxygen, special centrifuge tubes were constructed and used to wash the cells with anaerobic buffer, see section 6.2.2.4 for details on the construction of the tubes and the method of washing.

However, despite making the washing process and centrifugation anaerobic, it was not possible to make the cell disrupter anaerobic, so the cell solution was kept under nitrogen until put into the disrupter and immediately purged afterwards.

Another issue came from the in house made centrifuge tubes. Despite ensuring a very tight fit of the bungs, the forces involved in the centrifuging of the disrupted cells would sometimes force the bung through the lid and into the tube. Obviously this would result in that tube becoming aerobic and hence the contents were discarded. This would happen in around 50% of the tubes, making the protein yield from the harvest very low.

Despite efforts to keep the protein in as anaerobic conditions as possible, the hydrogenase assay would still show no activity.

6.2.4. Discussion

The hydrogenase from *Clostridium pasteurianum* proved to be too susceptible to oxygen, despite efforts to keep the enzymes as anaerobic as possible. With the cell disruption equipment available it was not possible to keep the anaerobic conditions and hence the hydrogenase would become permanently deactivated. Even following the disruption up to 50% of each batch was exposed to oxygen during the centrifuging, leaving a very small amount of protein to work with.

The greatest difficulty encountered in this study was that of not being able to extract hydrogenase from *Clostridium pasteurianum* without irreversibly deactivating it. This was put down to the enzymes having to be exposed to air during the extraction process as preliminary tests with the whole cells showed activity from the hydrogenase.

Despite all attempts to keep the process as anaerobic as possible, during the disruption of the cells they had to be exposed to air for a period of a few minutes. This was enough to stop any activity.

In order to avoid this problem in the future there are three courses of action that could be taken.

Firstly the whole process could be carried out inside a glove box or anaerobic chamber. However the chamber would need to be sufficiently large to contain all the equipment needed, such as the cell disruptor and possibly the centrifuge.

Secondly, a different technique might be employed to disrupt the cells, such as a freeze-thaw or chemical process. Care would be needed though to find a suitable

process that would not denature the hydrogenase. Unfortunately in this study the time was not available to invest in finding a different technique.

Thirdly and perhaps the easiest would be to change the species and type of hydrogenase that is being worked with. As discussed in the introduction it is known that NiFe-hydrogenases are less susceptible to O_2 inactivation. Recent studies by Vincent et al (Vincent, Parkin, et al. 2005) and Maness et al (Maness et al. 2002) have shown some hydrogenases from aerobes to be tolerant of oxygen and even continue to function in the presence of oxygen. Working with one of these hydrogenases, such as the hydrogenase of *Ralstonia eutroph* will allow the hydrogenase to be exposed, but will return to full activity when returned to an H_2 rich environment.

6.3. Appendix III: Potentiostat

As well as the BAS Epsilon system, a basic potentiostat was needed to maintain a potential at the electrode whilst it is scanned in the AFM. This circuit was based on the designs of Rudolf Doelling (Doelling 2000) and built in house.

6.3.1. Design and Construction

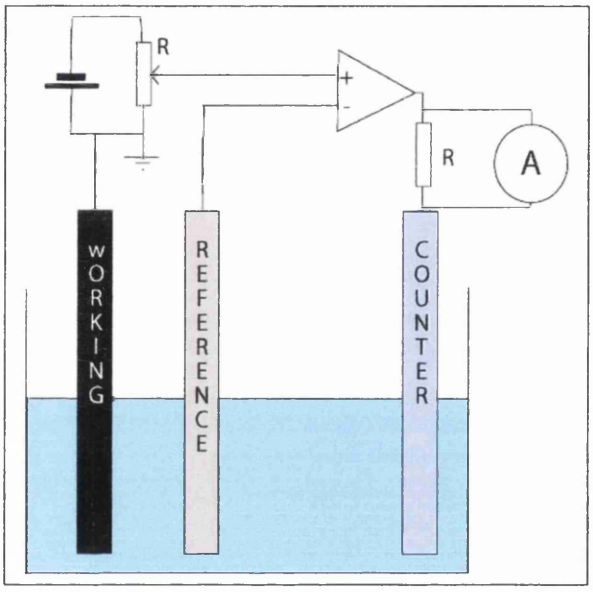

Figure 6.6- A basic potentiostat design allowing the potential difference to be controlled

A basic circuit, like the one in figure 6.6 and discussed in the introduction (section 1.4.1) would work as a potentiostat and would very quickly adjust to any changes in the potential between the reference and the working electrode. However, it would be unstable and may break into oscillations. This is due to the fact that, when the signal is amplified, the phase shift changes with frequency. At a certain frequency the phase shift will reach 180° and will result in growing oscillations until the amplifier reaches full power. To stop this from happening a small capacitance needs to be added to feed back to the inverting input, the capacitor corrects the phase shift and stops the oscillations from occurring.

Protection should also be considered for the circuit, in the form of a protection resistor between the reference electrode and the amplifier input. The resistor protects the amplifier from high voltage static shocks.

Another point to consider is that when current is drawn from a circuit, e.g. from the potential divider creating the working electrode offset, the potentials will change. To stop this happening and to try to take as accurate as possible potential readings, buffers are introduced to the circuit. These offer a high input resistance and a low output resistance, thus the potential can be maintained as only small currents are drawn from the circuit. The resulting circuit is shown in figure 6.7.

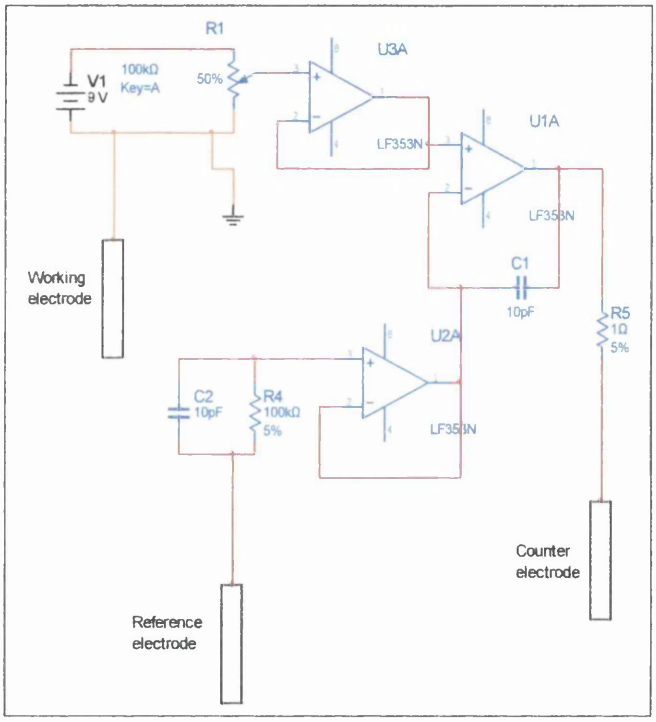

Figure 6.7- Basic potentiostat using buffers, stability capacitors and protection resistors

The final stage to be considered is the output of the circuit. The cell may require fairly large currents to get the correct potential. These currents may be too much for standard operation amplifiers, and thus a higher power amplifier was needed to be used.

A final addition to the circuit is to allow the potential to be both positive and negative. This was achieved by using a split rail power supply. Connecting the

potential divider from the positive to the negative rails gave the full range of adjustment. The potential from the divider is then added to the potential of the working electrode through the use of a summing amplifier.

For all the amplifiers in the circuit, except the power stage, the only requirements were to work on +9V to –9V split rail supply and to have a high slew rate that would adjust to any variations in the potential as swiftly as possible, but retain a high gain as the higher the gain, the closer the potential of the electrode becomes. For these applications the LF353N op-amp was chosen.

For the power stage an op-amp capable of supplying fairly large currents, based on an assumption of up to 1A was needed. This greatly exceeds the capability of the LF353N, which is capable of only a few milliamps. As well as the high power output, the amplifier must maintain the high slew rate, not a common characteristic in power amplifiers and hence would be very expensive. Audio amplifiers, however, do need both a higher power output and a high slew rate, their gain may not be as high as a power amplifier, but this is not important for a power stage.

The first amplifier tried was a LM3876, the specifications exceeded all those needed and the price was relatively low. However the supply voltage of +9V to –9V was the same as the minimum potential needed to power the amplifier. This caused a problem as with the circuit turned on the potential could drop below the required voltage and trigger the protection built into the chip, hence giving no output.

To solve the problem, the amplifier was changed to a lower power model that would still supply the current and meet the specifications, the TDA2030A. This chip did not have the same protection circuitry and hence would run off the desired voltage, giving the circuit shown in figure 6.8.

With the circuit built, a basic test was carried out by connecting 1 kΩ resistors between the counter electrode connection and the reference electrode connection, and between the reference electrode connection and the working electrode connection, these resistors simulated a basic cell. In this set up, the potential between the working electrode and the reference electrode followed the desired value.

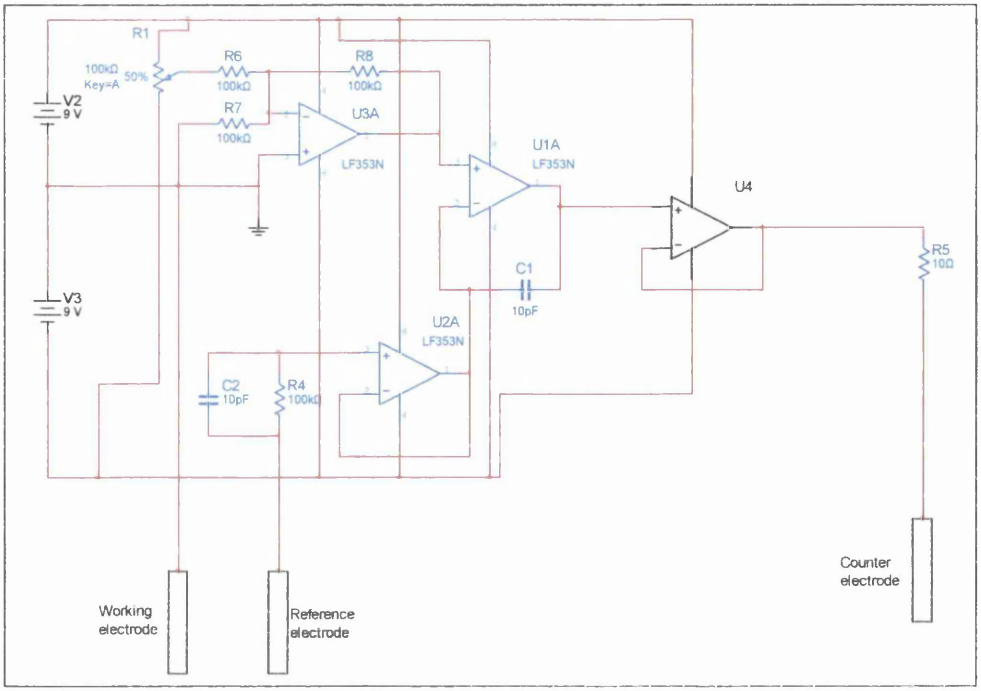

Figure 6.8- Circuit diagram of final potentiostat design

6.4. Appendix IV: AFM in Fluid

AFM in fluid presents more problems with getting an accurate scan of the surface, but can provide more information than a scan in air. By using the properties of the fluid, you can get more information about the surface. In this set of experiments, the scanning of the double layer above a submersed surface was used.

6.4.1. Method

6.4.1.1. AFM in fluid

With the equipment available, it was only possible to image using contact mode in fluid.

To use the AFM in fluid an appropriate head was used on both the Dimension and the Explorer to ensure it remained sealed. Both AFMs would then be set up as normal for contact mode. Once the tip was lowered close to the surface, a small amount of fluid was injected in to the gap between the head and the surface. This would cause the laser to bend, due to the refraction of the light. As a result the laser and sensor positions would have to be retuned to get the strongest signal.

Following the set up a calibration grid would often be scanned first to ensure the setup was good before scanning the sample.

As before, the set point, integral and proportional gains were used to gain a consistent trace and retrace before the scan was started. Fluid would then be added as needed to keep the surface wet.

6.4.1.2. Imaging of double layers

The double layer imaging was also carried out in using AFM in fluid and set up as in section 6.4.1.1.

Before the imaging took place, a force against setpoint curve was generated to allow the calculation of the force being applied in the scan. Once the tip had been brought down to the surface to start a scan, the set point was raised to a point that the tip would move above the surface and track the force exerted by the double

layer. The gains would then be adjusted to get a stable trace and retrace and a scan taken.

The ionic strength of the fluid would then be changed and the parameters kept the same to ensure the force stayed the same. A scan was then carried out at the new ionic strength. The resultant is taken above the surface at the point the new double layer exerts the same force.

6.4.2. Results of double layer imaging

Double layers are charged layers that form on surfaces when they are submerged in a liquid. The layer on the surface is either positively or negatively charged, the opposite charge to the charge of the surface. A second layer of ions, the opposite charge to the first layer, is then attracted to the first layer. These layers provide a force on the tip of the AFM as it is brought close to the surface, so if a low force is used the double layer is scanned instead of the surface. As the force is increased, the tip will scan closer to the surface giving more defined details. This can be seen on the scan of a calibration grid figures 6.9 and 6.10.

Both figures 6.9 and 6.10 were scanned in the same place, both in 1mM NaCl solution. Although there is no zero set point for the force, a test was run on the cantilever using the DI software and the force per nA of setpoint was 10.24 nN/nA. Thus the difference in force between the two scans is 307.2 nN. Comparing the scans it is possible to see that at -20 nA the edges of the grid are more defined and sharper, also the hole in the centre of the grid hole is smaller with a small groove running from it, in the -50 nA this all appears as one hole. This is all a result of the higher force pushing the tip further through the double layer.

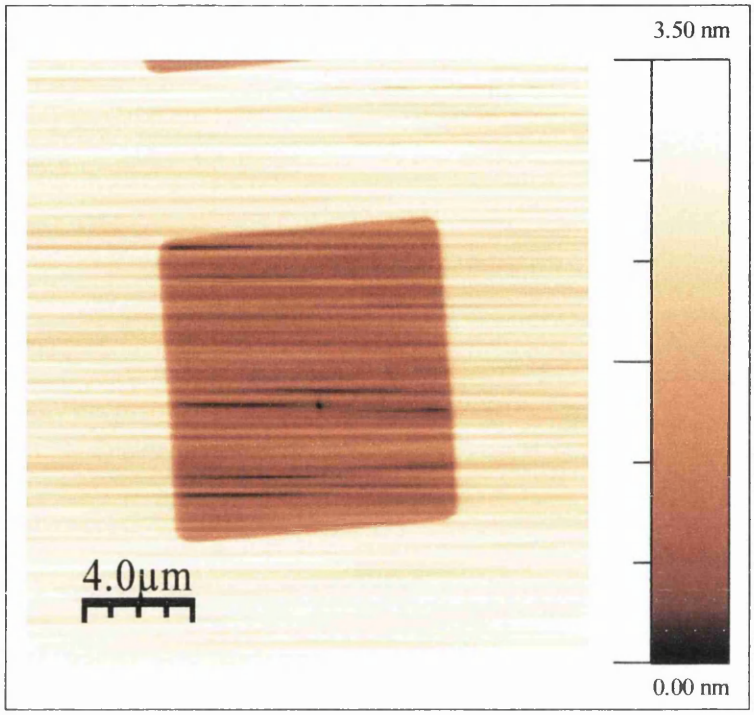

Figure 6.9- Scan of double layer on calibration grid at -20 nA

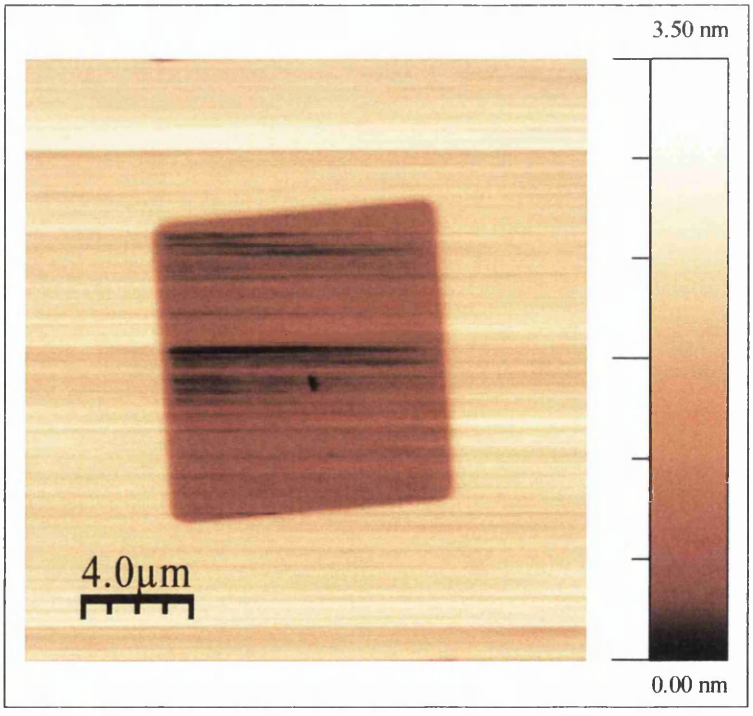

Figure 6.10- Scan of double layer on calibration grid at -50 nA

In the 3 dimension representations of figures 6.11 and 6.12 below, the sharpness of the calibration grid is even more obvious.

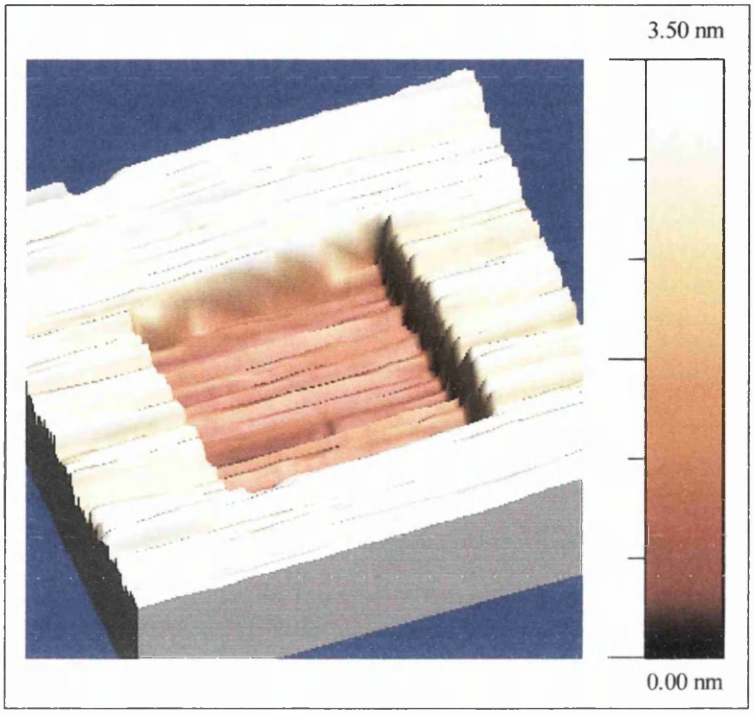

Figure 6.11- A 3D representation of figure 6.9

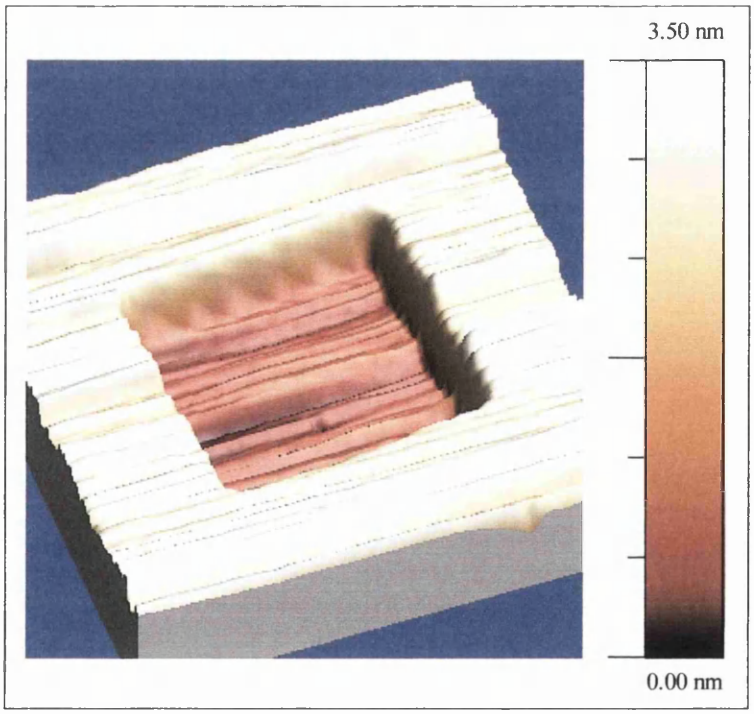

Figure 6.12- A 3D representation of figure 6.10

Increasing the ionic strength of the solution being used will reduce the height of the double layer, allowing the scan to be carried out nearer the surface and increasing the detail in the same way that using a higher force does.

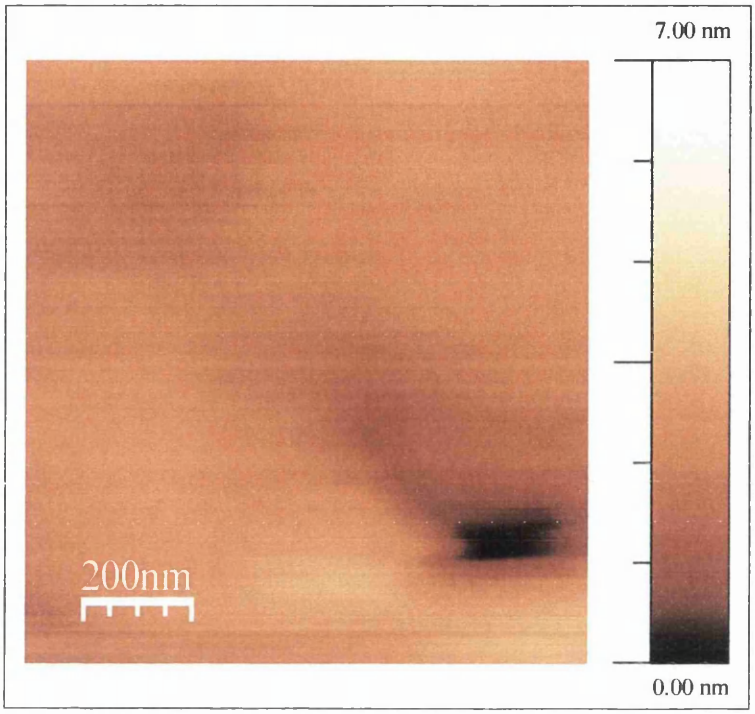

Figure 6.13- Scan of a Cyclopore membrane in 1mM NaCl solution

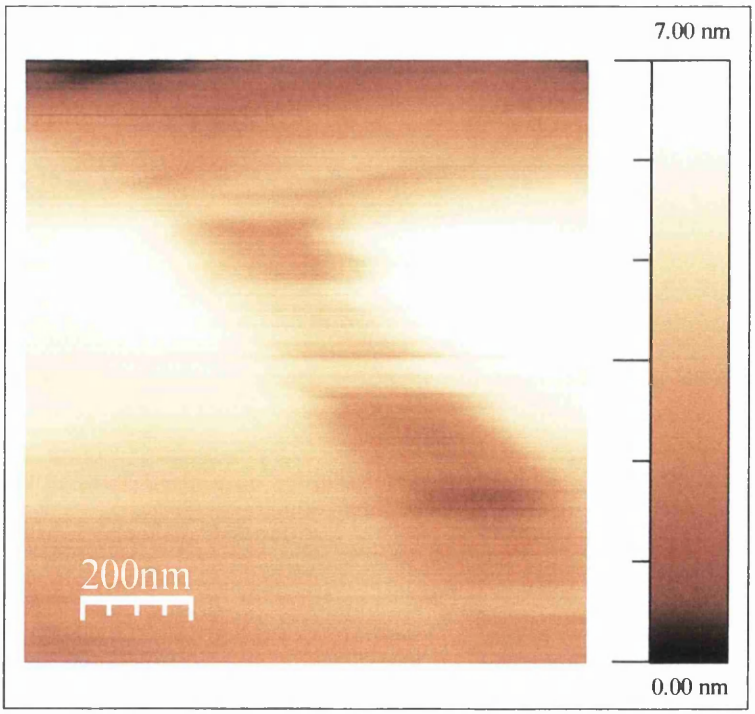

Figure 6.14- Scan of a Cyclopore membrane in 100mM NaCl solution

Figures 6.13 and 6.14 show a scan of a hole in the Cyclopore membrane scanned at the same force.

Although the images are not the most clear, it is possible to see that the 1mM NaCl image, figure 6.13, shows very little relief, the image is essentially flat except for the hole towards the bottom right of the image. The 100mM image, figure 6.14, shows higher areas to the right and left of the image and a second hole or dip just above the centre. These features can be seen more clearly on the three dimensional representations in figures 6.15 and 6.16.

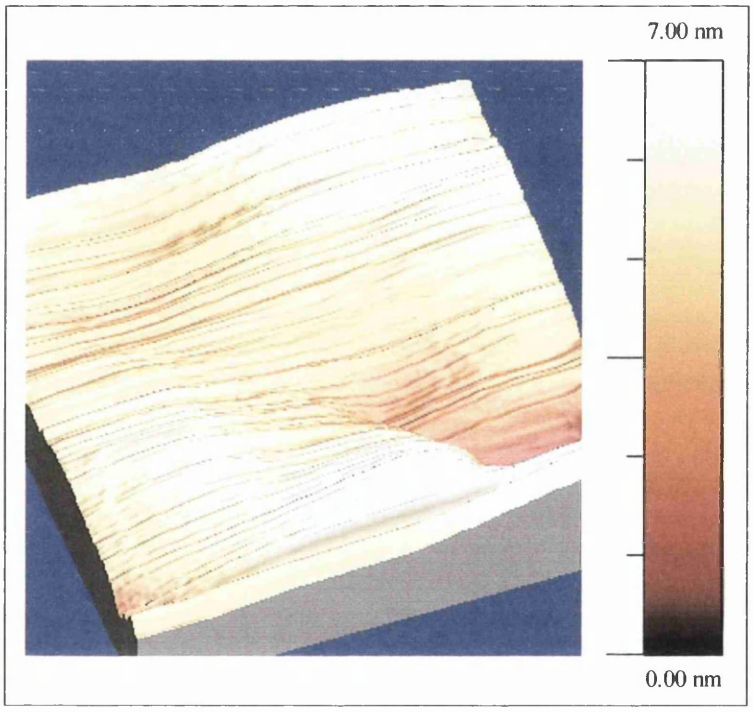

Figure 6.15- A 3D representation of figure 6.13

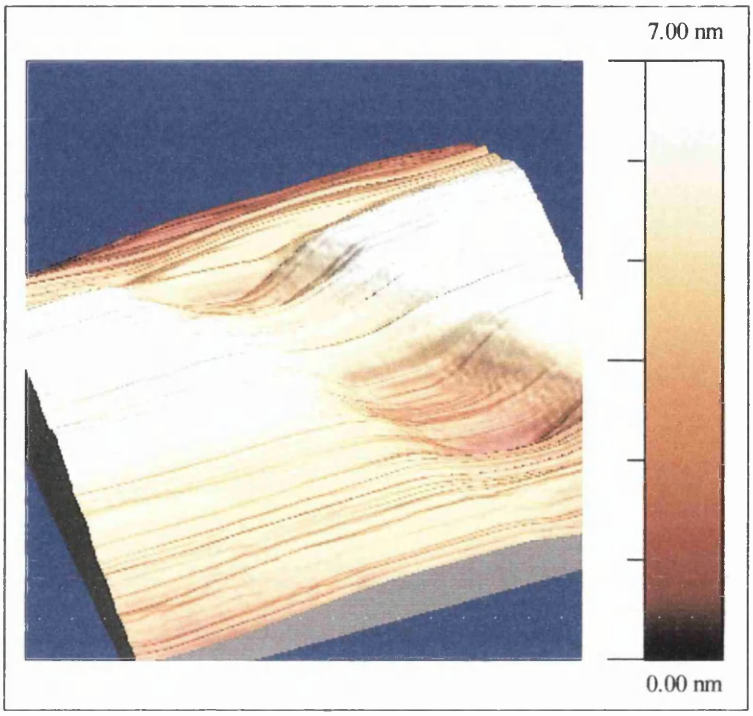

Figure 6.16- A 3D representation of image 6.14

The 3D representations show clearly that the stronger ionic solution defines the dips in the surface more sharply, with a more defined edge and shape.

6.4.2.1. Dicussion

In the AFM images it was possible to see the growth and shrinking of the layers with different ionic strengths. It follows that imaging a charged electrode in an ionic solution will show thicker and thinner double layers at the areas of charge on the surface as more ions are attracted or repelled from the areas as the charge on the surface of the electrode increases or decreases. This would give a better idea of current flow into a fluid than C-AFM in the dry can. However, it will require a potentiostat to charge the electrode. Assuming the need is only to charge the electrode and hold a potential, the potentiostat designed in parallel to this study (see appendix III) can be used.